OCA

REPORT

TO

GTE SPACENET CORPORATION

FINAL REPORT

for

Contract C-10070

RESEARCH AND DEVELOPMENT OF SATELLITE INTERFERENCE LOCATION SYSTEM (SILS) AT GEORGIA TECH

Paul G. Steffes, Principal Investigator

January 20, 1987 through June 30, 1990

Submitted by

Professor Paul G. Steffes
School of Electrical Engineering
Georgia Institute of Technology
Atlanta, Georgia 30332-0250
(404) 894-3128

REPORT

TO

GTE SPACENET CORPORATION

FINAL REPORT

for

Contract C-10070

RESEARCH AND DEVELOPMENT OF SATELLITE INTERFERENCE LOCATION SYSTEM (SILS) AT GEORGIA TECH

Paul G. Steffes, Principal Investigator

January 20, 1987 through June 30, 1990

Submitted by

Professor Paul G. Steffes
School of Electrical Engineering
Georgia Institute of Technology
Atlanta, Georgia 30332-0250
(404) 894-3128

Dedication

Benefits resulting from this dissertation are dedicated to all the friends, teachers, employers, mentors, and mostly to my parents who have done the tremendous jobs of putting up with me and making it possible for me to get to a point in life where I may contribute something back into this world.

Acknowledgments

I should like to thank my dissertation advisor, Professor Paul G. Steffes, for his assistance, teachings, and patience. I should also like to thank the faculty members who served on the various committees which are required to produce another Ph.D. student. I should specifically like to thank the following Georgia Tech professors for their technical and moral support:

Aubrey Bush
John Dorsey
Bob Feeney
Dave Hertling
Bob Roper
Bill Sayle
Steve Wicker

I should like to thank Mr. William P. Kinsella of the GTE Spacenet Corporation of McLean, Virginia for his moral support and for his company's financial support of this project.

I should like to thank Ms. Diana Fouts for her help and provision of resources for preparing much of the graphic content of this dissertation.

Finally, I thank Mr. Jim Norman and Dr. Sheila Azdell for being out there.

Table of Contents

List of Tables

List of Illustrations

Summary

This dissertation describes the design and development of a system for inferring the position of terrestrial satellite uplink stations using existing domestic satellites with minimal disruption to normal satellite operation. Two methods are presented by which a quantity measured at a terrestrial receiving site is mapped into a curve of possible uplink locations on the Earth's surface. One method involves measuring differential time delays of a single uplink signal observed through two adjacent spacecraft. Another method uses a short baseline interferometer composed of the two cross-polarized and spatially separated antenna feeds aboard an affected satellite. A unique location or two dimensional solution is obtained by employing an appropriate combination of the two presented methods. A system for measurement of the required differential delays and phases is described in addition to the experimental work performed to demonstrate the feasibility of these location methods.

1. Problem Statement and Potential Solutions

The objective of this research has been the development of a Satellite Interference Location System (SILS) for inferring the location of terrestrial satellite uplink stations using existing geosynchronous civilian repeater-type satellites with minimal disruption to normal satellite operation. Two methods are presented which together can produce a unique positional solution. Each method has been tested experimentally.

The first method is the Time Difference of Arrival (TDOA) system in which the propagation time for the uplink signal to a particular satellite is compared with the propagation time to an adjacent satellite. Given that the positions of the two spacecraft relative to the receiving station are precisely known, the difference in time of arrival over the two different paths isolates the possible uplink transmitter location to a one dimensional curve on the Earth's surface. Figures 1.1 and 1.2 show the two and three dimensional cases. Such a system requires a two channel receiving system capable of accurately estimating the differential delay between the two paths, as is illustrated in Figure 1.3. Because the level of the uplink signal through the adjacent satellite path is typically 30

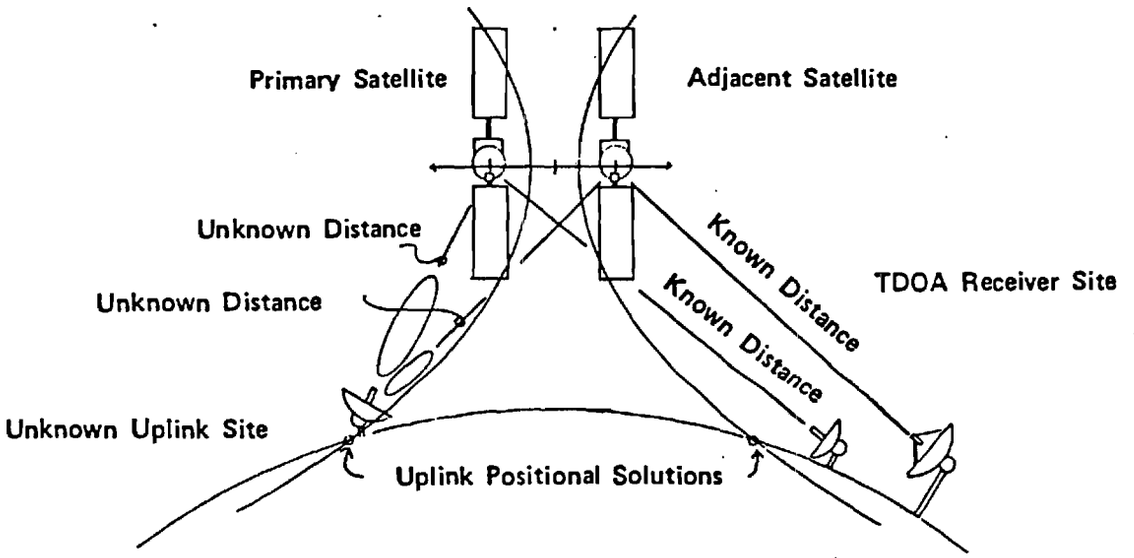

Two Dimensional TDOA Geometry
Hyperbolic Intersections

Figure 1.1

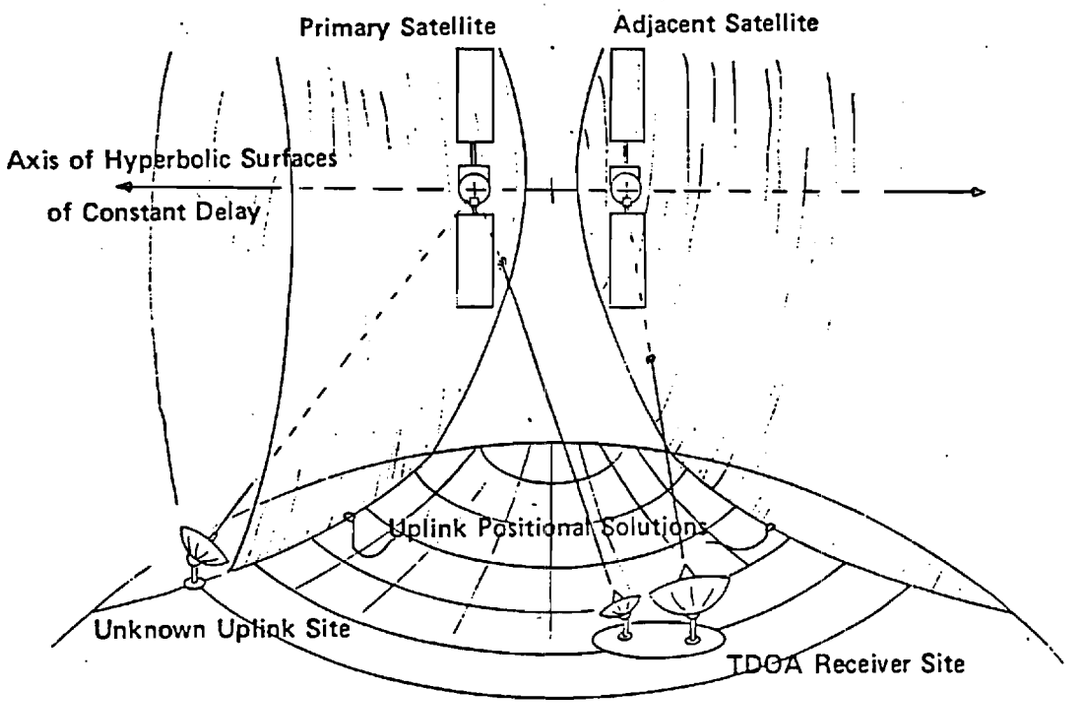

Three Dimensional TDOA Geometry
Hyperbolic Intersections

Figure 1.2

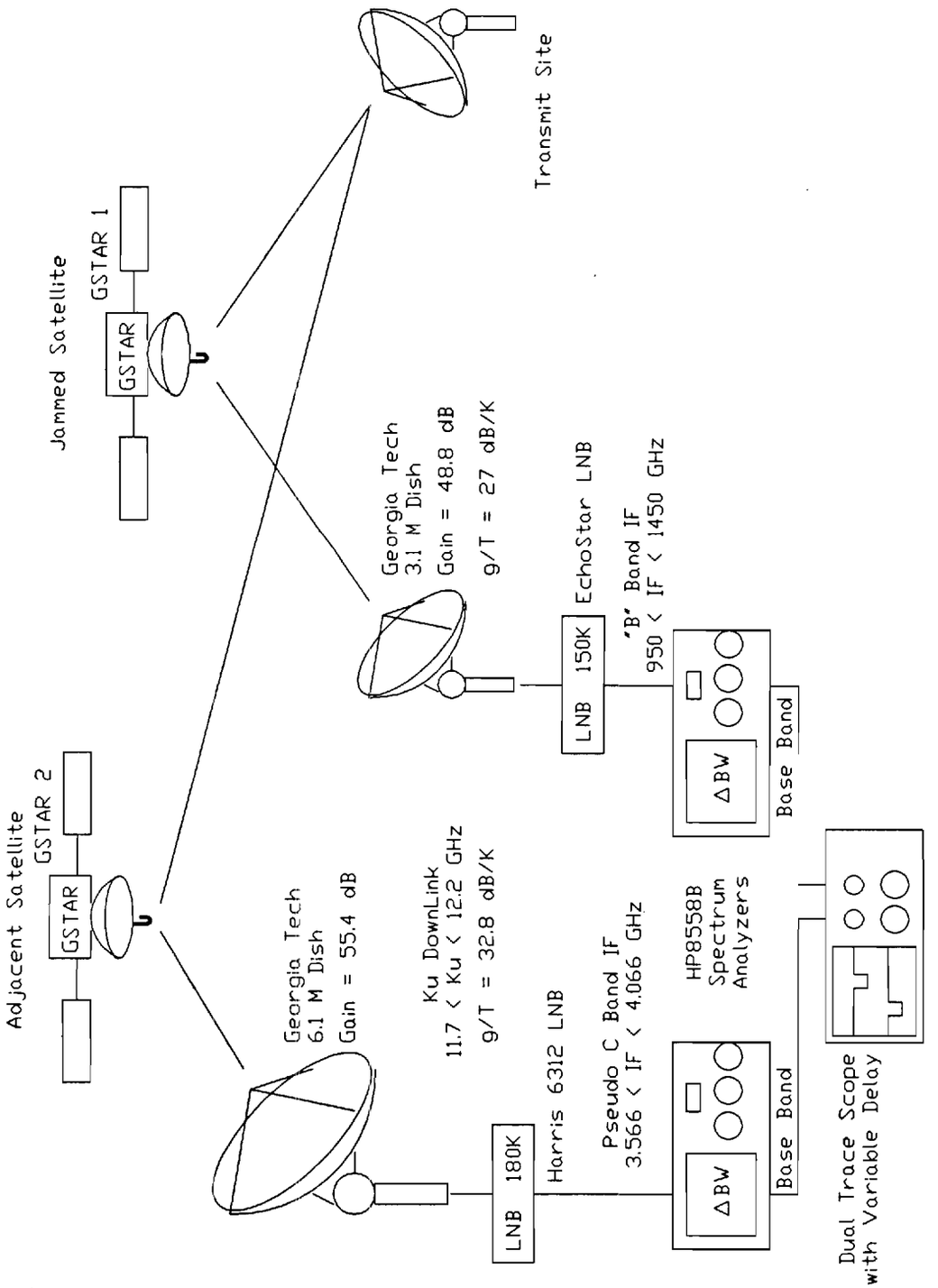

TDOA Developmental System
Hardware Configuration

Figure 1.3

to 40 dB lower than that through the primary satellite (for example, see [13,14] for uplink sidelobe performance), high sensitivity equipment is required for the adjacent satellite downlink. The corresponding transponder aboard the adjacent satellite should be only lightly occupied so as not to interfere with the relatively weak signal from the source of interest. Figure 1.4 shows a Mercator projection map of the Continental United States (CONUS) illustrating the family of curves of constant differential delay for GTE's GSTAR 1 (103 degrees west) and GSTAR 2 (105 degrees west) satellites.

The TDOA approach can be used to locate the sources of a wide range of signal types. Almost any modulated signal (video, audio, digital, etc.) can be located by using a measurement of the differential time delay between some unique portions of the two received waveforms. Even pseudo-random noise signals can be located using a variable time delay correlator to infer the differential time delay between the two satellite paths. However, unmodulated continuous wave (CW) signals present a special problem. Unless the differential time delay through the two paths is less than 1/f (where f is the frequency of the CW signal), it becomes impossible to identify unambiguously the location of the source of the CW signal.

Another technique for producing a one dimensional solution is interferometry, or the comparison of phases of

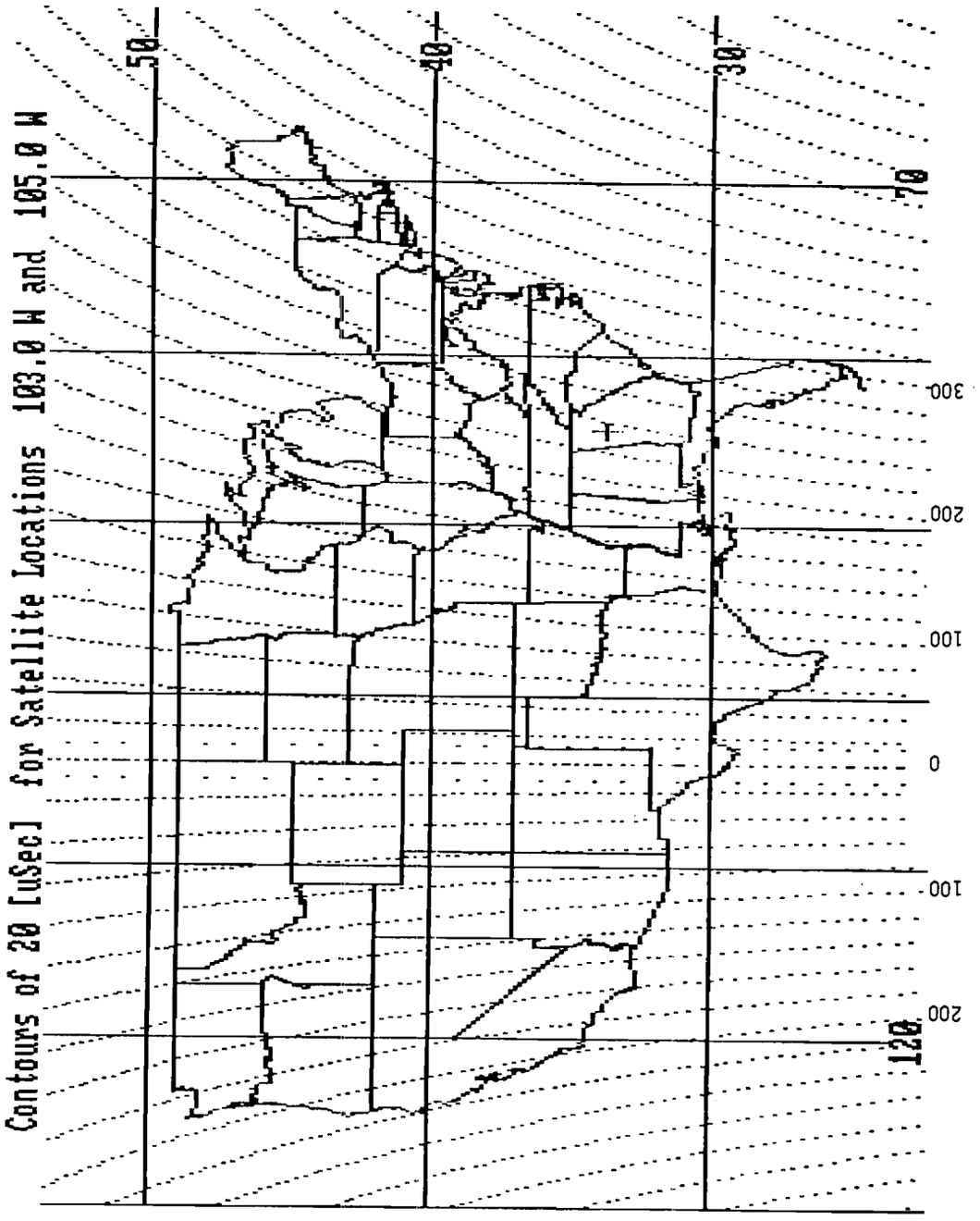

Contours of 20 Microsecond Differential Delay for GSTAR 1 & 2
Figure 1.4

an incoming signal at two spatially separated antenna locations. Given a differential electrical phase measurement made between two known and separate locations, one can determine the angle of arrival of incident radiation relative to an interferometric baseline formed by the line connecting the two receiving antennas. Figure 1.5 illustrates the relevant geometry for a dual antenna receiving system to relate the desired geometric angle to the antenna separation, wavelength of the incoming signal, and the measured differential phase between the antennas. This technique may be used with CW signals.

To employ this technique for a SILS effort, two antennas are required in a location which facilitates a useful terrestrial solution. The distance between adjacent geosynchronous satellites is too large to make unambiguous interferometric measurements of the direction of an incoming signal transmitted from within CONUS as viewed from a geosynchronous satellite. At the Ku-band frequencies used by some domestic satellites the distance between feeds used for the two orthogonal polarizations aboard a single satellite is usually smaller than one meter. Thus, a measurement of the differential phase of the uplink signal as measured by ground stations through each of the two orthogonally polarized feeds aboard the spacecraft may be used to infer the angle of arrival of incident radiation

Figure 1.5

Radio Interferometer
Geometry and Equation

Interferometric
Geometry at the
Satellite

Figure 1.6

Figure 1.7

Figures 1.5, 1.6, and 1.7

upon the satellite. This measured differential phase can be mapped into a terrestrial curve of possible locations of the uplink signal source.

Figure 1.6 illustrates the antenna feed locations aboard a GSTAR series satellite and relates this geometry to an interferometric baseline. Figure 1.7 shows the resulting cone of constant differential phase around the interferometric baseline and terrestrial intersection between this cone and the sphere of the Earth. Figure 1.8 shows a Mercator projection map of CONUS illustrating the family of curves of constant differential phase for GTE's GSTAR 1 (103 degrees west) satellite. Because the signal level through the cross-polarized transponder would be much weaker than that through the primary transponder (approximately -30dB based on manufacturers' data for typical ground antenna cross-polarization isolation), a more sensitive receiving system is required for that signal.

Employing a combination of the TDOA and interferometric techniques can localize the uplink transmitter's position through the determination of the intersection of the two curves. Figure 1.9 shows a map with overlaid curves of constant delay and differential phase for the TDOA and Interferometric methods specific to the case where time difference is measured between GSTAR 1 and GSTAR 2 and phase difference is measured between the orthogonally polarized

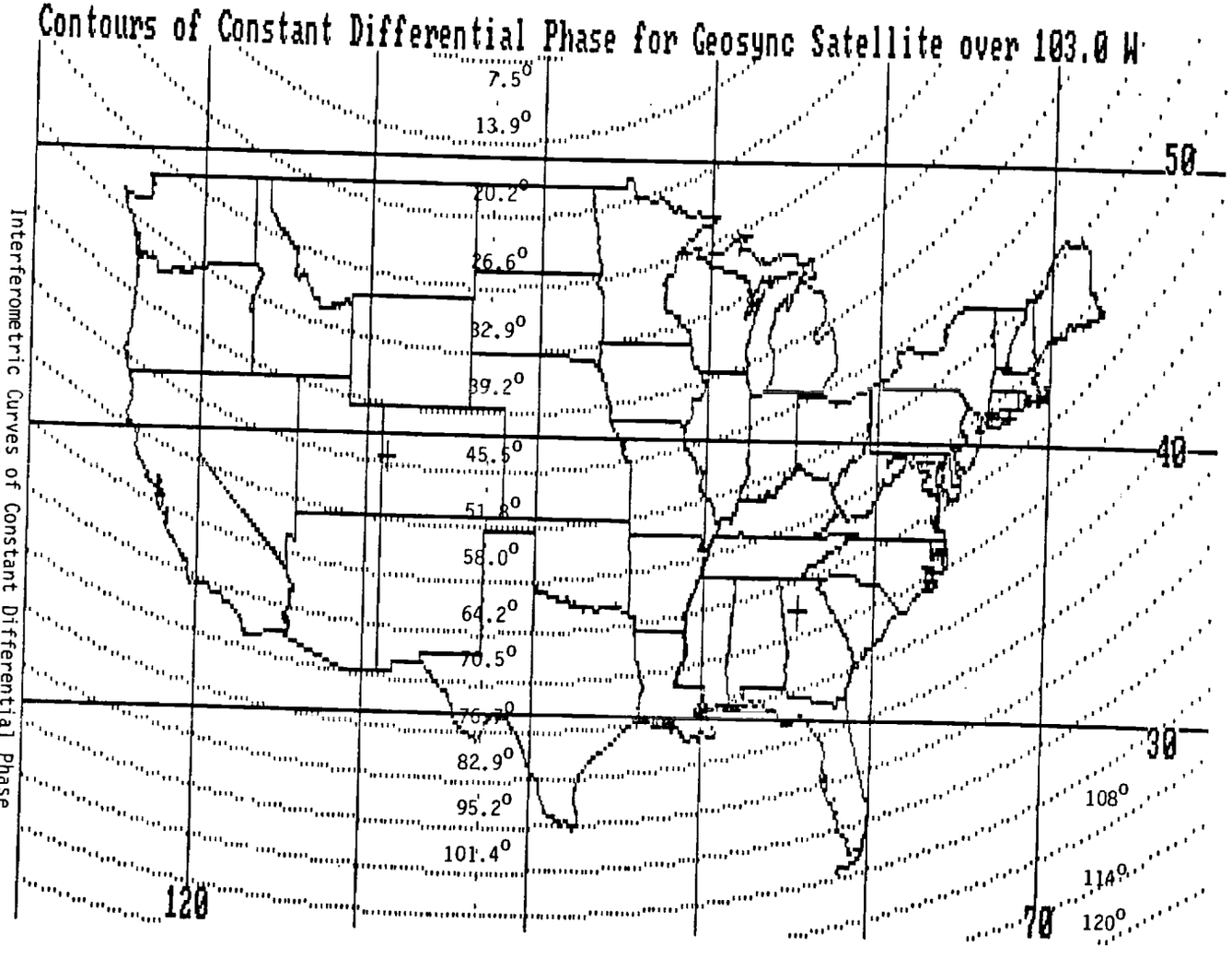

Interferometric Curves of Constant Differential Phase
Figure 1.8

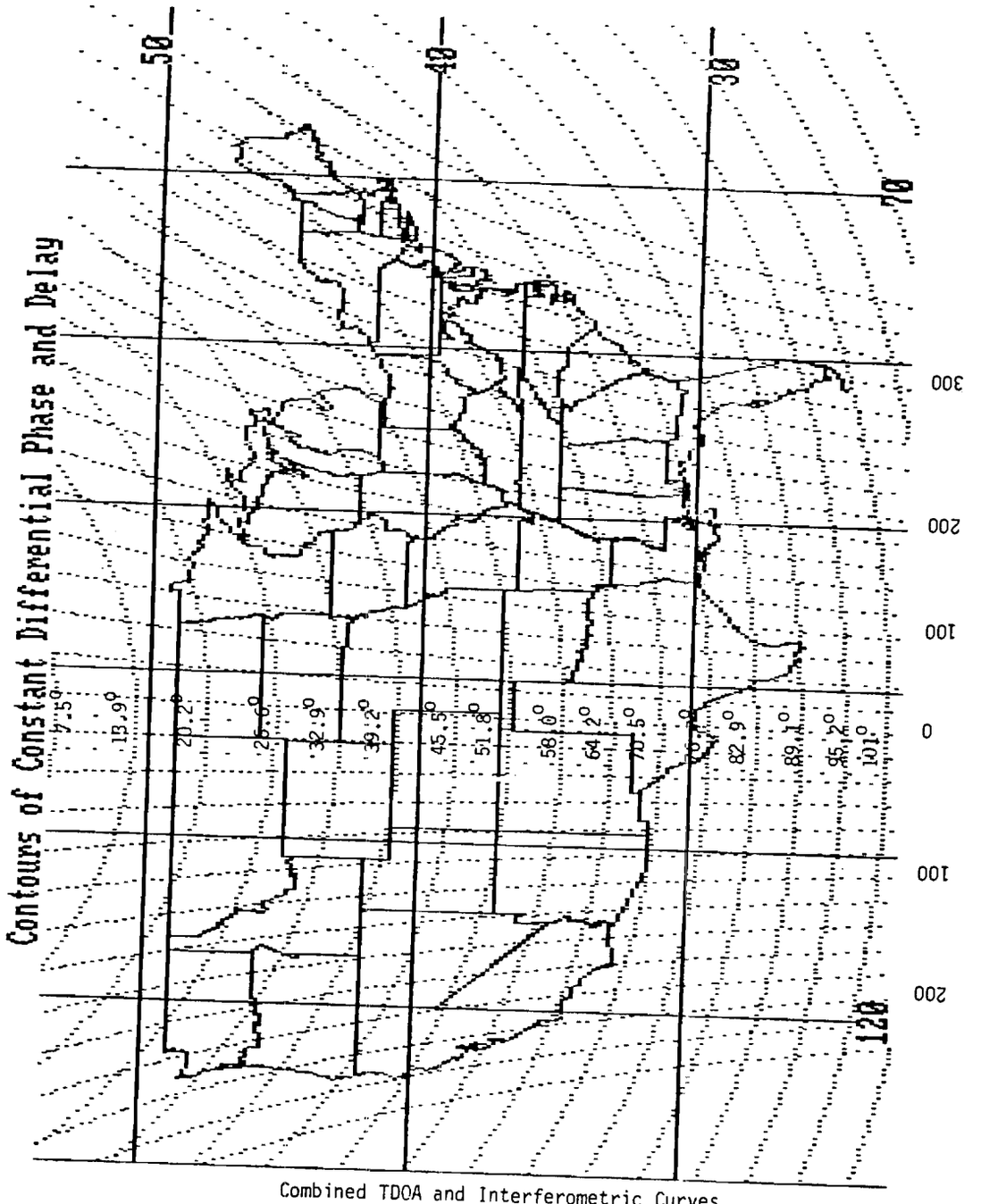

Combined TDOA and Interferometric Curves
Figure 1.9

antenna feeds aboard GSTAR 1. The combination of these two methods has the added advantage of requiring only two satellite paths and provides for locating the source of signals regardless of their purpose without disrupting normal communications through the spacecraft or requiring any additional spaceborne hardware.

Because the GTE Spacenet Corporation sponsored most of this research and GTE allowed the Georgia Tech investigators the use of much equipment and their GSTAR series of satellites, most of the examples and experiments presented herein are oriented around the use of the specific satellites GSTAR 1, GSTAR 2, and GSTAR 3. These are polarization re-use, repeater-type, Ku-band, geosynchronous United States domestic communications satellites located at longitudes 103, 105, and 93 degrees west respectively.

Both the Time Difference of Arrival and Interferometric techniques were successfully tested experimentally. The TDOA experiments were performed by measuring delays of "target-of-opportunity" signals. Because the interferometric tests required more elaborate signals and more complex processing schemes, a pair of experiments were performed using signals originating from Atlanta, Georgia and two GTE sites. The details of various experiments are discussed herein.

2. History

On 27 April 1986, someone operating under the title of "Captain Midnight" overwhelmed the Home Box Office commercial television C-band uplink signal between Hauppauge, Long Island and the geosynchronous Hughes Galaxy I satellite located over the Pacific at 134 degrees west longitude. The "Captain Midnight" incident [1-3] is relatively unique in that it received much press attention. However, intentional or inadvertent interference from man-made sources to satellite communications channels is a frequent occurrence. During the local evening television news time slots, one can find examples of poorly directed uplink radiation patterns from mobile satellite terminals striking more than their intended satellite target. In uplink transmitter hardware, radio frequency leakage into some intermediate frequency circuitry outside of the intended information passband may show up as unknown noise in an unintended satellite transponder. Many occurrences of illegal transponder usage also exist.

Most cases of interference may be corrected by taking action at the originating uplink station. However, a receiving station cannot typically determine the source of the uplink unless there is some easily demodulated and

identified artifact in the interfering signal. The satellite operators usually have no more information than an afflicted user, and an intentional jammer will not be trying to assist an identification effort.

The locations of unknown uplink stations are difficult to determine because of the wide range of potential locations of the interfering transmitters and because most satellite uplink stations direct their transmitted power away from the surface of the Earth, making detection with terrestrial receivers difficult except at relatively short ranges. Alternate approaches to location determination include detection from aircraft or low altitude spacecraft. Both share the difficulties of fairly long response times and extreme expense. The use of adaptive antennas aboard domestic spacecraft (i.e., movable "spot beams") either to locate the source of the unwanted signals or to minimize the effects of such signals is feasible, but requires the additional cost for spacecraft construction and launch [4]. The existing fleet of domestic satellites are not so equipped. The technique of physically moving a spacecraft so that the edge of its principle receiving beam scans past the undesired transmitter has been tried, but has the disadvantages of disrupting the traffic through other transponders on the same satellite and of consuming propellant [5]. Preferable are alternate techniques which

use the existing fleet of domestic satellites and require only a minimal disruption to normal spacecraft operation.

There are several possible signal processing methods for uplink station location which require no modification to spaceborne hardware. In cases where there is relative motion between the satellite and some combination of the receiver and transmitter, the knowledge of a satellite's orbital geometry and the propagation time changes or doppler shifts may be employed. Several satellites currently exist (i.e. the SARSAT series) whose mission is to find (by using doppler shifts) an activated Emergency Locator Transmitter (ELT) of the type carried aboard commercial aircraft. If the spacecraft has no motion relative to the receiver and transmitter as in the case of geosynchronous satellites, then remaining methods include the use of TDOA and interferometry as described above.

From investigations of the literature, Chestnut [6] appears to be the first to have discussed the TDOA method in the refereed press although he refers to other sources in his paper. To this author's best knowledge, single spacecraft short baseline interferometry was first described by Professor Paul Steffes of Georgia Tech in 1986. A short history of both the TDOA and interferometric methods follows with editorial emphasis on the underlying motivations of the participants.

In 1982, Chestnut [6] of ESL, Inc. (Sunnyvale, CA), proposed the Time Difference of Arrival method in the context of stochastic error analysis for a navigation system.

Richard Harris and Reed Burkhart of Hughes Aircraft released a TDOA "review package" dated 7 April 1986. The paper briefly discusses the TDOA method in the context of an interference locating system and primarily focuses on the error analysis presented by Chestnut.

In the Summer of 1986, Professor Paul Steffes presented a proposal for SILS research to Hughes Aircraft. They initially appeared to be interested in sponsoring research. However, their final response was negative. They stated that all external research had been halted after their corporate acquisition by General Motors.

In October of 1986, Professor Steffes and Smith presented a similar proposal for SILS research to the GTE Spacenet Corporation. GTE was interested and provided funding beginning in January 1987. This gave Georgia Tech access to GTE resources which include their various ground control facilities and their GSTAR series of Ku-band domestic geosynchronous communications satellites. The Georgia Tech Earth station facility had already been using the GSTAR series of satellites as part of the institute's regular AMCEE/NTU distribution of live and videotaped

technical classes.

Burkhart and Harris presented a reorganization of their 1986 TDOA review package as a conference paper [7] on 9 February 1987 in the context of a navigation system for providing an uplink operator's location with the implicit cooperation of the transmitting station and the employed transponder's owners. In their paper, the authors do not claim to have made any actual measurements and deal mostly with the error analysis in the style of Chestnut. The authors refer to the use of a third satellite to form another pair of signal paths from which a second set of terrestrial curves of constant differential delay may be determined whose intersection will contain the unknown uplink station. This discussion appears to imply that they had not made any actual measurements because the mathematical findings within this dissertation show that the intersections of these two sets of curves are almost tangential for useful adjacent satellite locations. The empirical discovery of the signal-to-noise levels on typical adjacent satellites as observed by the Georgia Tech researchers reduces the differential time measurement accuracy to a point where typical intersections of these two sets of noisy tangential curves can have intersections occupying not a well defined point but an area of thousands of square miles.

In the Spring of 1987, the Amateur Radio experimenter's publication, QEX, published plans by AMSAT president Vern Riportella to invoke a form of "Techno-Sports" which would include a determination of the location of an "unknown uplinker" employing doppler shifts through one of the OSCAR (Orbiting Satellite Carrying Amateur Radio) series of non-geosynchronous satellites. This author has since been contacted to model mathematically such an activity.

The June 1987 issue of Telecommunications magazine ran a short overview article by Dr. Michael J. Marcus of the FCC which discusses satellite security [4]. Marcus hints at ground electronics techniques for uplink locating but states, "There are legitimate reasons for avoiding public discussion of the technical details of these techniques..." This was written some time after an extensive telephone conversation in September of 1986 with Professor Steffes concerning satellite interference location techniques. Dr. Marcus led the investigation of the "Captain Midnight" incident during the summer of 1986.

In November 1987, Smith and Steffes submitted a manuscript concerning their theoretical and experimental Ku-band TDOA efforts to IEEE Transactions on Aerospace and Electronics Systems [8]. This paper included a discussion of the relevant theory, a closed form equation for determining the terrestrial curves of constant differential

delay, a system architecture description, and the Georgia Tech developmental system performance with an experimental case result consisting of oscilloscope photographs of propagation-delayed demodulated television using real unplanned signals, the computed possible locations, and the actual location of the signal source. After an unintentional delay in an associate editor's office, this paper was accepted for publication after peer review in the Spring of 1988 and published in March 1989. Note that this paper was presented as part of this author's Ph.D. Qualifying Examination on 1 April 1988.

The Georgia Tech researchers received a visit from the sponsor, Mr. Bill Kinsella of GTE Spacenet (McLean, VA), on 18 and 19 May 1988. Dr. Alireza Shoamanesh of Telesat Canada also appeared at Georgia Tech on Thursday 19 May 1988 with Mr. Kinsella. During the visit, Steffes and Smith demonstrated the Time Difference of Arrival method by blindly locating a San Francisco uplink station using signal paths through GSTAR 1 and GSTAR 2.

On 8 June 1988, a meeting consisting of representatives of the FCC, Georgia Tech (Professor Steffes), Hughes Aircraft, GTE Spacenet, AT&T, Intelsat, Comsat, and other satellite operating companies was held in Washington, DC concerning SILS activities. A decision was made to hold formal operating and technical meetings later in July. Mike

Marcus of the FCC verbally requested that Georgia Tech not publish information concerning satellite interference locating capabilities, giving as the reason his wish not to inform potential adversaries. The Georgia Tech investigators gracefully declined the censorship offer stating that the publication concerning the TDOA efforts had already been accepted by IEEE Transactions on Aerospace and Electronics Systems and that this research activity had been taken on only after written guarantees as to the freedom to publish all results were given.

The 22 July 1988 meeting, consisting of a similar group, presented two revelations. A restricted-distribution communication dated 29 January 1988 from Hughes to the FCC was revealed which included a report entitled "Transmitter Location System." This report describes the Hughes TDOA C-band experimental effort. Although Hughes did not appear to have achieved any better accuracy in their later geographical results as compared to that of the Georgia Tech team, they seem to have significant advantages in equipment, software, and manpower. Their experiments were performed under controlled conditions using large receiving reflectors and previously arranged uplink signals (video test patterns) from known uplink stations. The signals were processed digitally using Tektronix hardware and purchased software. In contrast, the Georgia Tech experiments used available

equipment and "targets-of-opportunity" which were discovered as various transponders of various satellites were examined.

In addition, the Interferometrics Corporation, which was represented at the meeting, released a report indicating their desire to build and maintain a SILS site which would perform TDOA measurements for the satellite operator community. They proposed an approach where direct pre-detection radio frequency correlation of the two incoming signals would be performed to determine the required differential delay. They claimed that this would have the benefit of better noise immunity in the presence of another transponder signal when compared to post-detection correlation. Direct RF correlation has been discussed at Georgia Tech, and the post-detection method of correlation was found to require less hardware and economic commitment, thus facilitating more rapid results. The key requirements for the former method involve the acquisition of sufficiently fast analog-to-digital converters or variable digital or analog delay hardware.

A paper entitled "Time Delay Techniques for a Satellite Interference Location System" by Smith and Steffes appeared in the March 1989 issue of IEEE Transactions on Aerospace and Electronic Systems [8].

On Tuesday 3 April 1990, Smith spoke with Reed Burkhart of Hughes at the National Association of Broadcasters

convention in Atlanta, Georgia. Mr. Burkhart told Mr. Smith that Hughes had presently ceased their pursuit of the TDOA method for financial and resource commitment considerations.

Most of this information has been gathered by discussions with members of the interested satellite operations community. Most parties who are interested in this subject tend to keep their information proprietary. An on-line abstract search (including the TECHDATA and Georgia Tech library databases) which accumulated more than one megabyte of keyword related abstracts failed to produce any other relevant documents.

To the knowledge of this author, there exists no available system which performs a similar signal source location function.

3. Time Difference of Arrival (TDOA) Techniques

The Time Difference of Arrival (TDOA) system is a technique by which the propagation time for the uplink signal to a particular satellite is compared with the propagation time to an adjacent satellite. Given that the positions of the two spacecraft relative to the receiving station are precisely known, the difference in time of arrival over the two different paths isolates the possible uplink transmitter location to a one dimensional curve on the Earth's surface. The key disciplines involved in the application of the TDOA techniques for locating Earth stations include geometry, RF link analysis, and signal processing.

Geometric issues include a determination of the relationship between the location of the receiving SILS site, the location of the primary and adjacent satellites, a measured differential delay between the signals traversing the two different paths, and a curve of constant differential delay. A set of equations which facilitate numerical generation of a geographic set of curves of constant differential delay as a function of satellite position were developed and are described below. Appendix A discusses the derivation of these equations, and Appendix B

lists a computer program for generation of various families of curves of constant delay.

RF link analysis issues include the determination that sufficient power and Carrier-to-Noise ratio (CNR) exist through both the primary and adjacent satellite signal paths to perform the desired differential delay measurement at a SILS receiver site. Receiving antenna dish sizes, typical transmitting antenna sidelobe strengths, and transponder loading become the important factors.

Signal processing issues involve the recovery of the differential time information between the two received signals. Possibilities include coherent versus non-coherent demodulation of an incoming RF signal, digital versus analog measurements of the time delay, and the practicality of the methods of choice.

3.1. TDOA Geometry: Terrestrial Curves of Constant Differential Delay

Whether friendly or not, the typical satellite uplink user is attempting to illuminate only one satellite at any one time. For several reasons, however, the uplink may be illuminating multiple satellites with enough power so that a receiving ground station may be able to detect the presence of the source station on adjacent satellites in addition to the uplink's goal satellite. Reasons for this include poor dish alignment procedures or equipment, a marginal antenna

aperture size which may not generate appropriately small beamwidths, sidelobes intrinsic to the uplink antenna, and a smaller apparent angle between satellites which are at low elevation angles relative to the uplink location. This last effect has been made more noticeable by the recent reduction of geosynchronous satellite spacing from three to two degrees.

The TDOA location method being presented depends on the ability to determine relative time delays due to the different lengths of two satellite signal paths as perceived by a receiving station. A curve on the Earth's surface containing the location of the signal's source may be determined given this time delay (which can be measured by simultaneously observing each of the two relevant satellites with receiving systems), the location of the receiving station, and the positions of the two satellites of interest. It is not unusual for satellite operators to know at all times the position of their satellites to within a few meters via the use of laser reflections obtained off cube-corner mirrors aboard the satellite or more typically from radio signal processing techniques.

The previously presented Figure 1.1 shows a two-dimensional view of the geometry pertinent to the TDOA technique. As illustrated, the positions of the two satellites, the location of the TDOA site, and thus the

distances from the satellites to the TDOA receiver site are known. The unknowns are the two remaining distances from each of the satellites to the unknown uplink station.

If the receiver site has two antennas connected to two receiving systems which can simultaneously monitor the signal through each satellite, a relative time delay between the two paths may be measured. Given this delay, a knowledge of the speed of the signal propagation through space, and the equivalent distance of any non-negligible signal processing time, the difference in path distances may be deduced. Subtracting out the known downlink distances and any other system offsets from the satellites to the TDOA receiver site leaves the remaining differential distance between the two unknown uplink distances. In the two-dimensional case, this differential distance determines two potential points for the location of the uplink station. These points are found by solving for the intersections of the Earth's circle and the two branches of the hyperbolas made from the two paths of equal length plus the inferred delay distance. Holding one arrival time as fixed and considering whether the other signal is leading or lagging this fixed time uniquely determines which of the two intersections is the uplink location.

Previously presented Figure 1.2 depicts the three-dimensional case. Only the unknown uplink portions of the

signal path need to be considered because the distances from the satellites to the TDOA receiver site are assumed to be known. As an extension of the two-dimensional case, the surfaces of constant delay between the satellites form a hyperboloid of two sheets centered along the axis of the line segment connecting both satellites and opening away from the segment's center point. The two intersections of these hyperbolic branch surfaces with the sphere of the Earth provide terrestrial curves of constant delay which include the location of the uplink station. As in the two-dimensional case, holding one arrival time as fixed and considering whether the other signal is leading or lagging this fixed time uniquely determines which of the two curves contains the uplink location. However, unlike the two-dimensional case, there is one less known input than is required to support the dimension of the desired solution. Therefore, the solution is one dimension higher than desired, and another piece of information is required to acquire a unique solution.

Figure 3.1 illustrates another viewpoint of the three-dimensional case where terrestrial curves of constant delay are determined by the locus of the intersections of concentric circles around the subsatellite points of the effected satellite pair. Let the radii of these subsatellite circles be determined by considering a general

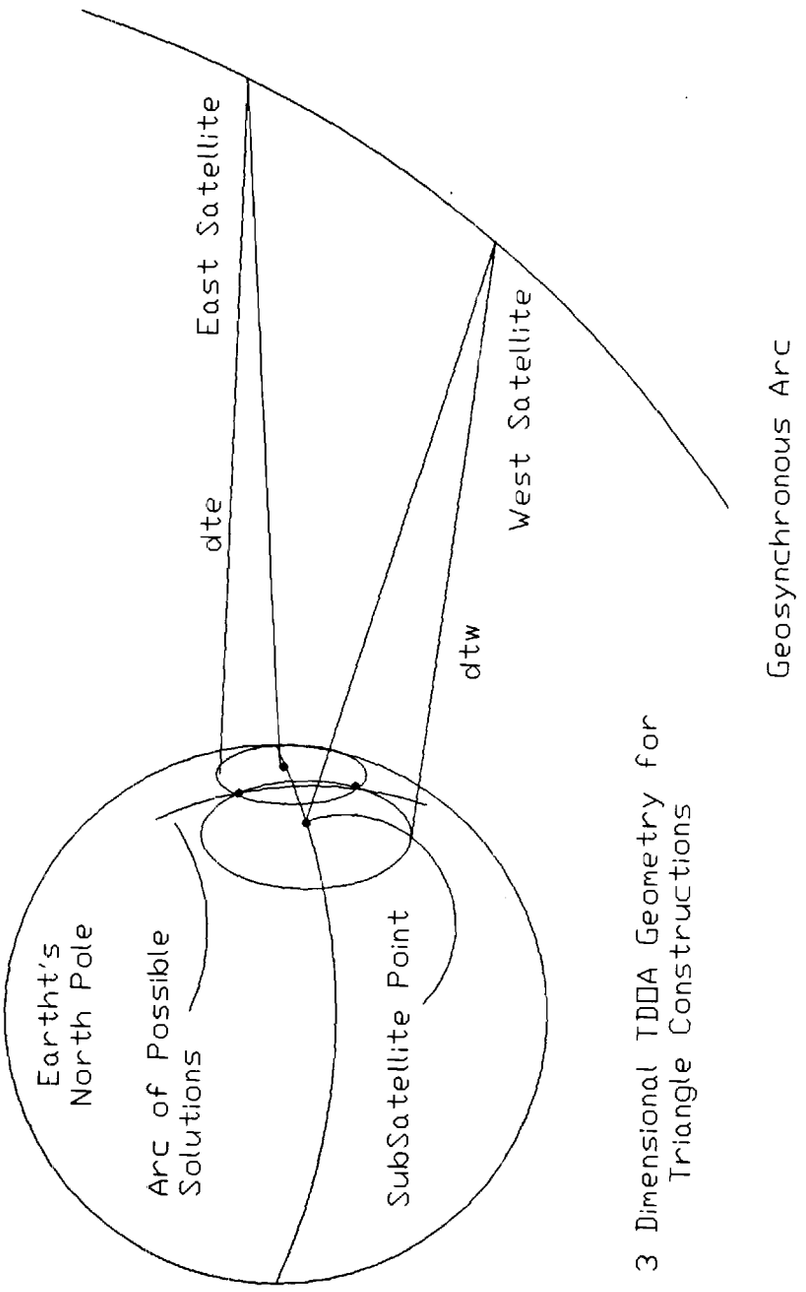

3 Dimensional TDOA Geometry for
Triangle Constructions

Figure 3.1

satellite-to-Earth distance (dte and dtw in Figure 3.1) which will be greater than or equal to the satellite-to-subsatellite point distance. Note that if the differential delay to the two satellites from a given uplink station is considered as a differential distance equal to the difference between the two uplink-to-satellite paths, then the uplink station must lie on the intersection of the two subsatellite circles.

From this construction, a family of curves of terrestrial solutions to the uplink location problem may be determined for various delays between satellite signal pairs. For a particular differential delay, the corresponding differential distance is computed. A reference uplink-to-satellite distance is then chosen. The other uplink-to-satellite distance is chosen to differ in length by the differential distance. A subsatellite circle is constructed for both distances. The intersections of these circles are a point or a pair of points on a curve of potential uplink locations for the given differential delay.

The entire curve is constructed by sweeping the reference uplink-to-satellite distance from its minimum at the subsatellite point to its maximum near the Earth's poles. The intersections form the entire curve for the given differential delay. A family of curves may be generated by performing this iteration over a number of

different differential delays.

In both the hyperbolic intersection and the subsatellite circle constructions, the goal is to relate time delay measurements and known geometric information to a curve along the Earth's surface which contains the unknown uplink's location. The subsatellite circle viewpoint for the three-dimensional case lends itself to a triangle construction which provides trigonometric equations that generate a latitude and longitude given a delay and the known geometric information. Details of this construction are discussed in Appendix A. Using a computer program similar to that found in Appendix B to sweep the appropriate variables generates a family of terrestrial curves of constant differential delay. Figure 1.4 showed these curves with 20 microsecond separation for GTE's geosynchronous GSTAR 1 (103 Degrees West) and GSTAR 2 (105 Degrees West) satellites projected onto a Mercator projection of the CONUS (CONtinental United States) area. Equations 3.1 through 3.4 relate the known geometry and the measured delay to a longitude and latitude for a fixed Earth-to-satellite distance. Sweeping over this distance generates one of the constant delay curves.

Equation 3.1

$$e = \arctan\left[\frac{\dfrac{(dtw^2 - r_p^2 - r_{sat}^2)}{(dte^2 - r_p^2 - r_{sat}^2)} - \cos(\,difflong\,)}{\sin(\,difflong\,)} \right]$$

[degrees]

Equation 3.2

Longitude =
  longe + e [degrees] if T>0 (Uplink west of satellites)
  longe - e [degrees] if T<0 (Uplink east of satellites)

Equation 3.3

$$Latitude = \arccos\left[\frac{r_p^2 + r_{sat}^2 - dte^2}{2 * r_p^2 * r_{sat}^2 * \cos(\,e\,)} \right] \text{ [degrees]}$$

Equation 3.4

$$T = (dte - dtw)/c \text{ [seconds]}$$

where:

longe = [degrees] Longitude of eastern satellite
longw = [degrees] Longitude of western satellite
difflong = [km] Absolute value of (longw - longe)
dte = [km] Swept distance from eastern satellite to eastern subsatellite circle
dtw = [km] Swept distance from western satellite to western subsatellite circle
r_{sat} = [42162 km] Radius of Earth geosynchronous orbit
r_p = [6378 km] Radius of Earth
e = [degrees] Intermediate offset longitude between subsatellite circle intersection and satellite longitude
T = [seconds] Differential time of arrival (Eastern Signal - Western Signal)
c = [2.997925×10^8 m/sec] Speed of Light

Assuming the use of the GSTAR 1 and 2 satellites, these equations, and subtracting out any additional delays for an arbitrary TDOA receiving location site, delays range over a magnitude of about 200 to 300 microseconds for the west and east coasts of the United states to zero along the western Great Plains beneath the satellites. Note that the latitude values should be takes as both positive and negatives as the resulting curves are symmetric about the equator. However, the antenna beam pattern GSTAR series satellites enforces only northern hemisphere service, therefore, the southern solutions would be unlikely uplink location candidates.

Note that the geometry of Figure 1.4 implies that the curves of constant delay associated with one pair of satellites would be almost tangential to the curves of another nearby pair of satellites for a large part of CONUS. Thus, the intersection from the TDOA curves of two nearby satellite pairs will not provide a high resolution solution due to the large areas of the intersections of terrestrial curves induced by signal noise. However, due to signal level constraints, any other satellite pair employed for TDOA measurements must be close to the primary satellite. Therefore, some technique other than this form of TDOA must be used to lower the dimension to a solution which uniquely locates an uplink station.

3.2 RF Link Analysis - Power Budgets

The satellite experiencing an interfering signal will usually be illuminated by an adequate amount of power to facilitate easy detection of the interfering signal (or else it would not be a interference problem). Therefore, the power critical signal path for TDOA purposes is that from the unknown uplink location through the adjacent satellite and back down to the SILS receiving site.

There are many possible scenarios by which a satellite may receive enough illumination to cause interference. An Earth station operator may incorrectly aim his dish antenna out of the plane containing geosynchronous satellites thus causing one or more satellites to experience his antenna's first sidelobe as he increases his transmission power. Most operators vary their output power level to adequately illuminate their target satellite to facilitate varying attenuation conditions. The antenna's pattern may be distorted due to mechanical distortions in the reflector or misalignment of the feeds at the reflector's focus. There also exist cases where there is inadequate illumination of an adjacent satellite for TDOA purposes.

The following example presents a simple link analysis for a typical scenario where GSTAR 1 is the afflicted satellite and GSTAR 2 is the adjacent satellite. This

example illustrates some of the points germane to TDOA operations. The goal is to determine how well a TDOA operator may be able to measure a delay from which he may infer a terrestrial curve of constant differential delay.

An operator in Atlanta, Georgia is using a Scientific-Atlanta Series 8060 6-meter antenna [13] in an attempt to saturate a Ku-band transponder aboard GSTAR 1 (103 degrees west) with a 32 MHz wide frequency modulated television signal. The antenna is correctly aimed at GSTAR 1 and needs an adequate amount of power at 14.25 GHz from its high power microwave amplifier to achieve the published [22] transponder input saturation flux density of -95.6 dBW/meter^2 at the satellite. (Although not realistic, this example assumes 100% efficiencies for all reflectors.)

Equation 3.5 [25] $$\text{Flux Density} = \frac{(\ \text{EIRP}\ )}{4 * \text{Pi} * r^2}$$

Equation 3.6 [25] $$\text{EIRP} = P_t * G_t$$

Where: P_t = Power from transmitter into antenna
G_t = Antenna Gain = 57.2 dBi @ 14.25 GHz = 524800
r = Distance to GSTAR 1 = 37369 km

Solving for power gives a required 9.2 watts or 9.6 dBW into the antenna and an EIRP for GSTAR 1 of 4.8 megawatts or 66.8 dBW.

To find the power level illuminating GSTAR 2 which is 2 degrees further west at 105 degrees longitude, one must

compute the sidelobe power levels emitted from this antenna. Part 25.209 of the Federal Communications Commission regulations [24] requires that a satellite uplink antenna have a sidelobe performance with emissions below an envelope defined by:

Equation 3.7 $$\text{Emitted Power [dBi]} = 29 - 25*\log(\theta) \quad \text{for } 1 \leq \theta \leq 7 \text{ [degrees]}$$

Scientific-Atlanta advertises that their 6-meter antenna meets or is better than this specification. Ignoring the slight angular offset due to parallax and assuming a worst case sidelobe performance at 2 degrees off boresite gives a power difference from the main lobe peak of 21.5 dB. Thus the apparent EIRP in the direction of GSTAR 2 is 45.3 dBW or 34 kilowatts which produces a flux density of 1.9 picowatts/m^2 or -117 dBW/m^2 at the satellite.

However, the absolute powers are less important than the link carrier-to-noise (CNR) ratios which determine the quality of the received RF signal. A CNR value should be contrasted to a signal-to-noise (SNR) value. A low CNR value may map into a higher SNR value for the communicated information content due to a processing gain achieved by a modulation or coding scheme such as the frequency modulation used to transmit television or voice through satellite

channels. CNR refers only to the final modulated RF carrier power to RF noise levels. CNR (which is a unit-less ratio as is SNR) may be defined as:

Equation 3.8 [25]

$$CNR = \frac{EIRP}{k} * L_p * \frac{G_r}{T_{eq}} * \frac{1}{BW}$$

where: k = Boltzmann's Constant = $1.379*10^{-23}$ W/K/Hz
= -228.6 dBW/K/Hz

G_r = Gain of Receiving Antenna
T_{eq} [K] = Equivalent Noise Temperature of the Receiving Antenna System
BW [Hz] = Bandwidth of Interest
L_p = "Space Loss" attenuation over distance from the Friis Transmission Equation if the transmitting and receiving antenna gains are removed and is given by:

Equation 3.9 [12]

$$L_p = \frac{(\text{wavelength})^2}{(4 * Pi * r)^2}$$

r = Distance (to GSTAR 2 = 37440 km)

At the uplink frequency of 14.25 GHz (wavelength = 2.1 cm) with GSTAR 2 being 37440 km from Atlanta, the "space loss" is found to be -206.8 dB from Equation 3.9. From this information, assuming a receiver bandwidth of 32 MHz, and the published G_r/T_{eq} of the satellite of 2.5 for Atlanta [22], uplink CNR is found to be -5.5 dB.

Downlink CNR is determined in the same way. The same model 6-meter dish with an equivalent noise temperature of

180 K is assumed to be used by the SILS receiving site which is also in Atlanta. The published gain of the aforementioned Scientific-Atlanta antenna is 55.9 dBi at the 12 GHz downlink frequency resulting in a receiver G_r/T_{eq} of 33.4 dB/K. The "space loss" for the downlink is a slightly different -205.5 dB due to the difference between uplink and downlink frequencies. Using the same bandwidth gives a downlink CNR of 2.6 dB. The uplink and downlink CNRs are combined (as are paralleled resistors) as shown in Equation 3.10 to give a total link CNR_T of -5.9 dB.

Combining Link CNRs

Equation 3.10 [25] $$(CNR_T)^{-1} = (CNR_{up})^{-1} + (CNR_{dn})^{-1}$$

As the noise is 5.9 dB stronger than the desired signal, this link CNR does not facilitate a differential measurement by observing a demodulated signal with an oscilloscope. Intuitively, one would observe only the channel noise floor were one to view this received signal with a spectrum analyzer. Inserting such an FM signal into a slope demodulator will produce only noise at its output. A typical extended CNR threshold satellite television receiver requires a CNR of at least 8 dB before it can lock onto the signal.

Fortunately, the SILS site need not recover the entire

modulated signal. The SILS requirement for TDOA is only that some time discernible feature of the signal be detectable for cross-correlation or direct delay observation.

The previous link analysis assumes the SILS site is attempting to recover the full 32 MHz wide frequency modulated television signal. If this goal is abandoned and only a 4.5 MHz portion of the signal is accepted via the use of bandpass filters, then a total link CNR of 2.4 dB is achieved.

Although the entire television signal is no longer available, this is not as great a loss as one may initially believe. A NTSC signal contains much timing information. The 15.75 kHz horizontal synchronization pulses and the 60 Hz vertical frame retrace information should be easily detectable by tuning through various portions of the original 32 MHz signal.

This reduced passband may now be slope demodulated to produce a signal which is visible on an oscilloscope or available to a cross-correlation device. This demodulated adjacent satellite signal may now be compared with the easily demodulated primary satellite signal for delay measurement purposes. Measurement of delays within television signals is particularly easy because of the consistent features available in the timing information.

Such measurements were successfully performed on a variety of television signals as is discussed throughout this dissertation.

3.3 Signal Processing

Signal processing issues involve the recovery of the differential time information between the two received signals. Possibilities include the demodulation of an incoming RF signal, digital versus analog cross-correlation to measure a time delay, and the practicality of the methods of choice.

The method chosen to perform the signal demodulation employed a pair of available HP 8558B spectrum analyzers to slope demodulate frequency modulated carriers such as satellite television or audio SCPC signals. Slope demodulation is facilitated in these devices by halting the sweeping of the local sweep oscillator and manually tuning it to the edge of the signal of interest. Thus any frequency modulation would show up as the amplitude information which drives the Y-axis of the spectrum analyzer's display. Such analyzers have ports available which provide voltage outputs proportional to the Y-axis information. Thus the slope demodulated information is available in analog form. The variable baseband and IF filters within these spectrum analyzers also facilitate a

manual ease of tuning. For these reasons, the spectrum analyzers were used as demodulators for this investigation.

Determination of differential time delays between signals traversing different satellite signal paths is required when using the TDOA method for locating uplink stations. The delay measurements were performed by manually observing the two spectrum analyzer demodulated time domain signals on an oscilloscope. This process and the ambient conditions which vary substantially require that the equipment operator be quick and completely aware of his job. To be more responsive to the realities of the end goal, attempts were made to employ computer correlation to provide the differential time measurement.

3.3.1 Cross-correlation: Digital Signal Processing Techniques

A commercially available Metrabyte analog-to-digital (ADC) converter accessory board was installed in a Hewlett Packard Vectra microcomputer (an IBM PC/AT compatible computer). This system sampled each of two channels at a rate of 25 kilosamples/second/channel (or a single channel at 50 kilosamples/second). A fixed length frame of analog samples was taken from each channel and correlated in software to produce a time domain graph where the maxima indicates the time of best correlation. The time of this

maxima corresponds to the differential time delay.

Cross correlation was performed by a "Turbo C" program which directly evaluates Equation 3.11 over the acquired data frames.

Cross Correlation Equation

Equation 3.11 $$c(T) = \sum_{\forall t} [\, x(t) * y(t+T) \,]$$

where: x, y acquired data frames
c resulting data frame
T index of delay

Performing this correlation required about 32 seconds on the computer using a frame length of 1024 samples with a dynamic range of 12 bits/sample.

The reader may notice that a more rapid response can be obtained by multiplying in the transform domain. (This is the equivalent of convolving the two incoming data frames if one of the frames is reversed in time.) The availability of data in the frequency domain would also provide the additional opportunity for employing various digital filtering techniques.

Figure 3.2 is a graph of a time domain "chirp" which is used as a input signal test pattern for the software. This 1024 sample frame has been auto-correlated to generate Figure 3.3. Figure 3.4 is an actual sampling of a slope

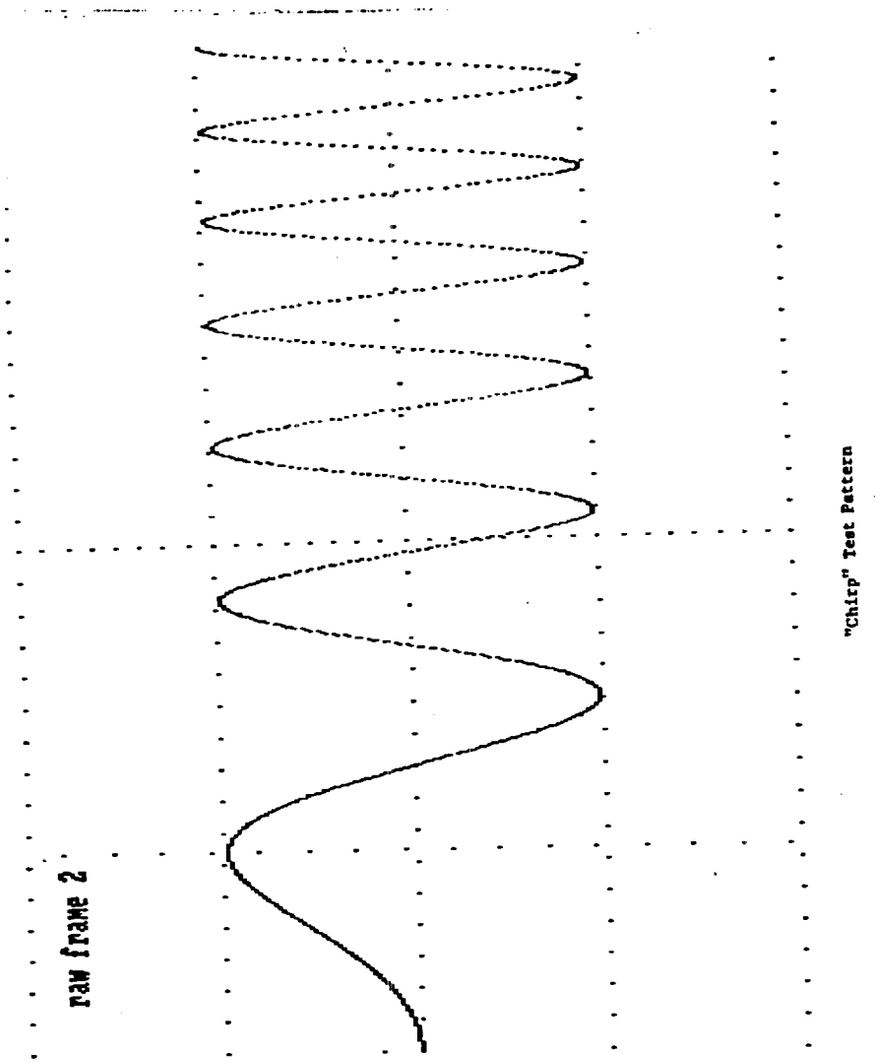

Digitized Chirp Test Signal
Figure 3.2

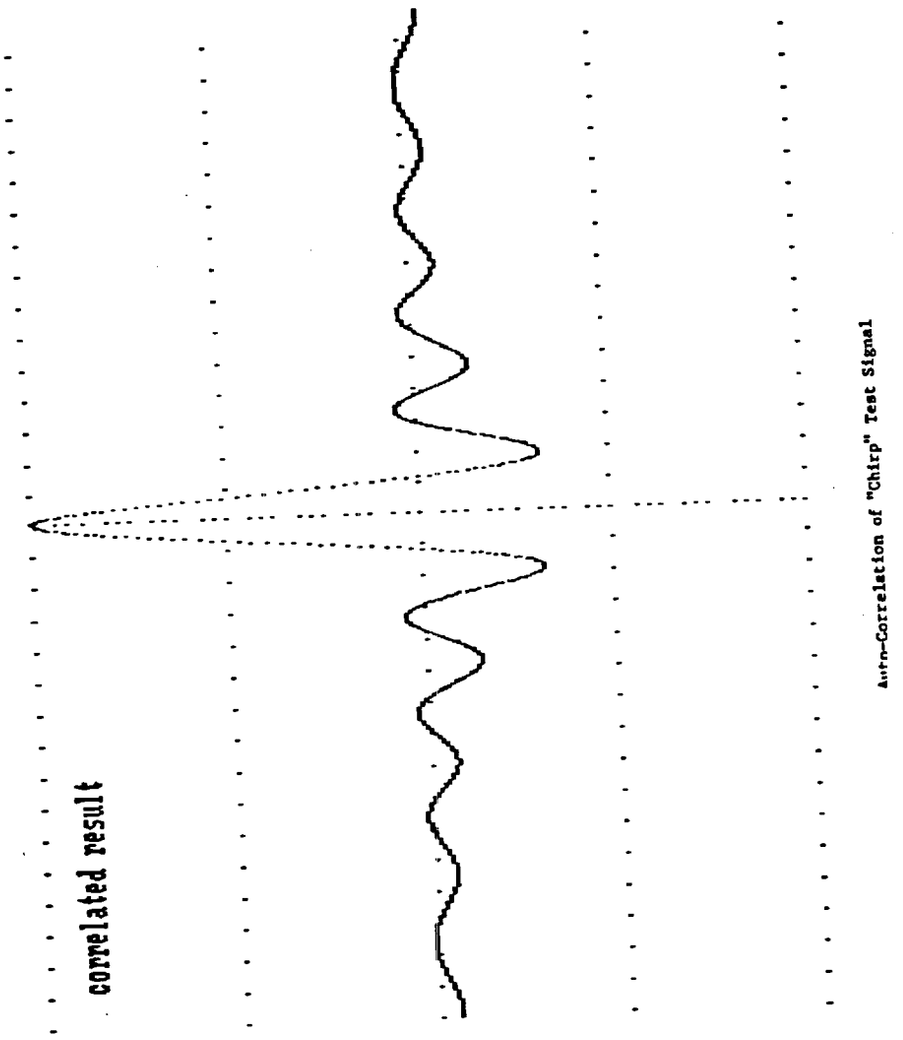

Auto-Correlated Chirp Test Signal
Figure 3.3

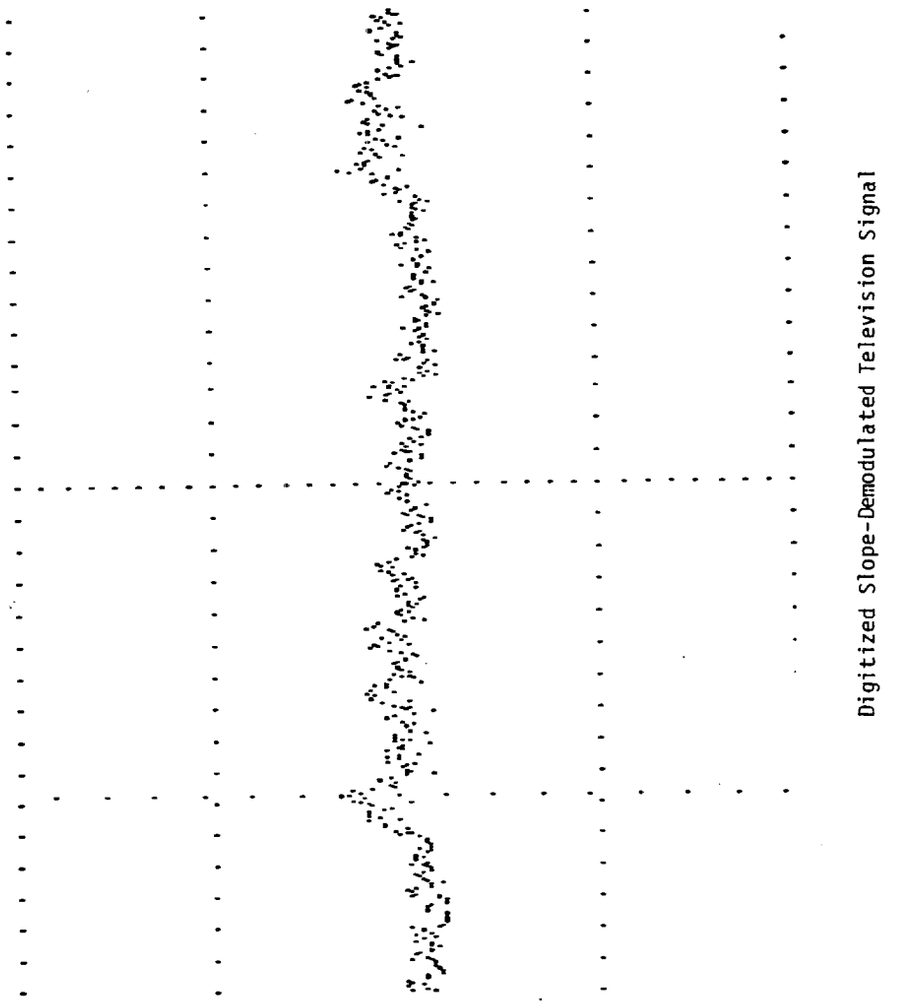

Digitized Slope-Demodulated Television Signal

Figure 3.4

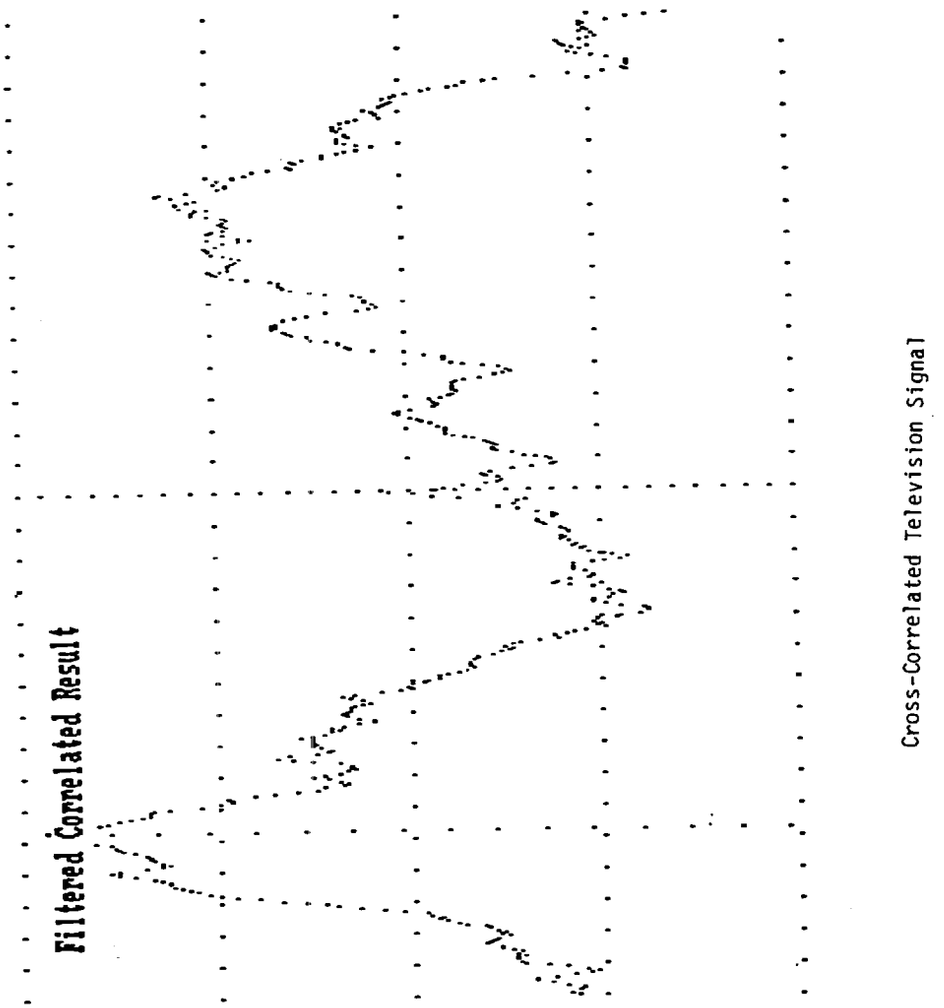

Cross-Correlated Television Signal ---------
Figure 3.5

demodulated satellite FM television signal which had a received CNR of approximately 10 dB. The picture content consisted of a color-bar test pattern. In this case, the sample frame length was 512 samples acquired at a rate of about 50 kilosamples/second. Note the two local peaks in the sampled signal which correspond to the 60 Hz vertical retrace portion of the NTSC video signal. Another frame was immediately sampled. These two frames were cross-correlated to produce the data of Figure 3.5. Note that the distance between the two peaks corresponds to the length in time of one television vertical retrace interval. As one would predict, successive television frames are interpreted similarly by the cross-correlation software.

In the context of observing satellite channel video signals, the 25 kilosamples/second/channel sampling rate is adequate to determine relationships between video frames. However, a much faster sampling rate than this is desired to determine the differential time delay measurements to the microsecond resolution (within individual video lines) required to acquire useful spatial TDOA results. Although speeds of up to 50 kilosamples/second/channel may have been acquired by implementing DMA techniques on the available hardware, the desired 100 to 1000 kilosamples/second rates require specialized hardware.

As such resources were not easily available and human

observations of oscilloscope displays provided a simple method for delay measurement, it was decided that work in this area will be pursued at a later time.

3.3.2. Cross-correlation: Analog Signal Processing Techniques

There are also several analog options for performing the cross-correlation function to determine the desired delay value. An analog cross-correlator may be realized by mixing two incoming signals where one of the signal paths contains a variable delay element. The DC component of the mixer output would peak as the variable delay was set to equal the actual delay between the signals. Were this to be done with the incoming RF without any form of demodulation, nulls would appear at every half wavelength. However, the voltage peaks would contain the desired cross-correlation information. A simple analog peak detector circuit with a discharge time constant appropriate to the delay sweep rate could provide a voltage related to the desired cross-correlation output.

The problem with this approach is constructing the delay circuit. Variable delay times of from -500 to +500 microseconds are required. Although dual-in-line-pin (DIP) package lumped element or transmission line delay devices are economically available in the tens of nanosecond ranges, their inherent distortions do not allow them to be cascaded

for the required delay lengths. Two other solutions are switched lengths of transmission line and surface acoustic delay devices.

Switched lengths of coaxial cable could produce the required delay. However, RG-58 50 ohm coaxial cable, which has a typical velocity factor of 66% (Belden 8259 [23]), would require a 99 km cable length to achieve a delay of 500 microseconds. This is obviously not a useful solution. Although a similar length of optical fiber requires a volume of less than a cubic meter, either type of cable would be expensive and present substantial amplitude losses.

Another method to realize such delays employs surface acoustic wave (SAW) delay devices. Also realizable as filters, these devices transform an incoming electrical waveform into a mechanical wave which propagates through a material medium at speeds substantially less than that of light. There may exist multiple taps for transforming the mechanical waves back into electrical signals at various distances from the input launching point thus realizing a multiply tapped delay line. The delay and phase distortions of SAW devices are well characterized by their manufacturers. The Sawtek Corporations sells a series of devices which would be useful in this application. Although these devices cost between $10 and $100 in single quantities, they better facilitate a compact electronic

design as their package size is less than that of a 40 pin DIP IC package.

3.4. Experimental Apparatus and Procedures

The choice was made to use Ku-band signals transmitted through GTE's GSTAR 1 and GSTAR 2 satellites for the differential time delay measurements because of the availability of these satellites through the courtesy of the GTE Spacenet Corporation. Two sets of Earth station receiving facilities located atop the Electrical Engineering building on the Georgia Tech campus were used for the experiments. One included a 6.1 meter Harris reflector with appropriate feeds for simultaneous transmission and reception of a standard Ku-band signal set as shown in Figure 3.6. A 180 K Harris 6312 low noise block converter (LNB) amplified and shifted the incoming signal from Ku-band down to a C band IF (3.566 to 4.066 GHz) from which the Harris 6531 receiver produced a 70 MHz IF and FM demodulated baseband NTSC video and audio. The second receiving system employed generic Ku-band TVRO components. It includes a smaller fiberglass 3.1 meter reflector, a 180 K LNB converter which converts to the TVRO industry standard "L band" IF of 950 to 1450 MHz. From here, a Drake model ERS 324S receiver generated a 70 MHz IF and demodulated baseband video and audio.

Although digital or analog correlation allows

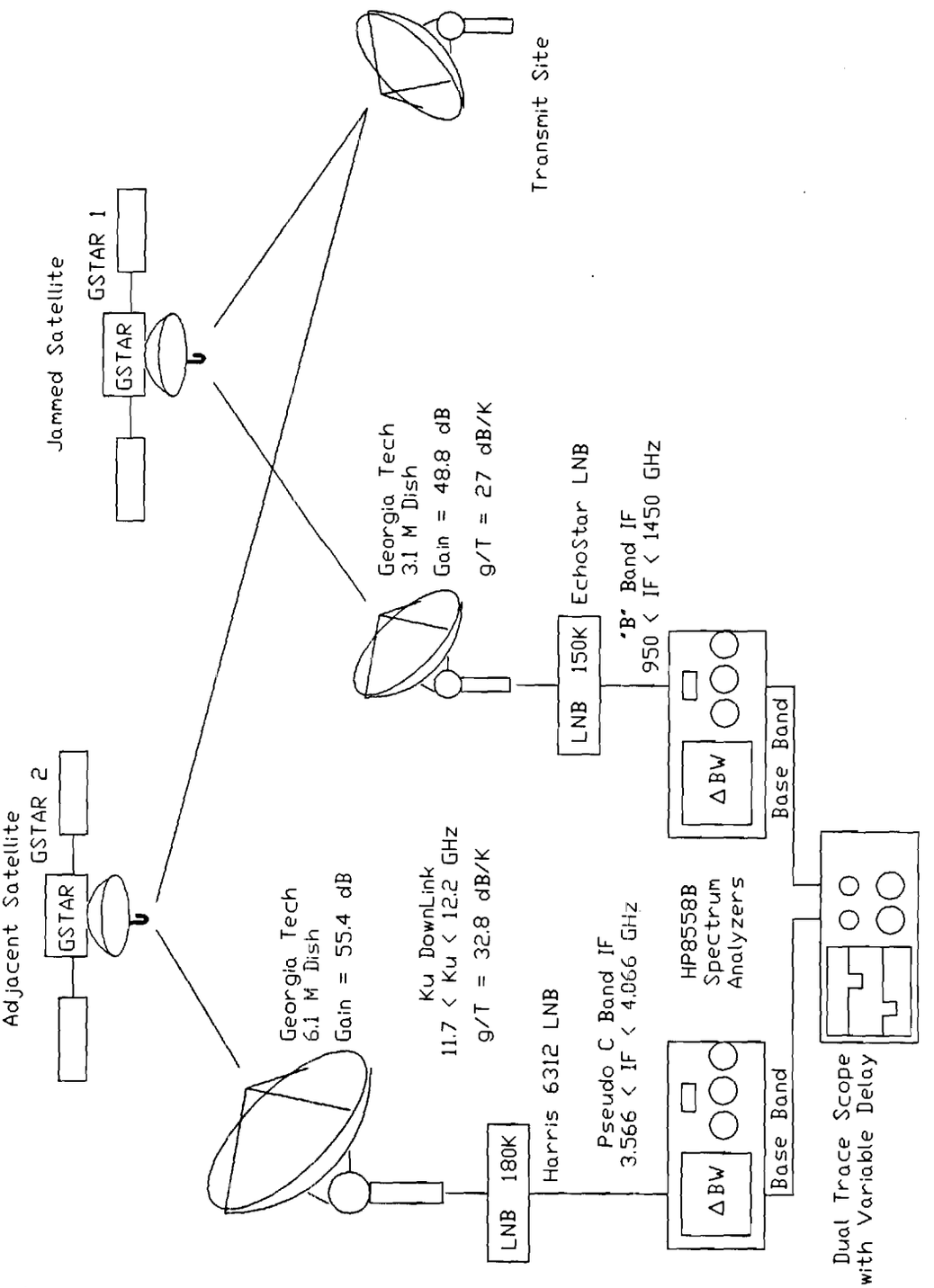

TDOA Developmental System
Hardware Configuration

Figure 3.6

measurement of the time displacement between pairs of most types of signals, a dual trace oscilloscope was chosen to view a pair of wideband FM television signals. Reasons for the use of TV signals included the variety of available source qualities and locations, the ease of demodulation, and the time domain features of an NTSC video signal. The use of the oscilloscope provided real time feedback to those performing the measurements. Demodulation and low level signal detection was performed by using two HP 8558B spectrum analyzers as slope detectors. These devices provided great flexibility in the degrees of freedom which they allow a user such as variable IF bandwidths from 3 kHz to 3 MHz, variable baseband lowpass filtering, IF frequency centering control, and logarithmic or linear amplitude demodulation.

Figure 3.6 shows the equipment configuration for the time delay measurements. The spectrum analyzers take the 70 MHz IF signals from both receivers and provide a baseband signal by using the analyzers' internal IF bandpass filter to perform slope detection of the frequency modulated video signal. The relevant characteristics of the baseband output are a function of the selected bandwidths of the analyzers' IF and baseband output filters.

Many signal pairs have been observed with this equipment configuration. The best results have been sourced

by remote evening news transmissions from mobile satellite terminals. These signals are uplinked from vehicles equipped with microwave transmitters and a reflector of minimal aperture size which is quickly erected, activated, and aimed upon arrival at the news site. Many times this is done too quickly as real time observations through multiple satellites confirm. Antenna misalignment, multiple sidelobes, a large main beam due to a small aperture size, or a "road-weary" dish contribute to signals appearing on transponders of adjacent satellites.

The Georgia Tech operators searched with the 3.1 meter system for a potential signal through GSTAR 2 which took the role of the primary satellite. Although any received video signal was available for full demodulation and viewing on a studio monitor, this was done only to ease and confirm signal acquisition. If a potential candidate was found (this was confirmed by viewing the content of the signal), searching began with the 6.1 meter system on the output of the corresponding transponder on GSTAR 1 which was only 2 degrees away on the geosynchronous arc and becomes the adjacent satellite. If the operator was fortunate and the GSTAR 1 transponder was not heavily occupied, he returned to the GSTAR 2 signal and used a spectrum analyzer to slope detect the RF video signal. This baseband output was fed to a Tektronix 2215 dual trace oscilloscope and was used as the

trigger source. The spectrum analyzer's IF and baseband filters and center frequency tuning were then optimized to facilitate the cleanest triggering of the oscilloscope. Next, the GSTAR 1 transponder's spectrum was searched for any vestige of the spectrum viewed through GSTAR 2.

Generally, there were many vestiges of frequency modulated video to be found. Potential ripples in the GSTAR 1 transponder spectrum being searched were slope detected by another spectrum analyzer, then routed to the other channel of the dual trace oscilloscope for visual correlation. With the oscilloscope's sweep rate set to show about one horizontal NTSC line (64 microseconds) on the trace containing the signal from GSTAR 2, the presence of another video signal in the noise from the GSTAR 1 trace was readily detectable. If the GSTAR 1 video signal was not from the same source as the GSTAR 2 video signal, then one observed relative drifting of the synchronization pulses between the two video signals due to different time base sources. But if clock rates were close and the user believed that he was viewing the same signal through both receivers, then reducing the oscilloscope's sweep rate to about one vertical period (1/60 second) showed the relative positions of the vertical retrace fields. If the fields were not nearly perfectly aligned, then these were two different signals because the maximum delays expected were on the order of

hundreds of microseconds. However, if the same signal was being viewed through both satellites, one would have observed no apparent drifting over time between the two signals, and a vertical retrace observation would have shown a maximum vertical sync field misalignment of only a few horizontal lines.

Adjacent satellite signal observations have included the barest vestiges of signals plucked from the noise of busy transponders with the skilled use of IF and baseband bandwidth and tuning controls. But other observations have included signals which were more than 4 dB above the noise floor on empty transponders, thus almost reaching a typical satellite receiver's direct FM demodulation threshold.

Figure 3.7 (Photo 1) shows an oscilloscope photograph of two differentially-delayed signals for the specific case of television station KARE's remote evening news uplink from Mankato, MN (50 miles southwest of Minneapolis), taken on 6 August 1987 at about 6:20 p.m. EDT. Note that the GSTAR 1 signal can be seen to be about 7 microseconds ahead of the GSTAR 2 signal with the sweep rate of 10 microseconds per time division. However, due to the repetitive nature of the horizontal lines, the delay could differ by an integer number of horizontal line periods. Figure 3.8 (Photo 2) shows that the vertical retrace intervals were indeed close to alignment with the sweep rate set to 2 milliseconds per

Photo 1
(Figure 3.7)

10 uSec/Div

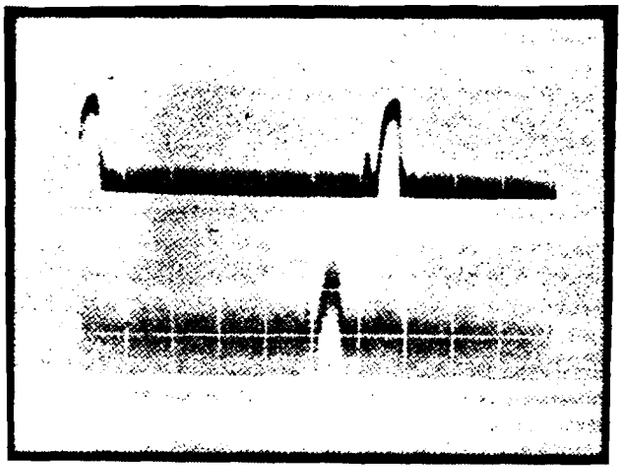

Photo 2
(Figure 3.8)

2 mSec/Div

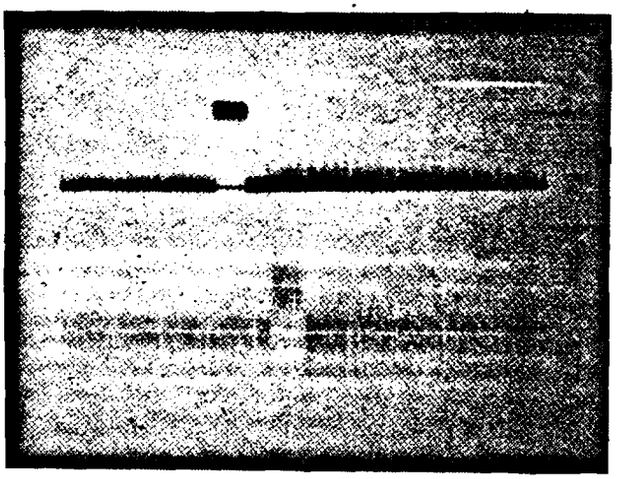

Photo 3
(Figure 3.9)

300 uSec/Div

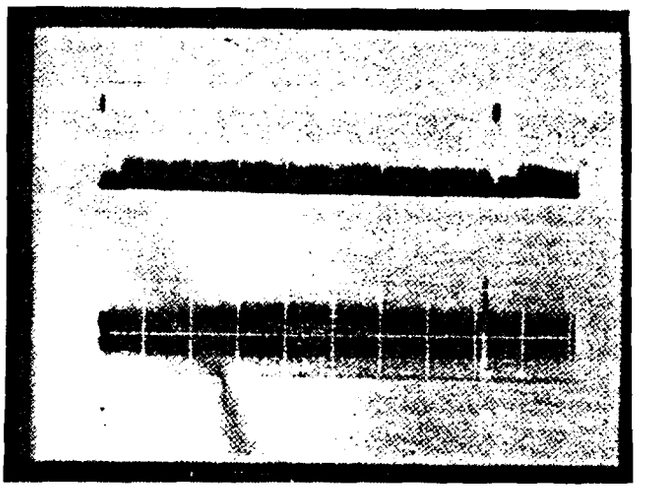

Oscilloscope Photographs for TDOA Example
Figures 3.7, 3.8, and 3.9

time division. Figure 3.9 (Photo 3) shows a close up view of the transition from vertical retrace pulses to video line sync pulses (about 300 microseconds, given 200 microseconds per time division). This compares favorably to the analytically computed delay of about 339 microseconds from Mankato, MN which includes the satellite-to-Atlanta differential delay. Note that a delay of 235 microseconds must be subtracted from this measured delay to remove the fixed differential delay specific to the Atlanta, Georgia receiver location. Table 3.1 lists calculated time delays for a variety of locations within CONUS.

Table 3.1: Calculated Delays within CONUS

Site		Distance to GSTAR I [km]	Distance to GSTAR II [km]	Differential Distance [km]	Differential Time [uSec]
Atlanta	GA	37369.5	37440.2	-70.7	-235.8
Van Buren	ME	38996.0	39091.6	-95.6	-318.9
Seattle	WA	38411.2	38358.7	52.5	175.2
San Deigo	CA	37148.8	37110.8	48.0	160.1
Dallas	TX	37012.1	37038.8	-22.6	-88.8
Greenbay	WI	38049.8	38098.2	-48.5	-161.7
Detroit	MI	38014.6	38079.9	-65.3	-217.8
Mankato	MN	37914.3	37945.1	-30.8	-102.8

Differential Time = time of arrival of (eastern signal - western signal)

3.5 TDOA Results

3.5.1 Mapping of Measurement Error

Because the delay measurement is a non-deterministic value with its own set of statistics, this random variable may be mapped from the measurement domain into the desired geographic contour domain. To do this in a mathematically rigorous form, the functions describing the mapping from the measurement to the geographic domains are required. Although these are given for computational purposes in Equations 3.1 through 3.4, they are non-linear and do not facilitate an easy mapping of the random variable's statistics.

The following example is included to facilitate an intuitive understanding of the relationship between the measurement statistics and the geographic consequences. After a series of measurements and data reduction, a typical TDOA delay measurement may be considered to be a gaussian random variable with a particular mean value of 235 microseconds with a standard deviation of 10 microseconds. Mapping this measured mean and the sum and difference of the standard deviations gives the three geographic contours shown projected onto the map of Figure 3.10. The enclosed area may be considered to be the statistical first sigma region for this particular measurement.

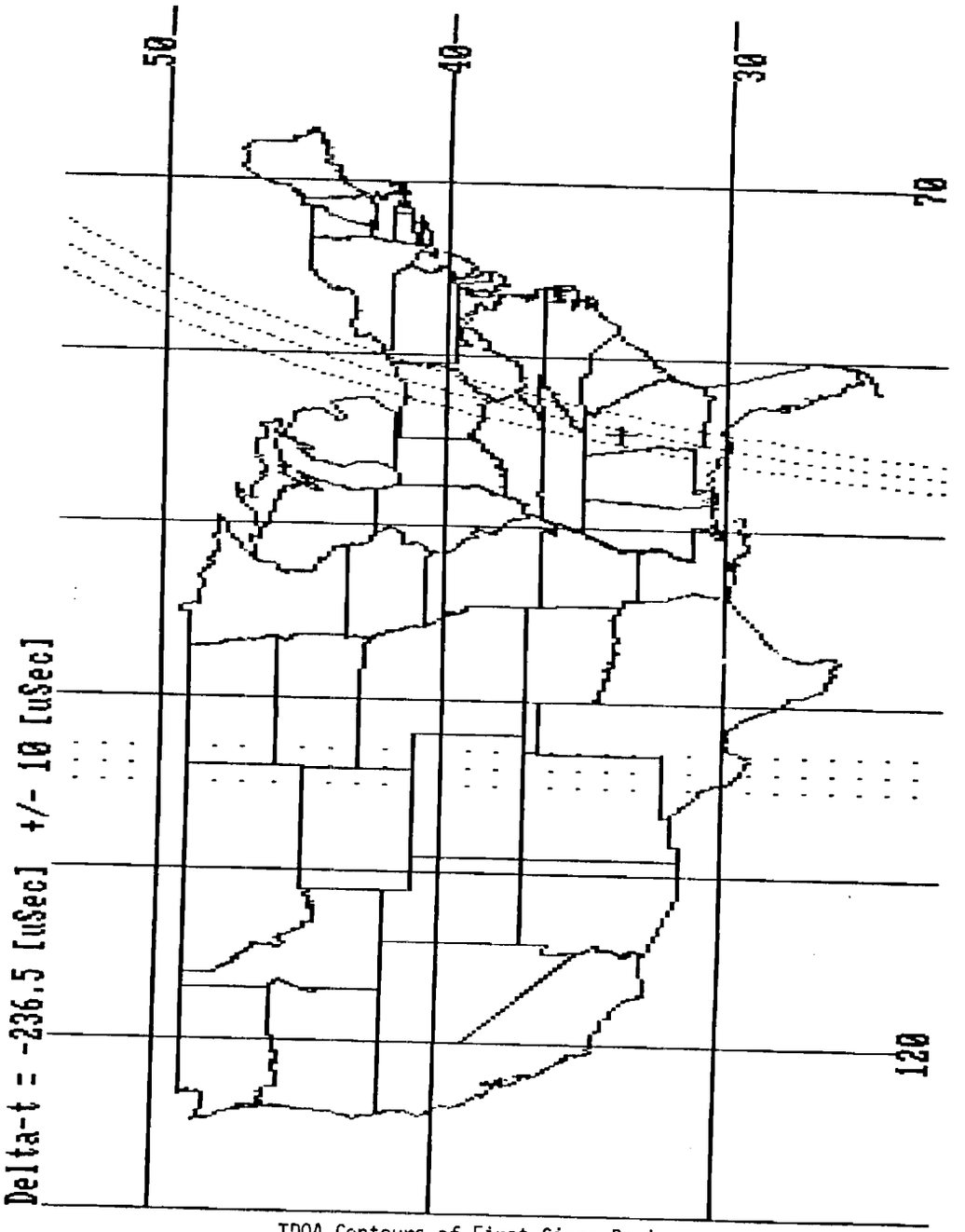

TDOA Contours of First Sigma Region
Figure 3.10

The literature provides several theoretical bounds for differential time and phase measurement accuracy as a function of signal-to-noise levels (for example [10-11]). Therefore, a determination of worst case CNR for a specific hardware configuration can be related to geographic error. One must note that CNRs will depend on site specific parameters such as antenna reflector sizes, amplifier noise levels, and phase and delay measurement hardware techniques.

3.5.2 Geographic Error versus CNR

Table 3.2 presents an empirically derived relationship between carrier-to-noise ratio, delay measurement error, and CONUS geographical error. This information was empirically derived because of the difficulty in mathematically manipulating the inherent non-linear mappings of noise statistics through the slope demodulation technique and the mapping from differential delay to a terrestrial curve of constant differential delay. Smith and Steffes [8] derived this relationship between adjacent satellite carrier-to-noise ratio (CNR) and geographical error across the center of CONUS specific to the Georgia Tech TDOA hardware. The table lists this relationship between adjacent satellite carrier-to-noise ratios, the measured differential time delay error, and the approximate east-west geographic error across a latitude of 40 degrees north which is about the

center of CONUS. This table was generated by taking a known frequency modulated television signal with a carrier-to-noise ratio of greater than 15 dB (high CNR) and comparing a slope demodulated copy with another attenuated (low CNR) then slope demodulated copy. These measurements were performed using the same equipment and the same procedure by which the differential time delay measurements were made.

Table 3.2

Empirically Derived Differential Time and Geographic Error versus Adjacent Satellite Carrier-to-Noise Ratio

CNR	Observed Differential Time Measurement Error	Geographic Error Across Center of CONUS
dB	Microseconds	Miles
2.2	3	15
1.8	4	20
1.4	4	20
1.0	4	20
0.8	5	25
0.7	20	100
0.5	20	100
0.4	60	300
0.3	70	350

Note that these results depend on the oscilloscope observation method for performing the time delay determination. Should any hardware change be made, such as the use of analog or digital correlation to determine the

signal delays, the errors inherent in these methods would need to be characterized and then mapped onto the Earth's surface as described above.

3.5.3. Uplink and Downlink dish size relationships for link CNR

Equation 3.12 describes the relationship between link CNR and the interfering uplink transmitter and SILS downlink site reflector diameters. This is derived from measurements taken and assumes:

Worst case uplink reflector sidelobe compliance with the FCC 29-25log(θ) rule,
The strongest measured uplink signals originated from the minimum legal 4.5 meter dish [17],
Operation on Ku Band frequency pairs,
Uplink reflector efficiencies of 50%,
Linear operation of the adjacent transponder.
The adjacent satellite is 2 degrees from the primary satellite.

$$\text{LINK CNR [dB]} = 10 \log\left\{\left(\frac{289 * L_t}{d_t * p_t^{1/2}} \right)^{2.5}\right\} + 10 \log\left\{\left(\frac{Pi * d_r}{L_r} \right)^2 * p_t\right\} + 58.2$$

Equation 3.12

where: d_t = uplink transmitter reflector diameter
d_r = downlink receiver reflector diameter
p_t = efficiency of uplink antenna
p_r = efficiency of downlink antenna
L_t = transmitting wavelength
L_r = receiving wavelength

Table 3.2 lists the link CNR for various dish diameters assuming 50% reflector efficiencies at both Earth stations

and the appropriate Ku Band frequencies.

Conclusions from Table 3.3 and Figure 3.11 include the intuitively appealing notion that the detectable signal threshold occurs when the downlink reflector diameter approaches that of the uplink reflector. However, closer inspection of the equation shows that the uplink station will eventually have the advantage as dish sizes increase. Equation 3.14 relates the 0 dB CNR level for Ku Band frequencies for reflector sizes in meters with 50% efficiencies.

Equation 3.14

$$\frac{d(xmit)^{2.5}}{d(recv)^2} = 2.9$$

Table 3.3: CNR vs Uplink and Downlink Reflector Diameters
(This table is derived from from Equation 3.13)

Diameter in meters	D(uplink) 4.5	6.1	7	11	13	20
D(down)						
3.1	-1.9	-5.2	-6.3	-12	-13	-18
4.5	1.4	-1.9	-3.4	-8.4	-10	-15
6.1	4.0	0.7	-0.8	-5.7	-7.5	-12
7	5.2	1.9	0.4	-4.5	-6.3	-11
11	9.1	5.8	4.3	-0.6	-2.4	-7.1
13	11	7.3	5.8	0.9	-1.0	-5.6
20	14	11	9.5	4.6	2.8	-1.9
	Above Demodulation Threshold			RF Detection		Not Detectable

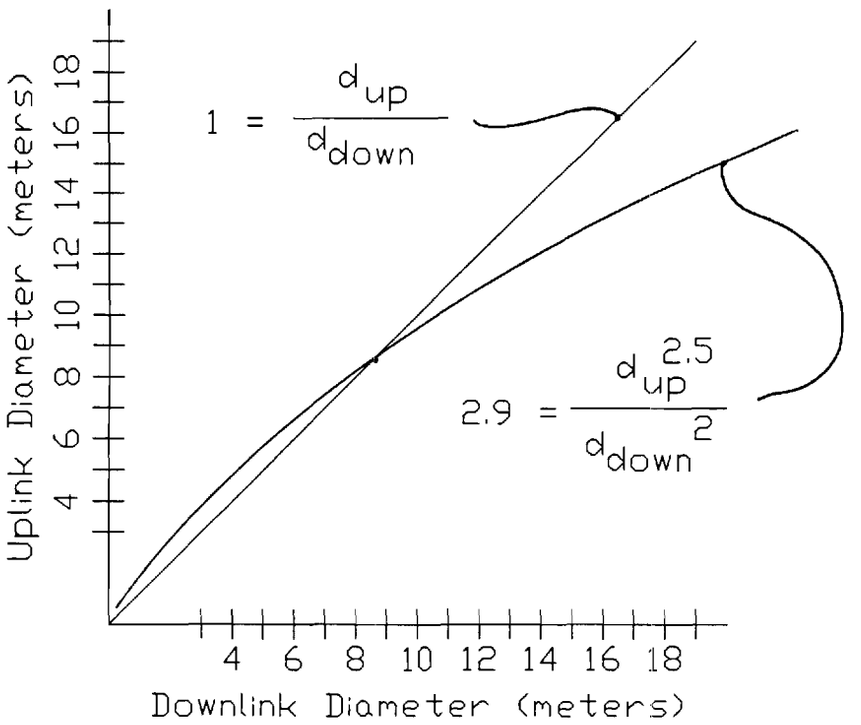

Graph Relating
Uplink and Downlink
Dish Diameters

Figure 3.11

4. Interferometry

Polarization re-use is a typical method employed in the satellite industry for doubling the available bandwidth of a given allocated frequency band. Typical domestic communications satellites use orthogonal linear polarization to achieve this doubling of capacity. To suit this end, there exists a pair of cross-polarized multi-horn beam-forming antenna feed assemblies at the focus of a typical satellite reflector antenna assembly. These feed assemblies are spatially offset from each other by a few inches.

Because of uplink antenna system imperfections or less than optimal operation of a transmitting site, uplinked radiation arriving at the intended satellite typically has some measurable cross-polarization component. Strong cross-polarization video transmissions were observed by the Georgia Tech investigators. Occasionally these signals were strong enough to facilitate direct demodulation.

The use of the offset dual polarization feeds aboard the GSTAR series satellites facilitates the measurement of the differential phase of a received signal between these two feeds which are connected to separate satellite transponder inputs. These cross-polarized signals are independently relayed to a SILS site via the orthogonally

polarized downlink channels. A differential phase measurement referenced to the satellite antenna feeds is then performed. This measurement is related to geographic solutions corresponding to possible uplink locations. A map of CONUS with calculated curves of constant differential phase for GSTAR 1 appears in Figure 4.1.

As discussed in the introduction, the theoretical issues for the interferometric method of uplink location include geometry, RF budget analysis, and signal processing. The geometry has been determined as a closed form expression which allows the generation of terrestrial curves of constant differential phase given the known position of a satellite, the known spatial locations of the dual polarization offset transponder antenna feeds, and the measured electrical phase. This relationship is illustrated in Figure 4.1 using curves of constant differential phase for GSTAR 1 at Ku-band frequencies overlaid upon a Mercator projection map of CONUS. Because there are a multiplicity of difficult-to-determine fixed phase shifts throughout the system, offset corrections are best implemented after calibration with signals from several known terrestrial sources.

The RF link analysis issues include determination of the signal level of each of the two polarization components in question into the satellite antenna feeds, the

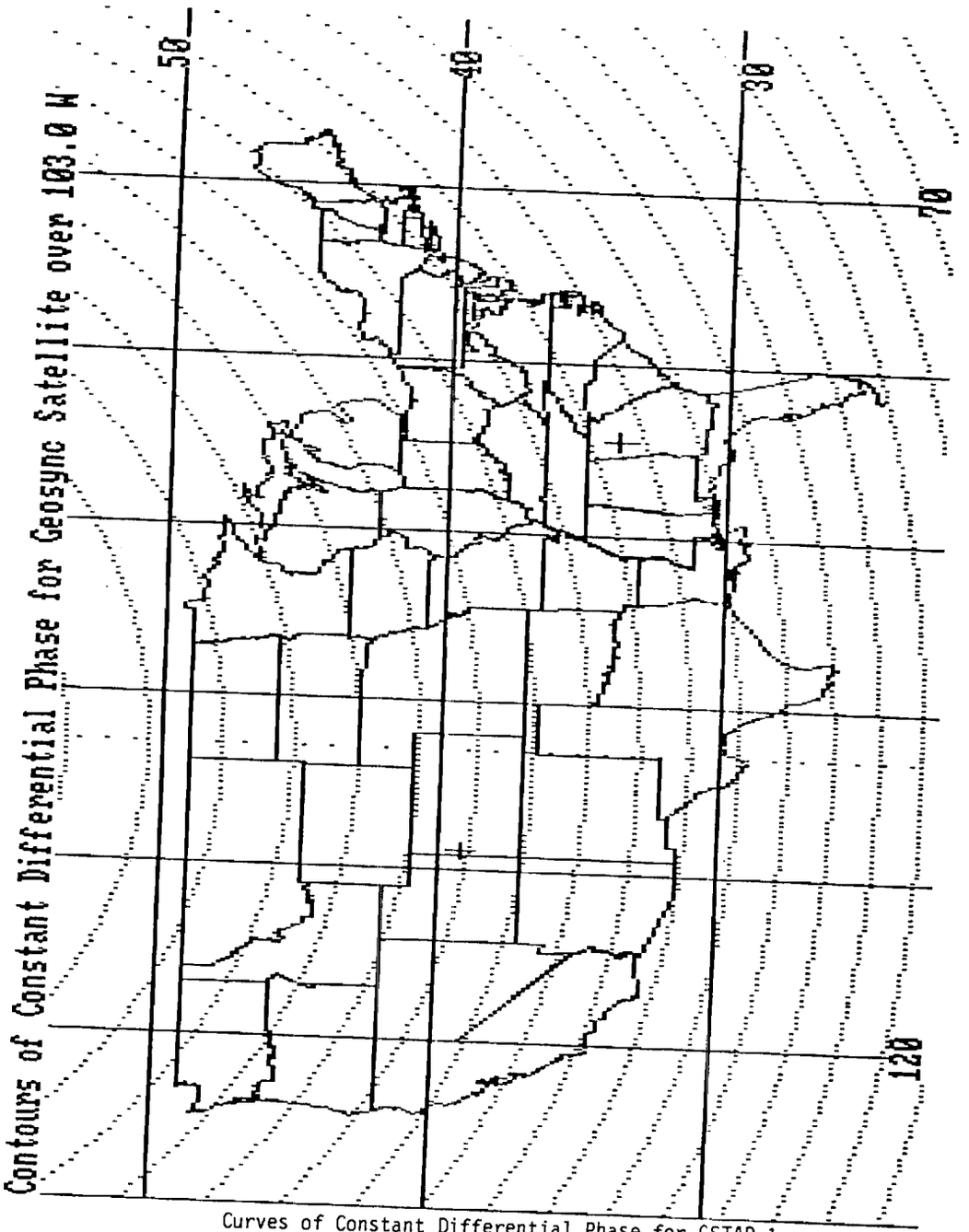

Curves of Constant Differential Phase for GSTAR 1
Figure 4.1

polarization isolation of each component of the system, and the phase stability of all components between the satellite received antenna feeds and the SILS site receiver outputs.

Signal processing issues involve the recovery of the carrier differential phase information as measured between the two cross-polarized feeds aboard the afflicted satellite. Although a simple mixing process between the two received cross-polarized channels would appear to produce a voltage related to the desired value, there are other effects for which there must be an accounting. Ku-band signals are typically uplinked at about 14 GHz then down-converted within the satellite to a downlink frequency of about 12 GHz. A pair of independent 2.3 GHz local oscillators are used for each polarization's set of 8 transponders on the GSTAR series of satellites. Because these oscillators are not locked to each other, the frequency shift in the spectra on the horizontal polarization's signals will rarely be exactly the same as the shift in the vertical polarization's signals. Calibration of the system to compensate for this net frequency offset requires the introduction into the transponder's passband of a reference carrier which is sourced from a cooperating and known site.

4.1 Geometry

4.1.1 Locating the Satellite's Interferometric Baseline

To employ the interferometric SILS method, the location of the interferometric baseline must be known. For the most general geometric case, one should know the three dimensional locations of the two orthogonally polarized phase centers of the receiving antennas onboard the satellite of interest to determine absolutely the location of the baseline. The mechanical diagrams for the GSTAR spacecraft show the receiving horns for each polarization to be in the spacecraft's XZ plane. This is the plane which contains both a line connecting the satellite and the subsatellite point and Earth's spin axis. Thus, the interferometric baseline must lie in the spacecraft's XZ plane that intersects Earth as the line of longitude above which the spacecraft resides. This is shown in Figure 4.2.

This terrestrial interpretation of the plane containing the interferometric baseline and the resulting contours of constant differential phase will change if there is any significant rotation of the spacecraft. However, since this condition would imply a catastrophic failure of the satellite system, such angular displacements are not anticipated.

Once the interferometric baseline is restricted to a

plane, only a single angle need be deduced. This was determined by learning the locations of the phase centers for each of the cross-polarized receiving horns aboard the spacecraft. This was done by reviewing the original GSTAR series antenna assembly mechanical drawings. However, phase offsets between channels are induced not only by the spatially displaced phase centers but also by the different signal paths through the satellite RF hardware, ground receiving RF hardware (which may change with experimental configuration), and through different downlink propagation paths which may change with time. Since it would be difficult to determine these phase offsets in an open loop fashion given the spacecraft mechanical configuration, it would be better to calibrate out these offsets by transmitting signals from known terrestrial sites through the spacecraft so as to determine the actual angle of the interferometric baseline.

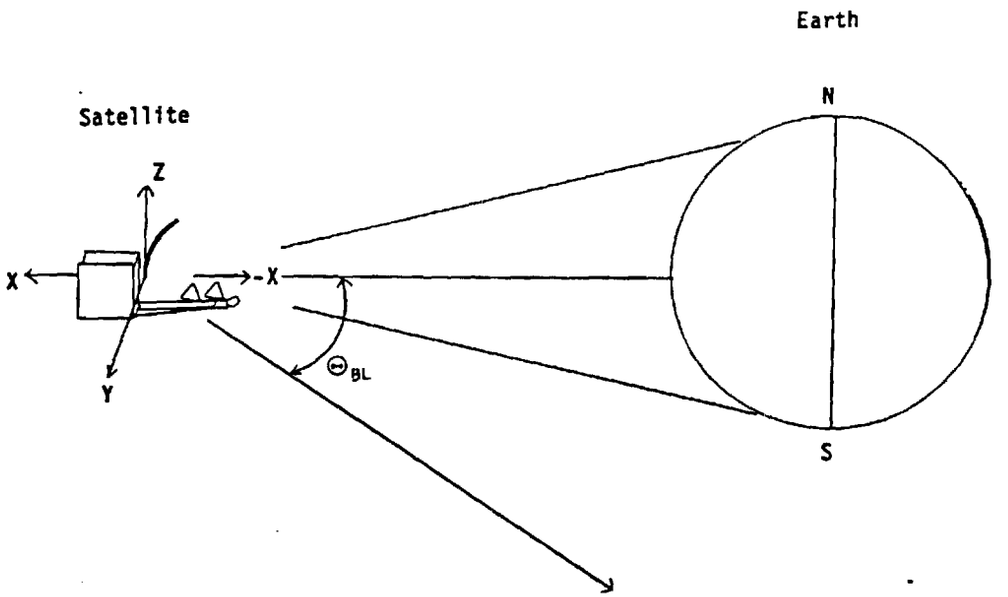

Location of Interferometric Baseline in Spacecraft XZ Plane

Interferometric Baseline in the Spacecraft XZ Plane

Figure 4.2

4.1.2 Terrestrial Curves of Constant Differential Phase

The relationship between measured electrical phase of signals at the GSTAR satellite feeds and possible uplink locations has been determined. Figure 1.7 shows the geometry relating the angle of a signal incident upon a GSTAR series satellite (and its associated interferometric baseline) to the desired terrestrial curve. Note that this geometry will change for a satellite with a different antenna feed configuration. Previously presented Figure 4.1 shows the desired result which illustrates curves of constant electrical differential phase across CONUS. This should be contrasted with previously presented Figure 1.4 which shows similar results for the Time Difference of Arrival method.

4.2. RF Link Analysis

The RF power budgets for each of the two signal paths of interest to the interferometry technique are similar and equally significant to that for the TDOA technique. However, the isolation between the two cross-polarized signals which traverse the cross-polarized paths from the "interfering" uplink station to the satellite and then to the SILS receiving antenna is a dominant factor in determining the realizability of the interferometric method. Therefore, experiments were performed to determine the

acceptability of the polarization isolation.

4.2.1. Cross-Polarization Isolation Experiment

One requirement for the proper operation of the interferometric system is that the unknown uplink signal contains some detectable cross-polarized component. Likewise, one must determine that the differential phase which is measured is actually due to imperfections in the polarization purity of the uplink in question. To be confident of this, the polarization purity of the other locations in the system where some polarization impurity may be introduced must be determined. Sources of cross-polarization impurity include:

1) The unknown uplink (desire impurity)
2) The satellite receive antenna (desire impurity)
3) The satellite transmit antenna (desire purity)
4) The SILS Site receive antenna (desire purity)

The satellites of interest typically employ a single antenna system for both the transmitters and receivers. Therefore, the desired purity of the satellite transmitting antenna will induce the same in the satellite receiving antenna if they are the same hardware. Thus, the most desired polarization impurity would be in the unknown uplink transmission system.

Experiments were developed to determine the polarization purity of the various portions of the hardware available to produce an interferometric system. They

involved the use of signals of various polarizations sent through various combinations of transponders some of which did or did not have an associated cross-polarized transponder.

As an example of a signal sent through two collocated (in frequency) cross-polarized transponders, Figure 4.3 shows a plot of relative received signal strength versus the polarization of the Georgia Tech Harris 6.1 meter receiving system. The signal strength was measured in dB above the local noise floor for a video signal feature downlinked through GSTAR 1 transponders 5 (horizontal) and 12 (vertical) at approximately 11950 MHz. Even when using a HP8558B spectrum analyzer's lowest resolution signal power scale to observe the Georgia Tech Harris 6531 receiver's 70 MHz IF output, the cross-polarized signal remained detectable in the "polarization null" which is 90 degrees from the desired polarization. In this case, it was desired that the observed cross-polarized component originate in the uplink's antenna system. Results from single transponder experiments with CW signals allowed determination of the polarization isolation for various portions of the system.

One can argue that the satellite antenna's polarization purity will be the best for the Georgia Tech experiments because of the offset reflector with polarization grid design which is employed in the present GSTAR series

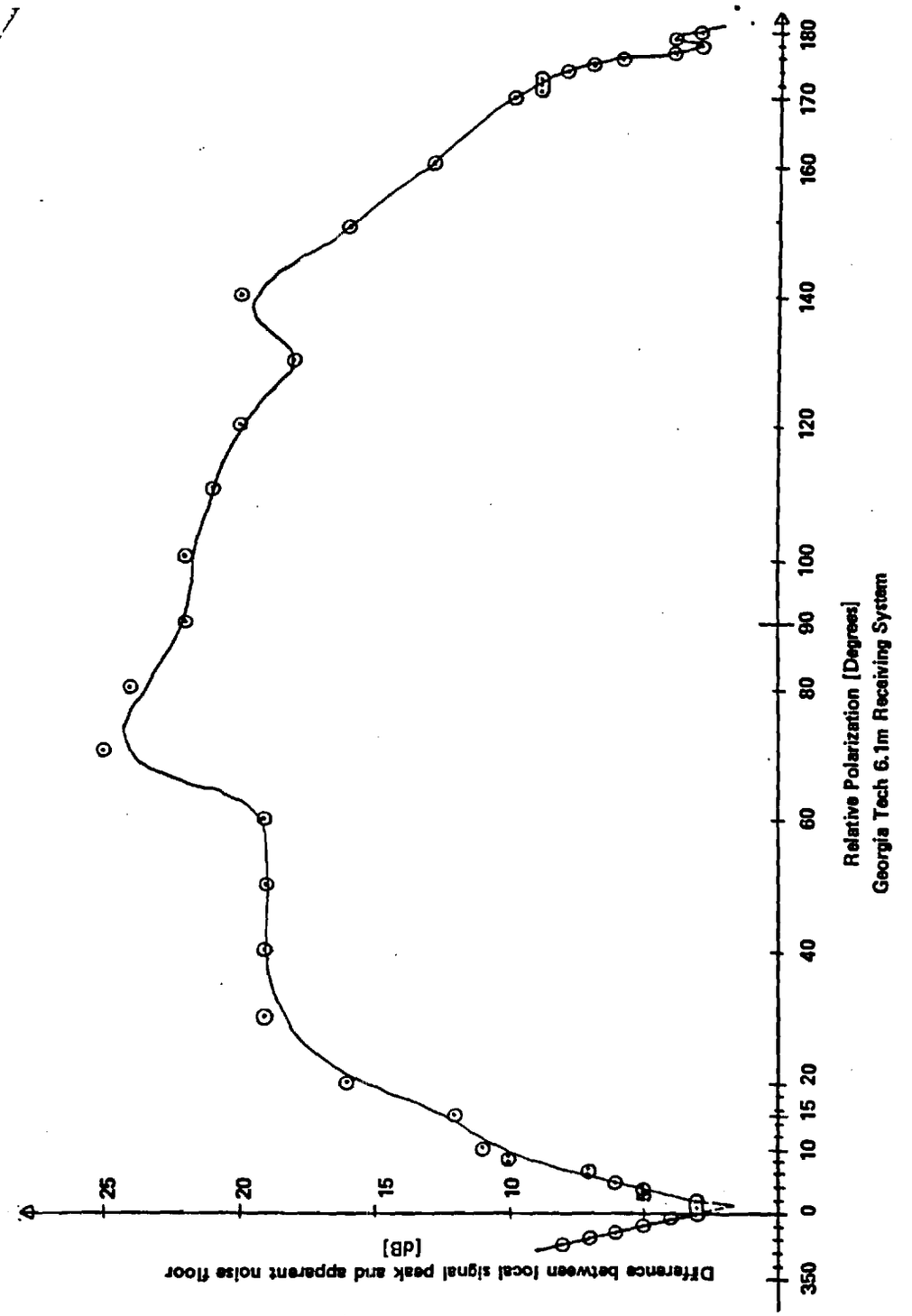

Georgia Tech 6.1m Antenna Polarization Purity Plot

Figure 4.3

satellites. The Georgia Tech Harris Delta Gain antenna also boasts a high degree of polarization purity [17] because of its unique feed design. However, a series of measurements were made which were designed to determine the polarization purity of the different parts of the available hardware.

An experimental goal was to test the satellite and the local SILS site receiving antenna's cross-polarization characteristics with the assumption that a carrier sourced by GTE's Tracking, Telemetry, and Control (TT&C) station had the best polarization purity in the system. To test the local antenna, it was necessary to guarantee that there existed no significant cross-polarization component radiating from the satellite. Therefore, a signal was uplinked into a portion of a transponder which shares no overlapping cross-polarized transponder. Once the local antenna's polarization characteristics were determined, the GTE sourced carrier was moved in frequency to a portion of a transponder passband which shares an overlapping cross-polarized transponder to observe the satellite receiving antenna's polarization purity. No signals originated at Georgia Tech because transmitter feed polarization and receiver feed polarization cannot be independently adjusted with the Georgia Tech system.

These polarization purity measurements were made by measuring received CW signal powers with the Georgia Tech

6.1 meter reflector system for various polarization rotations of the Georgia Tech antenna during four hours on 11 May 1988. GTE's Colorado TT&C station first transmitted a set of CW signals received at 12193 MHz with polarization angles of 0, 30, 60, and 90 degrees from the nominal satellite input polarization through a portion of transponder 16 on GSTAR 2 which has little overlapping cross-polarized transponder throughput. This set of transmissions of various polarizations was repeated at a received frequency of 12157 MHz which is in a segment of transponder 16 that overlaps cross-polarized transponder 8. Figure 4.4 shows the relationships between the transponder frequency band plan and the carrier frequencies employed.

Plots 1 through 8 (Figures 4.5 through 4.12) illustrate the received CNR levels for four TT&C polarization rotations through the overlapping and non-overlapping transponder passband segments. Although there were some problems with leakage of a cross-polarized component in the supposedly single channel portion of the transponder 16 passband due to the realistic filter characteristics of transponder 8, the results were as expected. CNR levels were measured by observing the difference in dB between the noise floor and CW signal peaks on a HP8558B spectrum analyzer which monitored the 70 MHz IF output of the Harris 6531 satellite receiver. The IF bandwidth of the spectrum analyzer was set

to 100 kHz. The Harris receiver's AGC system was temporarily defeated to facilitate impeding receiver induced changes in the observed noise floor.

The critical results are related to the depths of the notches in Plot 1 and Plot 4 (Figures 4.5 and 4.9) which respectively illustrate the cases of single transponder carrier transmission for a best aligned (co-polarized) uplink station and a worst aligned (cross-polarized) uplink station. For the scenario where power is transmitted from

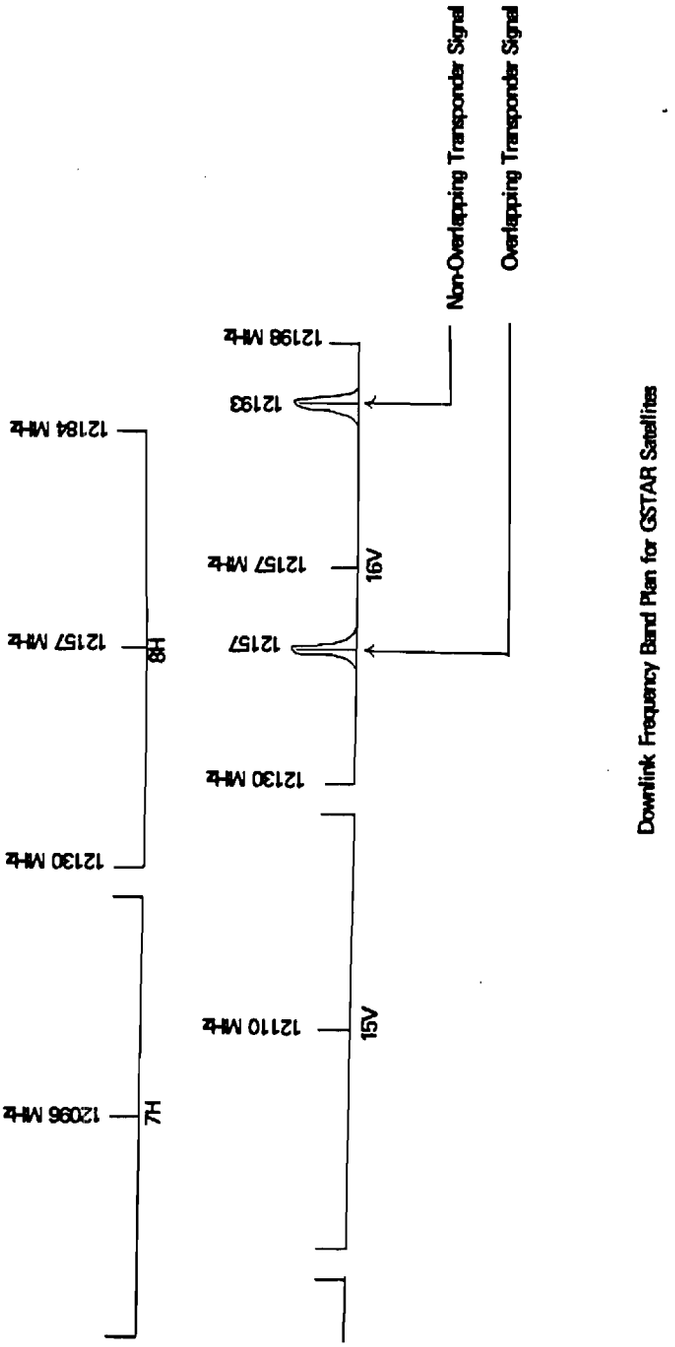

Satellite Polarization Purity Experiment Frequency Plan
Figure 4.4

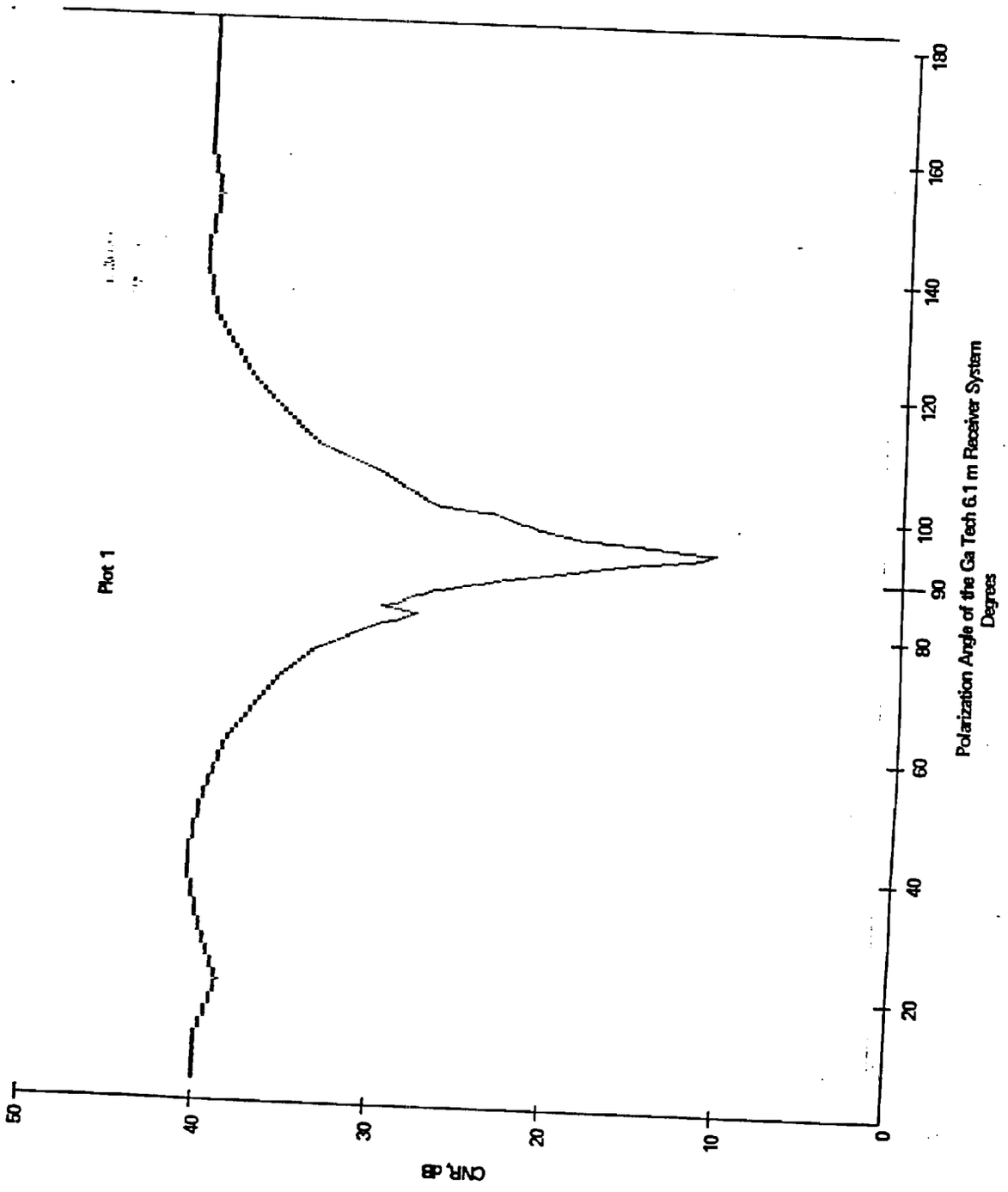

Uplink 0 Degrees from Best Copolarization
Single Transponder Transmission
Figure 4.5 - Plot 1

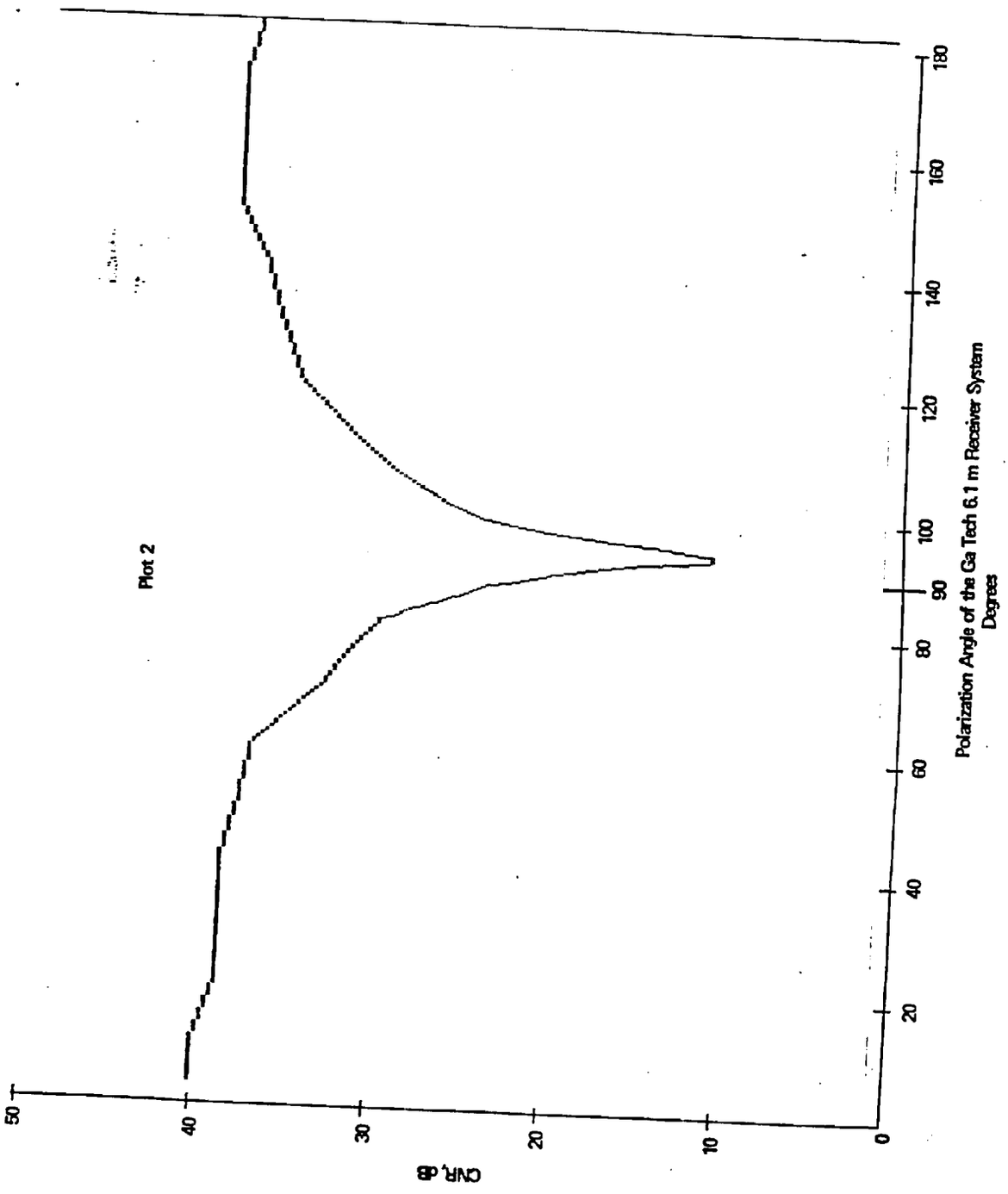

Uplink 30 Degrees from Best Copolarization
Single Transponder Transmission
Figure 4.6 - Plot 2

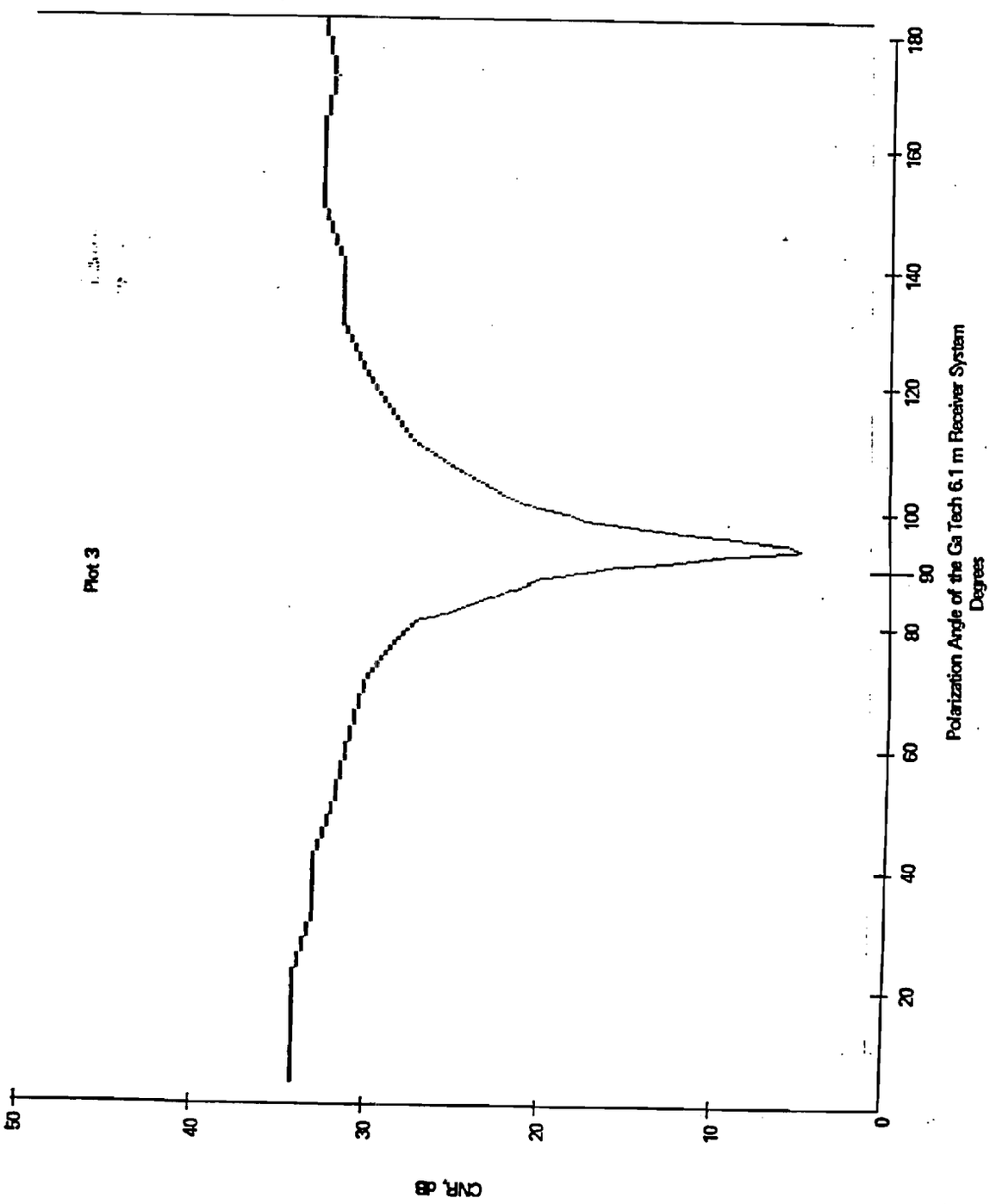

Uplink 60 Degrees from Best Copolarization
Single Transponder Transmission
Figure 4.7 - Plot 3

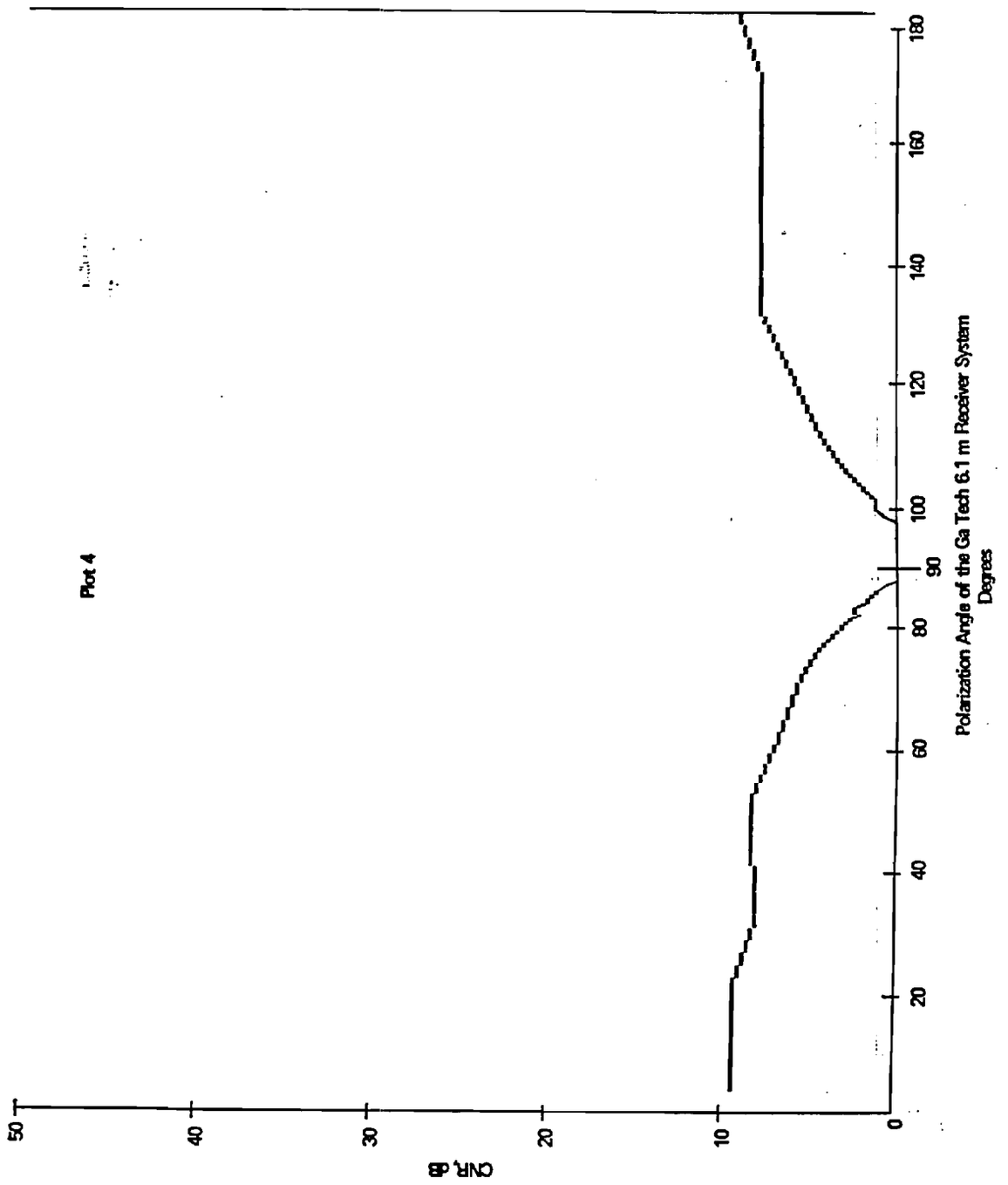

Uplink 90 Degrees from Best Copolarization
Single Transponder Transmission
Figure 4.8 - Plot 4

Uplink 0 Degrees from Best Copolarization
Dual Transponder Transmission
Figure 4.9 - Plot 5

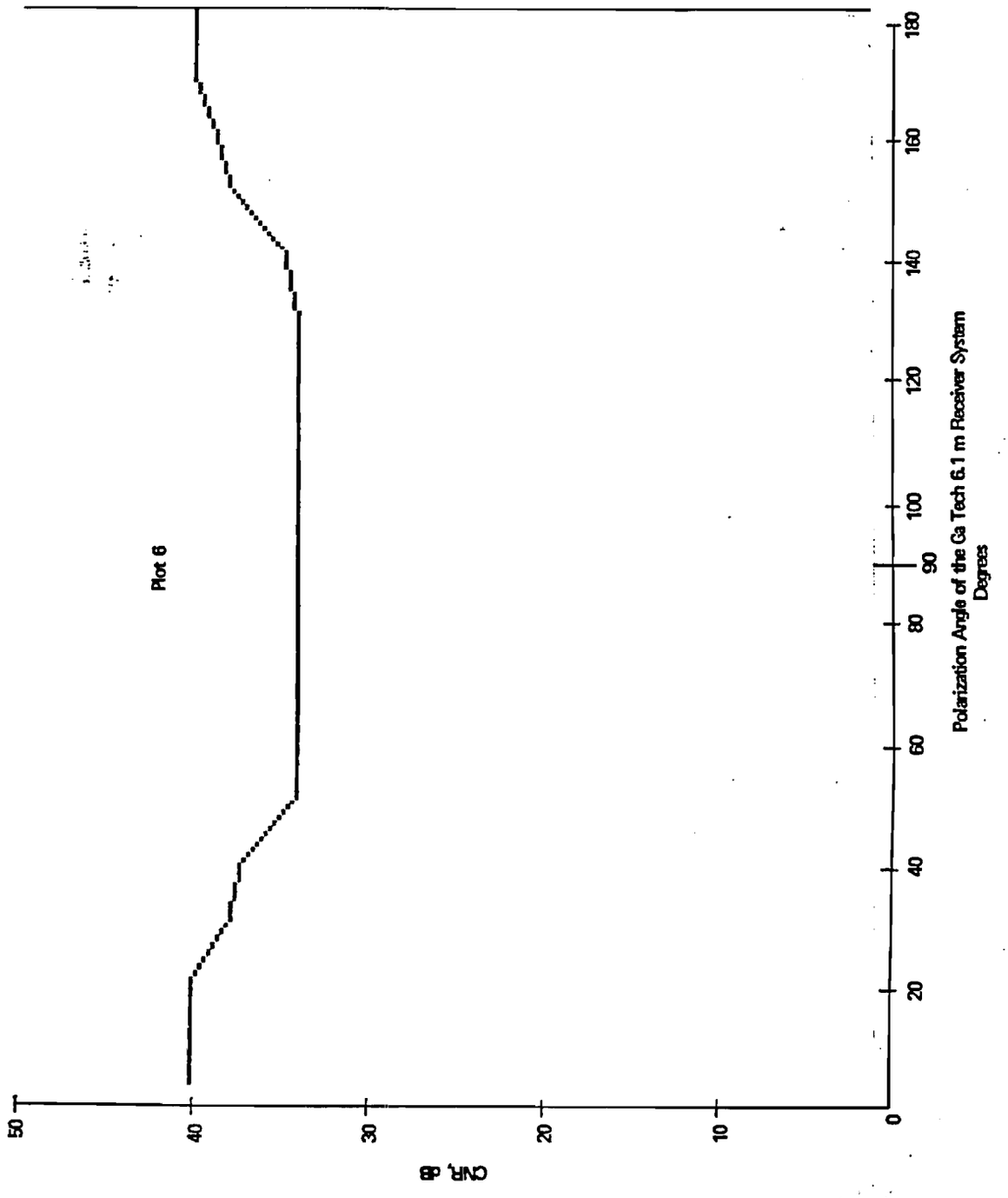

Uplink 30 Degrees from Best Copolarization
Dual Transponder Transmission
Figure 4.10 - Plot 6

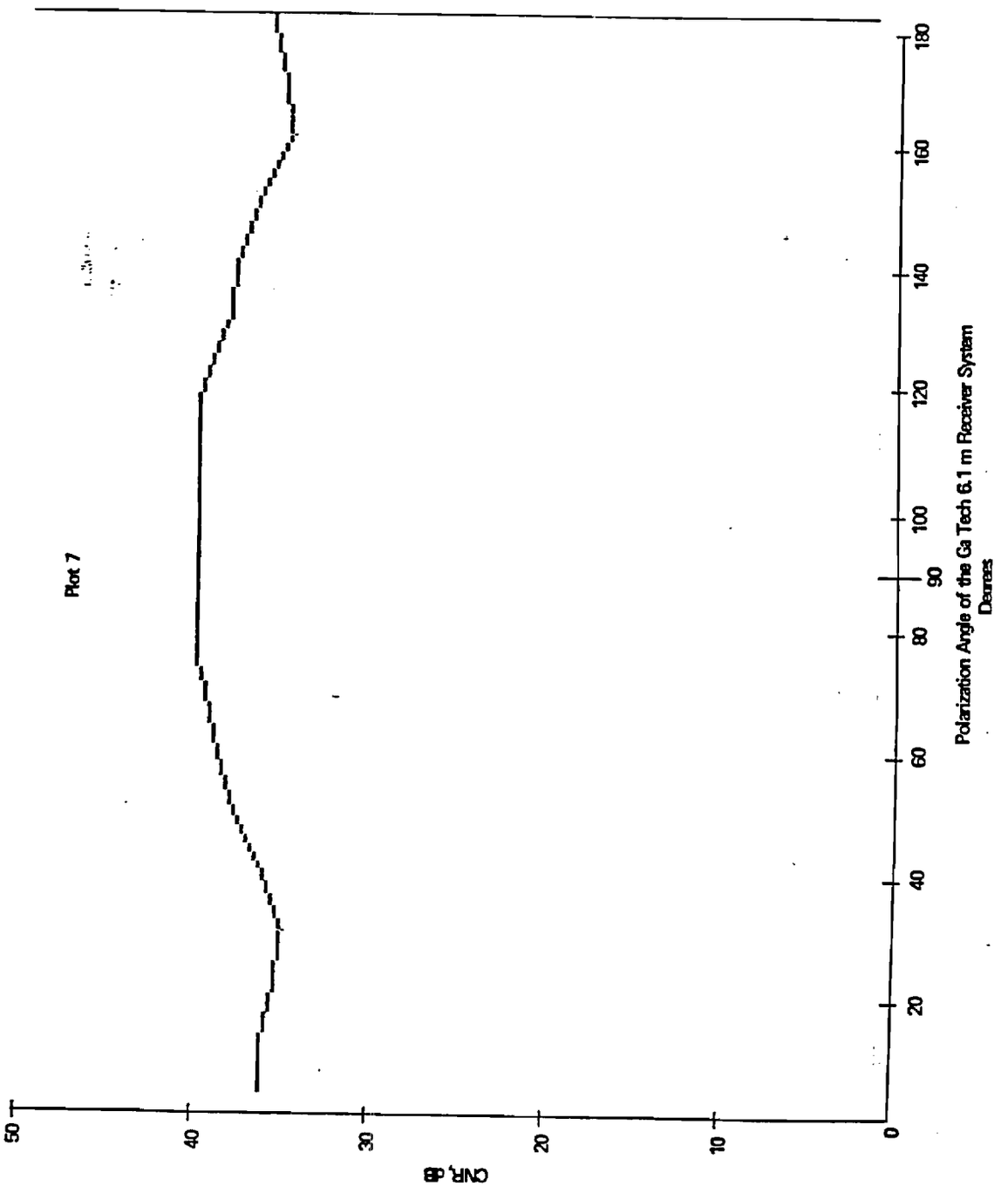

Uplink 60 Degrees from Best Copolarization
Dual Transponder Transmission
Figure 4.11 - Plot 7

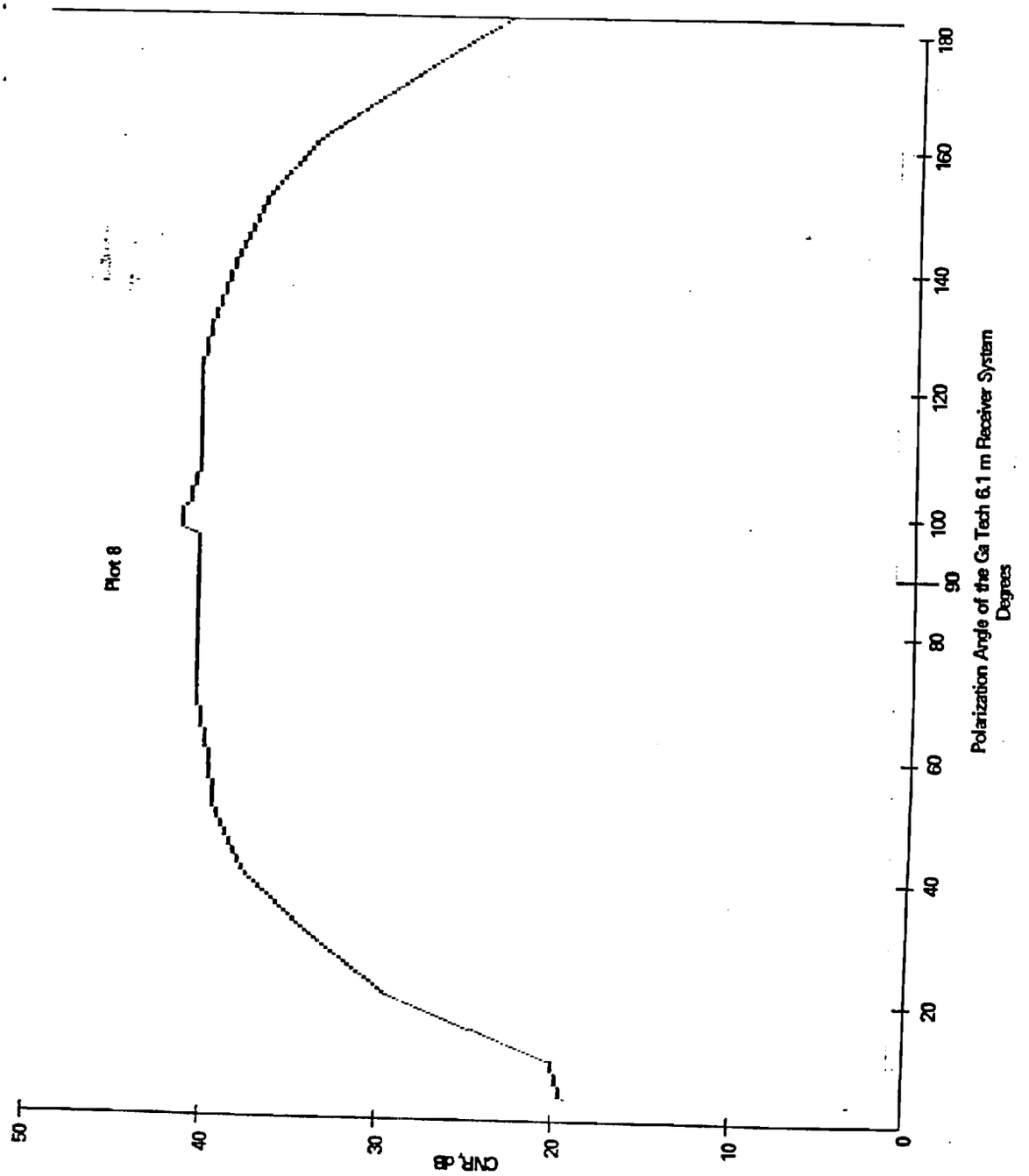

Uplink 90 Degrees from Best Copolarization
Dual Transponder Transmission
Figure 4.12 - Plot 8

the satellite in only one polarization, one would like to see zero power reception for an orthogonally rotated SILS receiving antenna in both cases. Plot 1 shows a CNR drop from about 40 dB to 10 dB at the receiving antenna cross-polarization angle providing the least power transmission. This may be attributed to some combination of imperfect orthogonal transponder rejection and imperfect polarization purity in the Georgia Tech receiving antenna. The complete loss of signal (less than 0.5 dB CNR measured) for the worst uplink polarization alignment angle (where the GTE sourced signal is 90 degrees from co-polarized) illustrated in Plot 4 suggests that the best polarization purity is in the satellite antenna. The other plots illustrate expected results for overlapping transponders.

The experimental result of a complete loss of signal for a cross-polarized uplink into a single polarization transponder channel indicates that there exists enough polarization purity in a full link using the Georgia Tech 6.1 meter SILS receiving system to allow isolation of a sufficiently strong cross-polarized component of an unknown signal for differential phase measurements. Uplinked signals with substantial cross-polarization components have been observed and sometimes directly demodulated. One may also conclude that better polarization isolation in the ground hardware at a permanent SILS site may provide

potentially better cross-polarization signal resolution than the equipment used for these experiments affords.

4.2.2 Phase Stability of the Georgia Tech Earth Station

Originally it was hoped that there would be no requirement to perform any sort of spectra realignment between the received pair of cross-polarized signals. Therefore, attempts were made to characterize the frequency and phase stability of the receivers at the Georgia Tech site. During a full loop transmission originating from Georgia Tech, the received CW signal which was locally sourced from a microwave frequency counter phase locked to a temperature compensated crystal oscillator was observed to drift more than 50 kHz over a 30 second period. This drift is far too large for performing the desired differential phase measurements. This local oscillator stability examination process was simplified by the loan of one of GTE Spacenet's test translators so as to avoid using satellite transponder time to operate the full uplink/downlink loop. There were numerous local oscillators involved in the full loop test to which the observed drift may be attributable. Some of these are in the Georgia Tech transmission path or the test translator which would not effect the receive paths of an interferometry system. Because of the inability to adequately stabilize or phase lock all the local oscillators together, a feedback approach was employed which uses a

reference signal.

4.3 Signal Processing

The paramount issues for the signal processing portion of the interferometric technique include the spectral realignment of the signals received from each polarization, the measurement of a differential phase between these two realigned signals, and the removal of any phase offsets induced by the paths traversed by these signals.

4.3.1. The Offset Spectra Problem

There is a spectra misalignment problem to overcome before acquiring a differential phase which may be mapped into the desired terrestrial curves of possible uplink locations. The goal is to perform a remote differential phase measurement referred to the two cross-polarized feeds aboard the afflicted satellite. Figure 4.13 shows the two signal paths from satellite antenna to terrestrial IF outputs at 70 MHz with an emphasis on the frequency sources for the receiver's mixing schemes. The frequency sources include several oscillator technologies: temperature compensated crystal locked, ambient temperature crystal locked, and digital synthesizer with a crystal source. The twin local oscillators aboard the satellite which shift each polarization's bank of transponder signals from the 14 GHz uplink passband to the desired 12 GHz downlink passband are

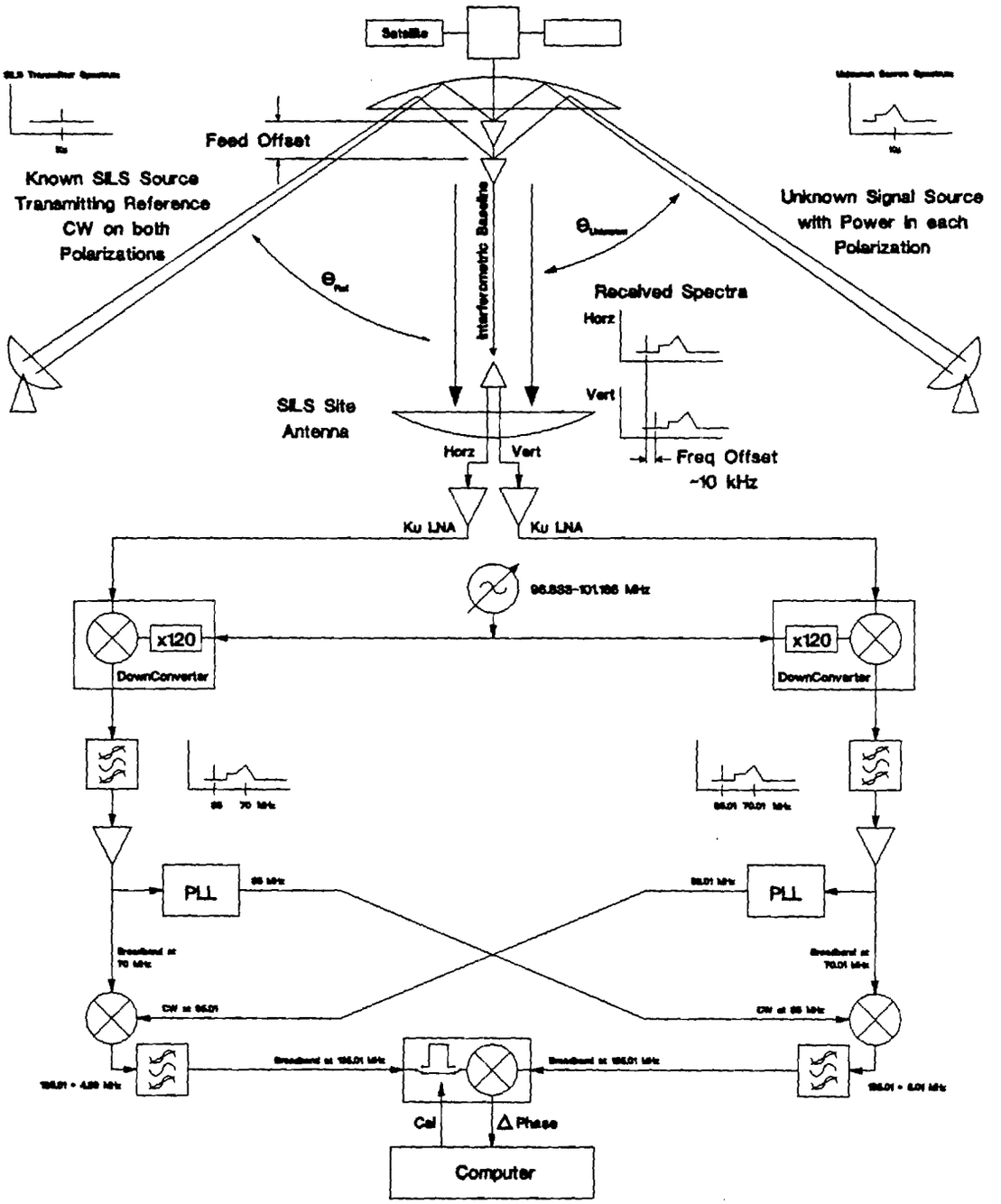

Interferometry System Block Diagram

Figure 4.13

not locked together. Thus, there are a multiplicity of sources for phase and frequency drift between the two signal paths. Therefore, there will exist some offset frequency between the two spectra presented at the receivers' IF outputs.

Even if the received and downshifted spectra were perfectly aligned, there exists the problem of interpreting the definition of differential phase for the situation where each signal occupies some non-zero bandwidth. For the trivial case of monochromatic signals, a mixer output provides a DC component which is related to the differential phase between the input signals. However, a typical satellite signal is often a broadband data or frequency modulated television signal.

4.3.1.1 Digital Signal Processing Approach

Several methods of correcting for the offset spectra have been proposed. One "total" digital signal processing solution involves shifting some portion of the spectrum of each signal close to baseband to facilitate the bandlimiting and digital sampling of a portion of each of two broadband transponder signals. The sampled frames from each signal path are transformed into the frequency domain. These digitally represented spectra are cross-correlated to determine their frequency offset by choosing the correlation

maximum as the offset frequency. One spectrum is shifted accordingly then the phase measurement is performed. The introduction of a known reference signal would greatly enhance this technique.

Drawbacks to the described DSP system include a lack of error frequency resolution due to both the minimum frequency increments of the discrete spectra and the potential broadness of a cross-correlation peak which would depend upon signal content. Were the frequency offset between spectra to exceed the filtered sampling bandwidth, a correction would be beyond the abilities of this method.

A problem analogous to that of the offset spectra is experienced by the Radio Astronomy community in the form of doppler shifts induced upon the spectra of signals received at antennas separated by this planet's diameter when astronomical Very Long Baseline Interferometry (VLBI) is performed. A sampling of both the literature and conversations with various Radio Astronomy authorities indicated that their offset spectra problem is resolved by either an a priori inference of the induced offset frequency and an open loop change in one receiver's (atomic clock referenced) local oscillator or the offset is determined from hours of off-line cross-correlation between long samples of the two received signals. Neither method was desirable for the SILS application.

4.3.1.2 Analog Spectra Realignment

Measurement of differential phase between two signals can be accomplished by directly comparing the phase of the two signals or by comparing the phase of each with a reference carrier. When performing phase measurements between a (reference) carrier and a broadband signal, the resulting energy within the passband of the mixer's product output can be so small as to elude simple detection.

Thus, it is preferable to mix a pair of broadband signals together to perform a phase measurement between them. Although it is possible that over large fractional bandwidths the phase would vary between time delayed signals, small fractional bandwidths produce consistent results. This was shown to be true in laboratory measurements between frequency modulated signals occupying hundreds of kilohertz centered near 70 MHz.

To facilitate the mixing of two broadband signals to determine their phase difference, the spectral misalignment or frequency offset induced by the two unlocked oscillators aboard the spacecraft must be removed before the phase measurement is performed.

Figure 4.15 shows the RF signal processing configuration used to perform the differential phase measurement between a pair of simulated satellite signals. A reference CW signal which would normally originate from a

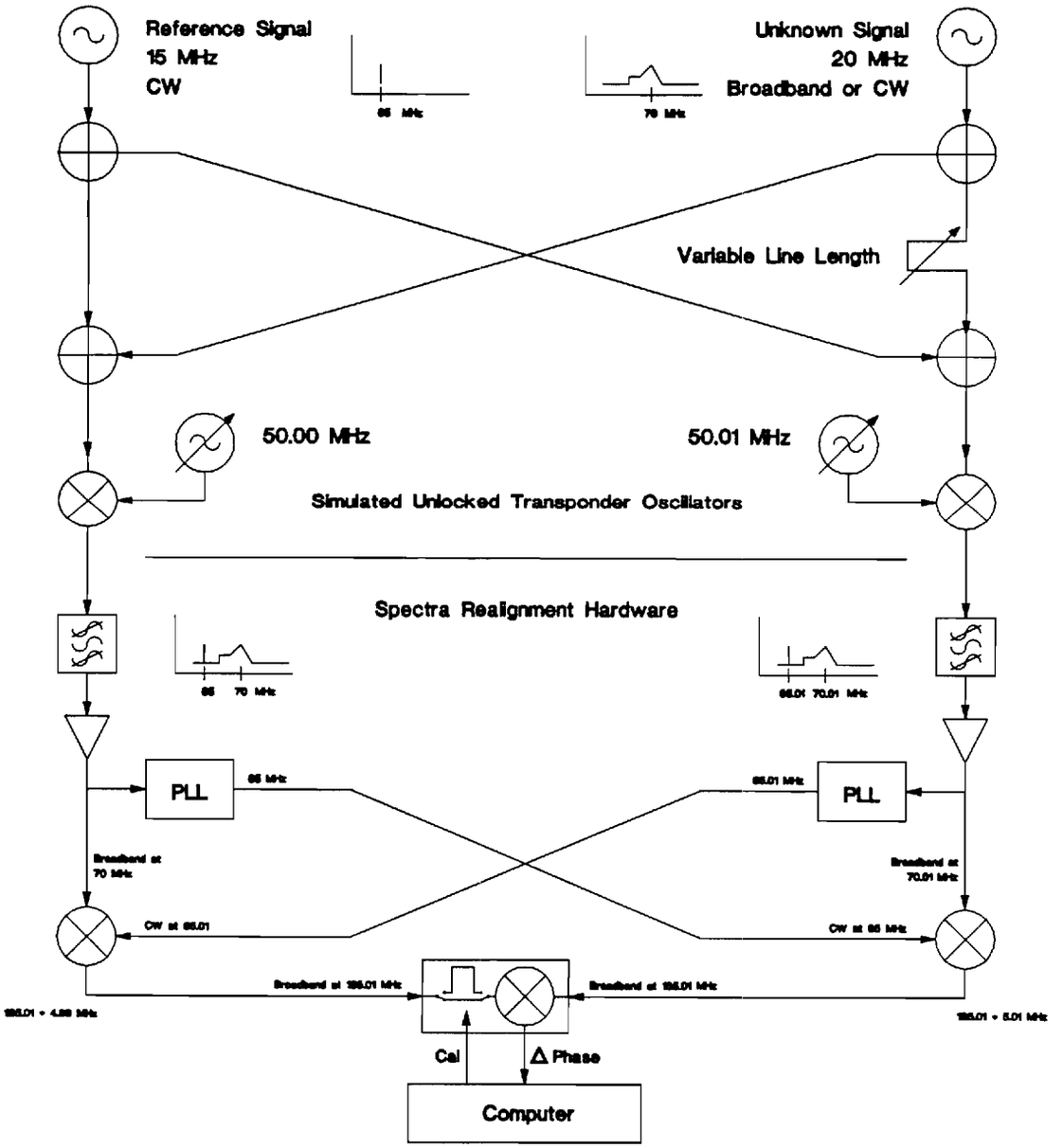

Simulated Satellite Signal Generation
with Offset Spectra Correction Hardware
for the Interferometric SILS Technique

Figure 4.15

friendly terrestrial source is used to realign the spectra. This signal is transmitted so as to be received by the satellite on each of the two cross-polarized feeds. At the terrestrial SILS receiving site, each reference carrier is regenerated by a phase locked loop (PLL).

The output of one PLL differs in frequency and phase from the other PLL by the difference induced by each transponder oscillator's frequency offset and the angle of arrival of the reference signal at the satellite antenna. One can know the angle of arrival of the friendly reference signal and thus the resulting differential phase between received channels. Any additional phase and the frequency offsets are due to elements in the signal processing path which signals from any other source must also experience.

Therefore, to realign the resulting spectra, each channel's received spectrum is upconverted by the regenerated reference carrier derived from the other channel's received spectrum. The output of the vertical channel's PLL reference generated carrier is mixed with the spectra of the received horizontal channel to produce a desired product spectra at a higher frequency. The same is done for the other channel.

Thus, the differences in frequency between the two resulting higher frequency spectra are canceled out. These two spectra are band pass filtered to isolate a signal of

interest. They are then mixed to produce a product which has a DC component related to the phase between the input spectra which may be measured and integrated by a computer. The known phase offset due to the angle of arrival of the reference carrier is then subtracted out along with any known fixed offsets to produce the desired resulting differential phase between the chosen signals. This phase may then be mapped into a terrestrial map to produce a curve of constant differential phase on which the chosen signal's source must reside.

4.3.2 Phase Budgets

Figure 4.14 shows the signal paths relevant to the interferometric method from the satellite receiving antenna to the terrestrial SILS interferometric phase detector with an emphasis on the elements which effect frequency and phase. Radiation from both the interfering and reference uplink sources was present at the antenna. The incident radiation's geometric angle at the antenna induced an electrical phase difference between the cross-polarized receive feeds. Thus, the independent vertical and horizontal paths contained both signals but corresponding signals had different geometry dependent phases at points 1 and 2 in Figure 4.14. To facilitate the hardware which is later described, both signals are assumed to be unmodulated

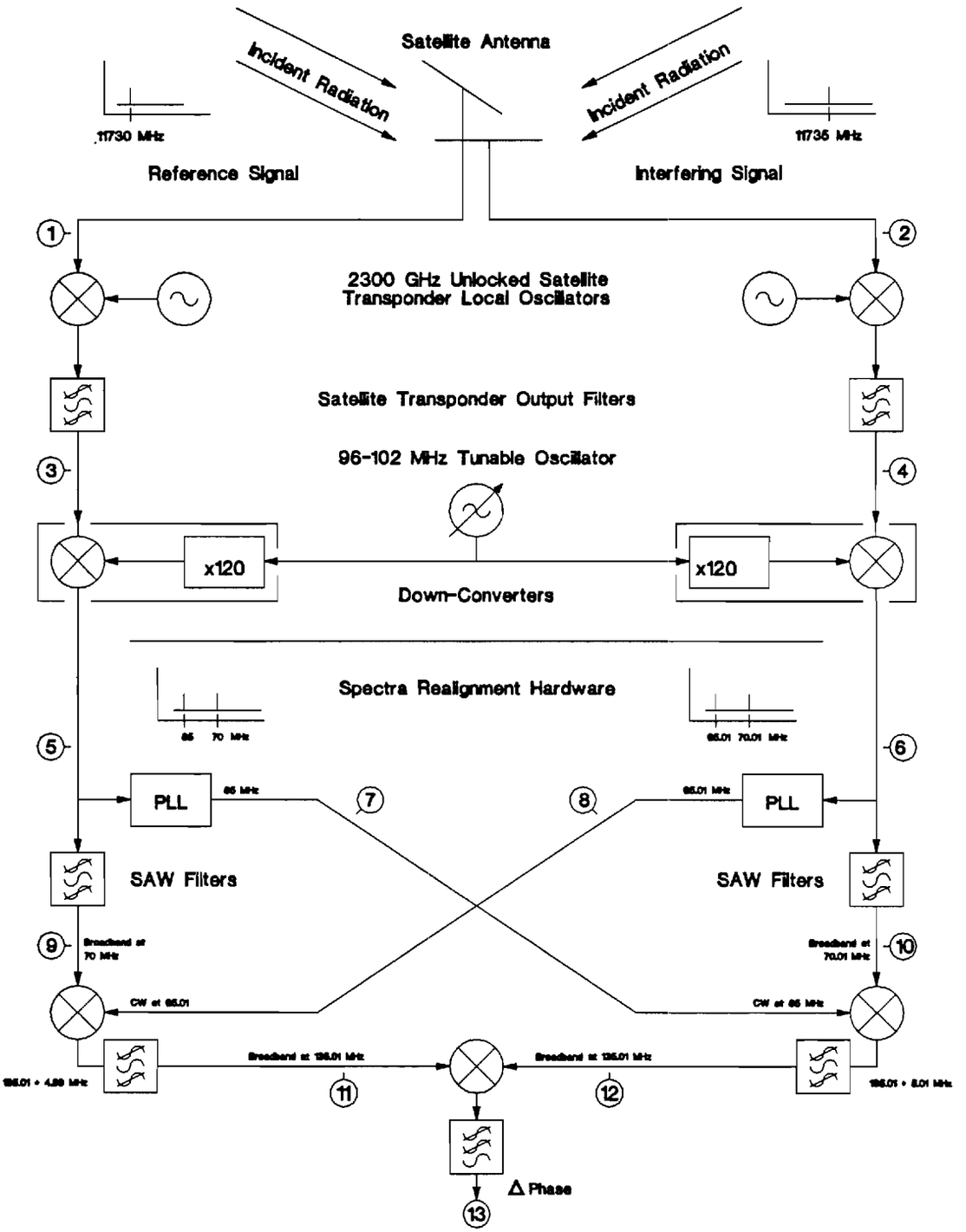

Phase and Frequency Control Elements
for the Interferometric SILS System

Figure 4.14

carriers, and the frequency difference between the reference and interfering signals is assumed to be 5 MHz with the reference signal being the lower.

Throughout the following equations, this notation holds:

r: refers to the reference carrier
s: refers to the interfering signal
h: refers to the horizontally polarized channel
v: refers to the vertically polarized channel
L: refers to the SILS site downconverter local oscillator

Incident Reference and Interfering Radiation

Equation 4.1: $r_i = A_{ir} * \cos(w_r t)$
Equation 4.2: $s_i = A_{is} * \cos(w_s t)$

where: w_r = Reference uplink frequency
w_s = Interfering uplink frequency
A_x = Various signal amplitudes
θ_x = Various signal phases
r_i = Incident Reference Carrier
s_i = Incident Interfering Signal

Signals at Point 1

Equation 4.3: $r_1 = A_{r1} * \cos(w_r t + \theta_{rv})$
Equation 4.4: $s_1 = A_{s1} * \cos(w_s t + \theta_{sv})$

Signals at Point 2

Equation 4.5: $r_2 = A_{r2} * \cos(w_r t + \theta_{rh})$
Equation 4.6: $s_2 = A_{s2} * \cos(w_s t + \theta_{sh})$

The signals next experienced the mixing stage for conversion from the 14 GHz uplink band to the 12 GHz downlink band. Because the two independent onboard oscillators were not locked, the spectra at points 3 and 4

in Figure 4.14 are now offset in frequency by the difference between the 2300 MHz oscillators. The microwave filters following the mixing stage rejected the higher mixing product and the other products developed from the typically saturated amplifier used by full transponder signals.

Signals at Point 3

Equation 4.7: $r_3 = A_{r3} * \cos[(w_r - w_v)t + \theta_{rv} - \theta_v]$

Equation 4.8: $s_3 = A_{s3} * \cos[(w_s - w_v)t + \theta_{sv} - \theta_v]$

Signals at Point 4

Equation 4.9: $r_4 = A_{r4} * \cos[(w_r - w_h)t + \theta_{rh} - \theta_h]$

Equation 4.10: $s_4 = A_{s4} * \cos[(w_s - w_h)t + \theta_{sh} - \theta_h]$

where: w_v = Vertical transponder LO frequency
w_h = Horizontal transponder LO frequency
θ_v = Vertical transponder LO phase
θ_h = Horizontal transponder LO phase

The signals were then transmitted back to Earth where they were collected and amplified at the SILS site and down-converted in a pair of phase locked downconverters. These downconverters generated their internal microwave local oscillator frequencies by multiplying an externally generated and shared VHF signal. The received signals appear at the output of the downconverters at points 5 and 6 in an intermediate frequency band centered at 70 MHz. The SILS site local oscillator is tuned to center the

interfering signal at 70 MHz and the reference signal at 65 MHz. The channels retained their frequency offset from each other by the difference between the satellite's local oscillators.

Multiplied Local Oscillator
before Mixing in the Downconverter

Equation 4.11: $LO = A_{LO} * \cos(w_L t + \theta_L)$

Signals at Point 5

Equation 4.12: $r_5 = A_{r5} * \cos[(w_r - w_v - w_L)t + \theta_{rv} - \theta_v - \theta_L]$

Equation 4.13: $s_5 = A_{s5} * \cos[(w_s - w_v - w_L)t + \theta_{sv} - \theta_v - \theta_L]$

Signals at Point 6

Equation 4.14: $r_6 = A_{r6} * \cos[(w_r - w_h - w_L)t + \theta_{rh} - \theta_h - \theta_L]$

Equation 4.15: $s_6 = A_{s6} * \cos[(w_s - w_h - w_L)t + \theta_{sh} - \theta_h - \theta_L]$

where: w_L = SILS LO frequency
θ_L = SILS LO phase

The phase locked loops regenerated only the 65 MHz reference carriers. Therefore, only the CW reference carriers appeared at points 7 and 8 following the PLLs.

Signals at Points 7 and 8

Equation 4.16: $r_7 = A_{r7} * \cos[(w_r - w_v - w_L)t + \theta_{rv} - \theta_v - \theta_L]$

Equation 4.17: $r_8 = A_{r8} * \cos[(w_r - w_h - w_L)t + \theta_{rh} - \theta_h - \theta_L]$

Helical resonator and SAW Bandpass filters centered at

70 MHz isolated the interfering signal. Thus the interfering signals appeared alone at points 9 and 10.

Signals at Points 9 and 10

Equation 4.18 $$s_9 = A_{s9} * \cos[(w_s-w_v-w_L)t + \theta_{sv}-\theta_v-\theta_L]$$

Equation 4.19: $$s_{10} = A_{s10} * \cos[(w_s-w_h-w_L)t + \theta_{sh}-\theta_h-\theta_L]$$

The interfering signal at point 9 was mixed with the the regenerated reference signal at point 8. The higher product is retained by the following filter. This adds all the accumulated phases and shifts the frequency from earlier stages to produce the signal at point 11. The same is done with the signals at points 7 and 10 to produce the signal at point 12.

Signals at Points 11 and 12

Equation 4.20:

$$s_{11} = A_{11}*\cos[(w_s-w_v-w_L+w_r-w_h-w_L)t + (\theta_{sv}-\theta_v-\theta_L+\theta_{rv}-\theta_h-\theta_L)]$$

Equation 4.21:

$$s_{12} = A_{12}*\cos[(w_r-w_v-w_L+w_s-w_h-w_L)t + (\theta_{rv}-\theta_v-\theta_L+\theta_{sh}-\theta_h-\theta_L)]$$

Each of the signals at points 11 and 12 had the same frequency. Therefore, this pair of signals was mixed and lowpass filtered to produce a DC term which contained an unknown amplitude, a known reference differential phase, and the desired but unknown interfering signal's differential

phase. This final amplitude consisted of the phase detector's losses and the amplitudes of the signals entering the phase detector. Section 4.3.3 discusses the removal of the unknown amplitude. This leaves only the desired unknown differential phase from the interfering uplink transmitter.

The Resulting DC Term at Point 13

Equation 4.22: $V_{13} = A_{13} * \cos[\ (\theta_{rh} - \theta_{rv}) + (\theta_{sv} - \theta_{sh})\ ]$

where:
V_{13} = The measurable (known) mixer output voltage
A_{13} = An unknown scaling factor due to losses and earlier signal amplitudes
$(\theta_{rh} - \theta_{rv})$ = The known electrical phase induced by the known incident angle of the reference signal
$(\theta_{sv} - \theta_{sh})$ = The unknown electrical phase induced by the unknown incident angle of the interfering signal

4.3.3. Amplitude Independent Phase Measurement

A Metrabyte interface card provided by GTE was used in an IBM XT compatible computer to sample digitally the voltage output of the phase detector and to control the phase detector calibration circuitry. Note that the phase detector employed is a stock RF mixer which has been optimized to provide a larger DC output to facilitate phase measurement. The output from the phase detector was low pass filtered to about 1 kHz by an analog circuit to facilitate digital sampling and removal of higher mixing products. This low frequency signal was then oversampled by

the computer. The computer integrated (averaged) over thousands of samples to determine the average DC level output from the phase detector which was related to the phase difference between signals entering the phase detector.

Because the average DC level output from this type of phase detector is related to not only the desired phase difference but also the entering signal amplitudes, a method was needed for removing these possibly unknown amplitudes from the formula for computing the desired numerical phase angle. This is traditionally done in interferometric direction finding (DF) systems by hard limiting both incoming channels to a known power level and then mixing the two signals to achieve a DC voltage which corresponds to the desired phase angle. The SILS system employed a different approach.

The RF signal amplitude ambiguities were removed by alternately inserting and removing a known length of cable into and from one of the entering RF signal paths to induce a specific phase shift at the known frequency of measurement. This provides two equations for the two unknowns of differential phase and amplitude. By measuring the mixer's lowpassed DC outputs both with and without the extra cable length inserted, it is possible to solve numerically the underlying non-linear equations for both

signal amplitude and phase difference. This is illustrated below.

A pair of voltage signals are modeled as:

Equation 4.23 $V_1 = A_1 * \cos(w_1 t + p_1)$ [volts]

Equation 4.24 $V_2 = A_2 * \cos(w_2 t + p_2)$ [volts]

where: V = [volts] Measurable voltage
A = [volts] Amplitude
w = [rad/sec] Angular frequency
t = [sec] Time
p = [rad] Phase

Ignoring higher mixing products by assuming that a mixer is a perfect multiplier, the mixing of this pair of signals gives at the mixer output:

Equation 4.25

$$V_{mix} = A_1*A_2*A_{mix}*\{ \cos[(w_2+w_1)t + p_2+p_1] + \cos[(w_2-w_1)t + p_2-p_1]\}$$

If the frequencies are the same ($w_1=w_2$), then:

Equation 4.26

$$V_{mix} = A_1*A_2*A_{mix}*\{ \cos[(2*w_1)t + p_2+p_1] + \cos[p_2-p_1]\}$$

Lowpass filtering to remove the double frequency product term gives:

Equation 4.27

$$V_{mix|lpf} = A_1 * A_2 * A_{mix} * A_{lpf} \{ \cos(p_2 - p_1) \} \text{ [volts]}$$

$$= A_T * \{ \cos(p_2 - p_1) \} \text{ [volts]}$$

where: A_1 = Signal 1's original voltage amplitude
A_2 = Signal 2's original voltage amplitude
A_{mix} = Amplitude changes attributable to the mixer
A_{lpf} = Amplitude changes attributable to the lowpass filter
A_T = The combined total amplitude

The signal amplitudes, mixer losses, and lowpass filter losses will all vary depending on the strength of the incoming signals and variations in the RF signal processing components. Thus, the measurable voltage, $V_{mix|lpf}$, is related to not only the desired differential phase, p_2-p_1, but is also proportional to the unknown total amplitude A_T.

The insertion and removal of the known length of transmission line at one of the mixer inputs produces a phase shift, p_L which depends on the known frequency of the mixer's input signals. Now two equations are available. One relates a measurable mixer output voltage to the differential phase without the line inserted. The other relates the measurable voltage to the phase difference plus the additional phase induced by the additional transmission line length. The new equations are:

Equation 4.28 $$V_{short} = A_T * \{ \cos(p_2 - p_1) \} \text{ [volts]}$$

Equation 4.29 $$V_{long} = A_T * \{ \cos(p_2 - p_1 + p_L) \} \text{ [volts]}$$

Finding p_2-p_1 requires the solution of Equations 4.28 and 4.29. Because they are non-linear, the following equation is numerically solved for p_2-p_1 knowing V_{long}, V_{short}, and p_L:

Equation 4.30

$$V_{long} * \cos(p_2-p_1) = V_{short} * \cos(p_2-p_1 + p_L)$$

Computer software solved these equations and controlled both the phase detector output sampling and cable switching. The addition of computer controlled measurements reduced the time to make the measurements from a manual time of about a half hour to a few seconds with judicious adjustment of the sampling frequency, number of samples, and the analog filter characteristics.

4.4 Experimental Apparatus and Procedures

To test the offset spectra correction and other signal processing hardware, a series of laboratory tests were performed. This was done before attempting the more expensive live satellite tests. The laboratory tests required the generation of a pair of frequency shiftable spectra containing a reference carrier and a phase shiftable broadband or CW "interfering" signal. The satellite tests required signal transmissions from geographically separated pairs of locations which provided sufficient phase differences to illustrate desirable operation of the

interferometric technique. ..*** from month14

4.4.1 Differential Phase Measurements with Laboratory Signals

To make laboratory measurements to test the interferometric technique, there was a need to generate two sets of signals with a frequency offset typical of that found at the IF outputs of the pair of satellite receivers local to the SILS site. Figure 4.15 illustrated the test configuration with the pseudo-transponders occupying the upper half of the illustration and the actual phase measurement hardware occupying the lower half.

Two signal generators are employed to provide the equivalent of transponder input signals. The 19 MHz oscillator is considered to be the cooperative SILS reference carrier. The 20 MHz oscillator is considered to be the non-cooperative unknown signal of interest. These signals are summed as illustrated to produce the equivalent of inputs into two transponders aboard a satellite. One of the paths from the 20 MHz "unfriendly" oscillator is connected to a variable length transmission line (ganged trombone sections or different lengths of coaxial cable) to simulate varying differential phase shifts and thus varying angles of incidence for the corresponding "unfriendly" radiation arriving at the satellite antenna. The angle of

incidence for the SILS reference carrier's radiation is assumed to be known because the location of the SILS uplink site and the orientation of the spacecraft is known.

The simulated transponder inputs at about 20 MHz are then mixed with approximately 50 MHz outputs from another pair of signal generators which are purposefully set to have frequency differences of about 0 to 10 kHz. These two signal generators with their slight offsets correspond to the two unlocked local oscillators aboard the satellite which feed the two sets of transponders associated with the two orthogonally polarized antenna feeds. The two spacecraft oscillators are expected to have frequency differences of less than 3 kHz.

The outputs from this pair of mixers provided a pair of spectra like that expected at the 70 MHz IF output ports for each of the orthogonally polarized receiving channels at a SILS site. Each spectrum consisted of a reference and an "unfriendly" CW signal.

Because interference is expected from broadband modulated signals (FM TV, PSK), the "unfriendly" source signal had the ability to be frequency modulated to give it a substantial bandwidth. The choice of 19 and 20 MHz for the simulated uplinked signals was motivated by the availability of signal generators. Although microwave signals could be used and fed into the receivers, the

results at the 70 MHz intermediate frequency are the primary concern for laboratory test of the offset spectra correction and phase measuring hardware.

4.4.2 Differential Phase Measurement with Live Satellite Signals

Figure 4.13 showed the total satellite signal path topology assumed with the two paths of interest being that of the reference and the interfering signal. As was previously discussed, this method of locating an interfering unknown uplink signal requires that an additional reference signal be present nearby in frequency. Because the Georgia Tech Earth station was hardware limited in its ability to transmit and receive simultaneously on two polarizations, it was requested that GTE supply the satellite signals.

To determine whether the interferometry method was indeed working, the "interfering" signal needed to be transmitted from at least two geographically separate sites to induce a substantial phase difference between the orthogonally polarized antenna feeds aboard the satellite of interest. The Grand Junction, Colorado TT&C site and the McLean, Virginia site of GTE presented a sufficient difference in the differential phase measured between the two spacecraft antenna feeds to demonstrate the effectiveness of this system if either GSTAR 1 (103 degrees west longitude) or GSTAR 2 (105 degrees west longitude) was

used and the model which generates the illustrated curves of constant differential phase was correct. However, this was not true for the case of GSTAR 3 which was located at 93 degrees west longitude and should have nearly identical differential phase shifts for signals originating at the Grand Junction and McLean sites.

After being informed by GTE that GSTAR 3 would be the satellite used for the interferometric tests, plots of the associated contours of constant differential phase were generated to learn the expected differential phase measurement results between the probable uplink sites. Figure 4.16 shows this plot against a Mercator projection of the continental United States with cross marks at the approximate locations of Grand Junction, Colorado, Atlanta, Georgia, and McLean, Virginia.

Figure 4.17 illustrates the CW signals which were transmitted from each of the two different sites during the two different portions of the experiment. Each signal appeared on frequency overlapping transponders in each polarization as is shown in the example of Figure 4.17. The lower frequency signal served as the reference CW signal with the higher frequency signal being the unknown or interfering signal. Due to the limitations of the experimental hardware, the signals needed to be separated by no less than 5 MHz and no more than 10 MHz and were to be as

powerful as is possible. The reference CW signals were locked with the phase locked loops, the offset spectra were realigned, then the two interfering signals were mixed together to produce the desired differential phase.

Each experiment involved two measurements. For the first measurement, the reference and interfering signal came from the same uplink site. For the second measurement, the interfering signal came from a geographically different site with the reference signal continuing to originate from the previous site. A knowledge of the location of both sites provided for observations of a difference in phase between the two sites and determination of any satellite specific phase shifts.

The experiments were planned so that one half hour was allocated to each pair of signals from each site. The accuracy of these measurements greatly depended on the phase purity and signal-to-noise ratio of the reference CW signal, therefore, the cleanest and most powerful reference carrier was requested.

Figure 4.13 shows a pair of band pass filters centered at 140 MHz preceding the inputs to the phase detector. These filters were not included in the experimental hardware. Fortunately, the mixing product that these filters should reject consists of the pair of received spectra which have been offset in frequency by twice their

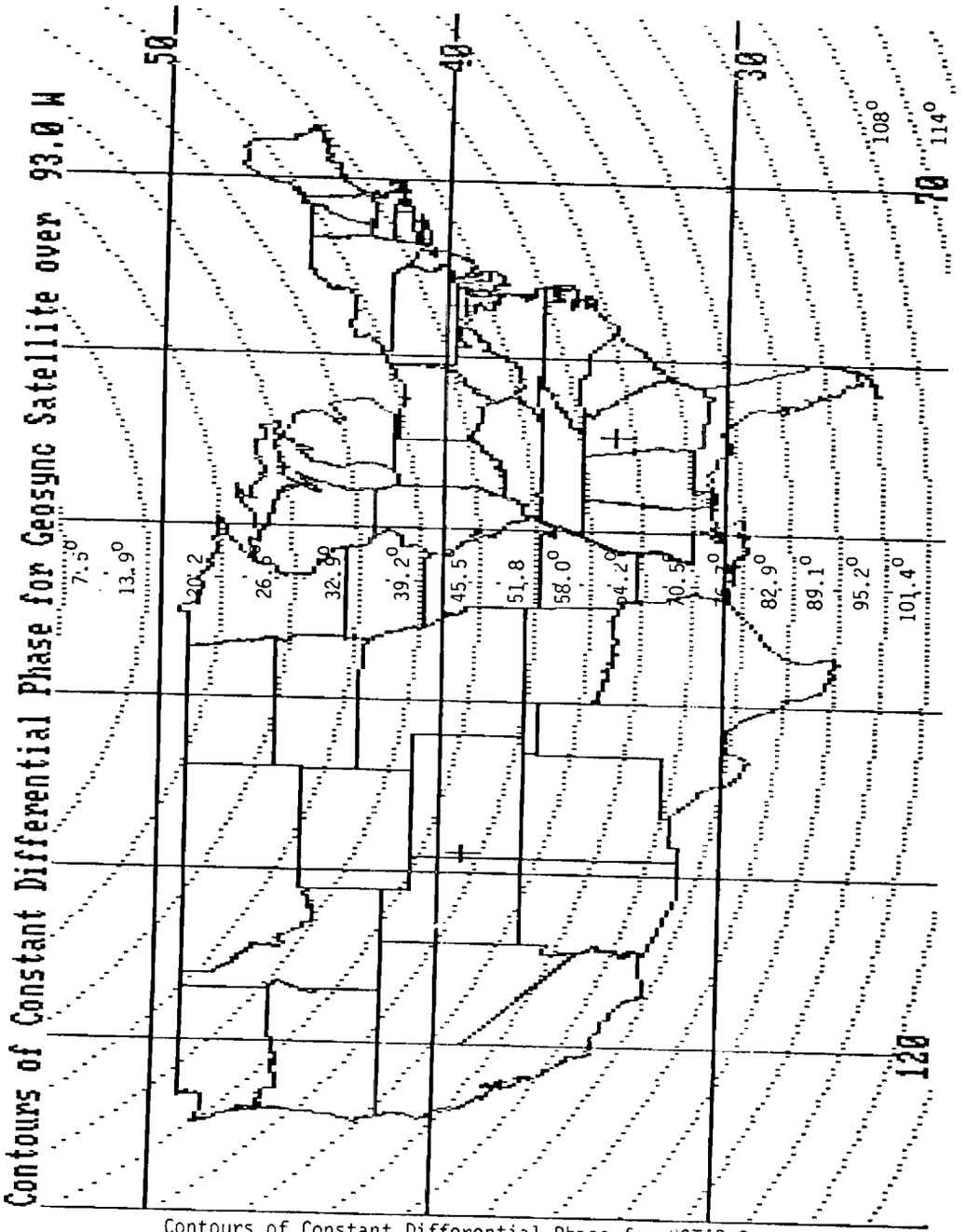

Contours of Constant Differential Phase for GSTAR 3
Figure 4.16

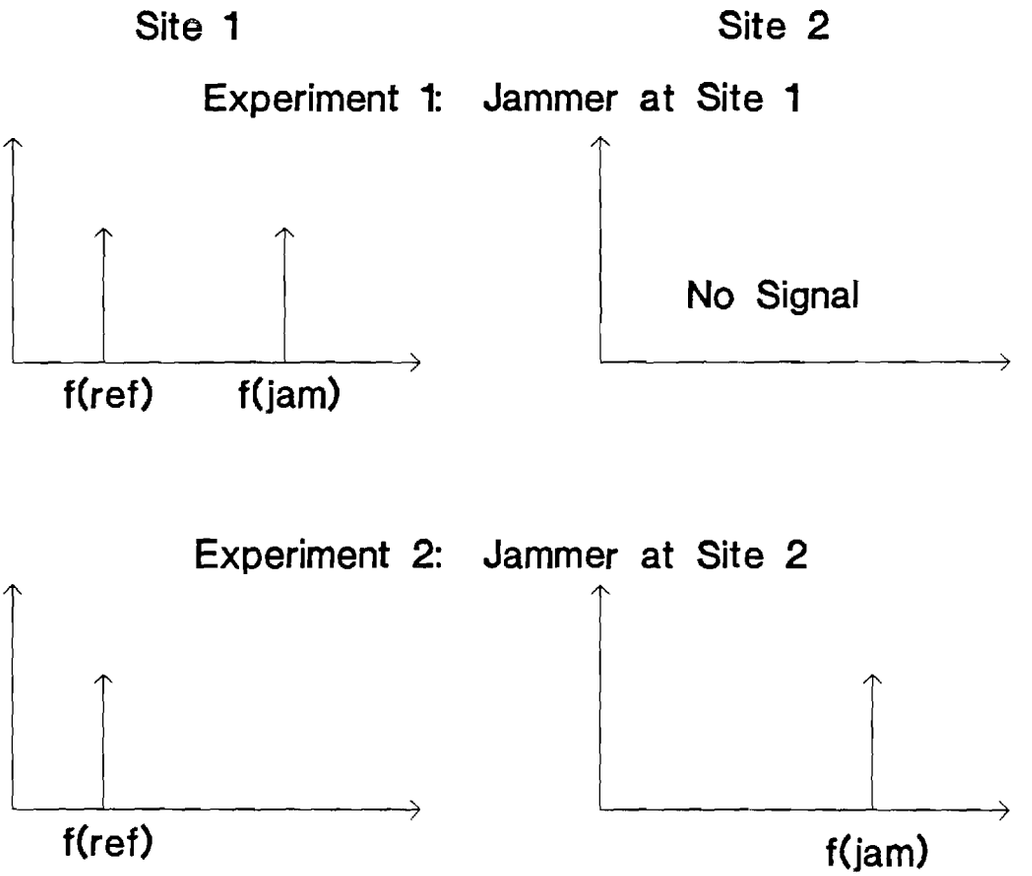

Desired Transmissions for Interferometry Experiment

Figure 4.17

GSTAR 3 Signals for Interferometry Experiment

Both Signals Should Appear on Each Polarization

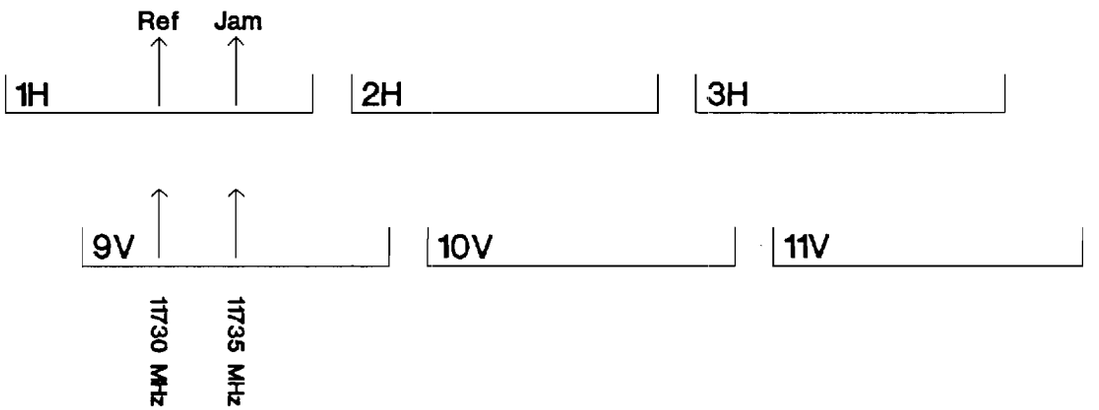

Figure 4.18

original error offset and thus should not correlate to produce a DC term within the phase detector.

The first experiment occurred on Thursday 15 February 1990 between 9 and 11 pm EST. GTE offered to provide the signals requested as is described above from Grand Junction and the McLean site with the Grand Junction uplink site providing the reference signal in addition to an "unknown" signal. The McLean signal originated with GTE's Ku-band Satellite News Gathering (SNG) truck which was parked outside their McLean, Virginia facility (immediately outside of Washington, DC). The second experiment occurred a week later on Thursday 22 February 1990 between 8:30 and 10:16 pm EST. Again, the Grand Junction site provided both reference and "unknown" signals with the second site being an Atlanta located and based Ku-band equipped SNG truck belonging to the local WXIA Channel 11 television station.

These choices of satellite and uplink locations result in several interesting observations. First, the predicted phase difference between Grand Junction and McLean was on the order of one degree or less while that between Atlanta and Grand Junction was about 12 degrees. Thus, one would expect to measure about the same differential phase between the Grand Junction and McLean signals assuming the differential phase contour model is correct.

A second point worth noting is that GSTAR 3 suffered an

accident during its trip to geosynchronous orbit which, amongst other things, resulted in its occupying an inclined orbit. This orbit requires that a terrestrial observer track the satellite through a celestial "figure eight" pattern during a 24 hour period which occupies an angular box with peak-to-peak widths of about 1.5 degrees of longitude and about 5 degrees of latitude. Because the satellite appeared to a terrestrial observer to be moving at its maximum northwesternly angular velocity at about 10 pm EST at the time of these experiments, all involved terrestrial antennas were required to constantly realign their azimuths and elevations to maintain relatively constant received power levels. This caused a continuous change to the received signal CNR levels. To a lesser degree, polarization purity is effected by a satellite moving out of the main radiation lobe of a linearly polarized terrestrial antenna and thus into a region of the antenna's pattern where some power from each of the spatially orthogonal polarization components may be emitted or detected.

On each of the above mentioned evenings, GTE's Grand Junction TT&C began transmitting a pair of CW signals at 14030 and 14035 MHz with the lower frequency signal being the reference and the other signal being the "unknown" uplink signal. These signals were transmitted from a

linearly polarized antenna which had been rotated approximately 45 degrees from either of GSTAR 3's horizontal or vertical polarization orientations. These signals were received by GSTAR 3, amplified and converted by the pair of onboard oscillators to signals at approximately 11730 and 11735 MHz then retransmitted back to Earth.

As Figure 4.13 illustrates, each orthogonally polarized pair of signals was received at Georgia Tech's dual feed 6.1 meter antenna, amplified by a pair of Ku-band low noise amplifiers (LNAs), then transported through coaxial cable at Ku-band frequencies to an identical pair of phase locked down-converters which mixed the signals down to 65 and 70 MHz. The dual polarity feeds of the Georgia Tech 6.1 meter antenna were used to receive the pair of cross-polarized signals. Phase locked loops were then locked to the now 65 MHz reference signals. The regenerated CW pair of signals were employed to realign the spectra from each received polarization which had become slightly offset due to the independent local oscillators onboard the satellite. Two 250 kHz wide surface acoustic wave (SAW) bandpass filters, centered at 70 MHz, were employed to isolate the "unknown" 70 MHz signals from the reference signal and other noise components in the received passband. This spectral realignment process resulted in the pair of 70 MHz "unknown" signals being centered at about 135 MHz where they were

mixed together to produce DC voltages related to their phase offsets.

The computer controlled sampling process previously described was used to remove the amplitude ambiguity and integrate out any remaining AC components in the voltage measurement. A computer program then inferred the phase difference between the two RF channels. These measurements were made continuously for periods of many minutes with results being intermittently written to the computer's hard disc.

4.5. Interferometric Results

4.5.1 Experimental Results - Laboratory and Live Signal Tests

Laboratory experiments demonstrated the desired operation of the the offset spectra correction and differential phase measuring hardware using the experimental configuration described above in section 4.4.1. Various lengths of transmission line were employed as the variable phase element for one of the "unfriendly" signal paths. Available trombone sections provided a change in phase of only 5 degrees at 20 MHz. Larger phase changes were realized by using various lengths of coaxial cable. However, the use of coax cables required the breaking and then acquisition of phase lock as the cables were disconnected and reconnected. The use of trombone sections

facilitated the direct observation of a change of phase as the trombone sections' lengths were changed.

During the live satellite signal tests, attempts were made to equalize the received reference and "jammer" signal CNRs. However, as is discussed above, the constant angular motion of GSTAR 3 required periodic antenna realignment at each of the participating Earth stations. Thus the received signal powers and therefore CNRs appeared to change with time. The phase locked loops were able to remain locked to the reference signals throughout all of their power level changes during all experiments except for one instance when all GSTAR 3 signals were lost while attempting to realign the Georgia Tech antenna.

The "jammer" signal emitted during the transmission from the GTE SNG truck at the McLean, Virginia site was observed on a spectrum analyzer at the Georgia Tech site to occupy about 100 kHz as compared to the relatively low phase noise CW (narrowband) signals which were experienced for all other portions of the experiments. The equipment performed equally well with the wideband signal as with the carriers.

From the measured and averaged voltage values taken during the live satellite experiments, angles and powers were inferred as is discussed in section 4.3.2. From these results, mean differential phases and variances of the accumulated data from each of the four transmissions (Grand

Junction, McLean, Grand Junction, and Atlanta) were generated. These statistical results are presented in Tables 4.1 through 4.4 with data included as a function of lowering received power thresholds. The last column in the table indicates the percentage of the available data which had an inferred power level greater than the listed power threshold. As the actual measured voltage values for these two experiments would require a minimum of 20 pages to print, this data is not listed in this report.

Table 4.1
Reduced Data from First Grand Junction Transmission

Mean, Standard Deviation, and Percent of Data Used
versus
Power Threshold

Power Threshold [dBm]	Mean [deg]	Standard Deviation [deg]	Fraction of Data Used [%]
-2.0	16.64	3.24	30.5
-3.0	9.11	7.65	72.6
-4.0	6.05	9.90	87.2
-5.0	4.63	11.08	93.3
-6.0	4.29	11.40	94.5
-7.0	4.29	11.40	94.5
-8.0	4.29	11.40	94.5
-9.0	4.29	11.40	94.5
-10.0	4.29	11.40	94.5
-11.0	4.29	11.40	94.5
-12.0	4.29	11.40	94.5
-13.0	4.29	11.40	94.5
-14.0	4.56	11.87	95.1
-15.0	4.56	11.87	95.1
-16.0	4.56	11.87	95.1
-17.0	4.56	11.87	95.1
-18.0	4.56	11.87	95.1
-19.0	4.56	11.87	95.1
-20.0	4.56	11.87	95.1
-21.0	8.12	25.18	97.6
-22.0	11.42	32.52	100.0

Table 4.2
Reduced Data from McLean, VA Transmission

Mean, Standard Deviation, and Percent of Data Used
versus
Power Threshold

Power Threshold [dBm]	Mean [deg]	Standard Deviation [deg]	Fraction of Data Used [%]
-3.0	3.41	7.66	12.0
-4.0	1.21	7.57	25.3
-5.0	0.88	7.60	26.3
-6.0	0.88	7.60	26.3
-7.0	1.04	7.69	26.7
-8.0	3.65	9.17	32.7
-9.0	3.65	9.17	32.7
-10.0	5.36	10.12	36.3
-11.0	6.13	10.03	40.0
-12.0	6.71	9.79	44.7
-13.0	6.66	9.80	47.0
-14.0	6.55	9.77	47.7
-15.0	6.67	9.83	48.3
-16.0	6.89	9.95	49.0
-17.0	8.23	10.57	53.3
-18.0	9.56	12.78	56.0
-19.0	10.98	16.16	59.7
-20.0	15.12	23.53	65.7
-21.0	37.14	52.61	81.3
-22.0	39.80	54.33	84.0
-23.0	41.67	55.00	86.3
-24.0	44.96	56.27	90.3
-25.0	46.47	56.39	93.0
-26.0	47.24	56.28	94.7
-27.0	48.17	55.93	97.0
-28.0	48.85	55.86	98.3
-29.0	49.87	56.22	99.7
-30.0	49.87	56.22	99.7
-31.0	49.87	56.22	99.7
-32.0	49.87	56.22	99.7
-33.0	49.87	56.22	99.7
-34.0	49.96	56.15	100.0

Table 4.3
Reduced Data from Second Grand Junction Transmission

Mean, Standard Deviation, and Percent of Data Used
versus
Power Threshold

Power Threshold [dBm]	Mean [deg]	Standard Deviation [deg]	Fraction of Data Used [%]
-1.0	-27.36	34.15	1.2
-2.0	-27.02	28.06	94.9
-3.0	-27.12	28.18	95.7
-4.0	-27.12	28.18	95.7
-5.0	-27.13	28.19	96.1
-6.0	-27.13	28.19	96.1
-7.0	-27.13	28.19	96.1
-8.0	-27.13	28.19	96.1
-9.0	-27.05	28.13	96.5
-10.0	-27.05	28.13	96.5
-11.0	-27.05	28.13	96.5
-12.0	-27.05	28.13	96.5
-13.0	-27.05	28.13	96.5
-14.0	-27.05	28.13	96.5
-15.0	-27.05	28.13	96.5
-16.0	-26.67	28.38	96.9
-17.0	-26.67	28.38	96.9
-18.0	-25.99	29.75	97.3
-19.0	-25.99	29.75	97.3
-20.0	-25.99	29.75	97.3
-21.0	-23.30	34.59	98.8
-22.0	-21.33	37.81	100.0

Table 4.4
Reduced Data from Atlanta, GA Transmission

Mean, Standard Deviation, and Percent of Data Used versus Power Threshold

Power Threshold [dBm]	Mean [deg]	Standard Deviation [deg]	Fraction of Data Used [%]
-2.0	-57.95	8.21	0.6
-3.0	-50.15	6.13	29.4
-4.0	-54.02	7.99	60.5
-5.0	-55.74	7.22	92.4
-6.0	-55.91	7.01	99.7
-7.0	-55.93	7.01	100.0

Tables 4.1 and 4.2 show the reduced data sorted by power threshold for the first experiment which was a measurement of the phase angle between Grand Junction and McLean. The standard deviation of the inferred angles for the samples above the higher -3.0 dBm power threshold is not the minimum deviation listed in the table. Thus, to choose a mean value to use as the estimated angle, a lower threshold was chosen which has a relatively low standard deviation for the included data. This was done in lieu of choosing the most powerful few samples or all the samples because this better removes transients (high power signals)

or periods when the computer continued to take samples but there were no desired signals present (low power signals).

Choosing the power threshold of -8.0 dBm for both the Grand Junction and McLean data gives mean angle values of 4.3 and 3.6 degrees respectively for the first day of measurements. Thus, a differential phase angle of less than one degree was acquired. Similarly choosing a power threshold of -3.0 dBm to minimize the standard deviation for the data of the second set of measurements resulted -27 and -50 degrees for Grand Junction and Atlanta respectively. This data is listed in Tables 4.3 and 4.4 and produced a differential phase angle of about 23 degrees which is a 3.1% error from the expected 12 degree result out of a possible 360 degree measurement.

Values of 4.3 and -27 degrees were measured for similar signals originating from Grand Junction for the two experiments. During the week between the experiments, parts of the hardware at the Georgia Tech site were reconfigured. This and other changes elsewhere along the signal paths may explain the difference in measured values. The absolute estimates are expected to vary with time. The differential estimates are the values of most interest.

The results from the first experiment reflect the expected small differential angle between the Grand Junction and McLean sites. Although the second experiment did result

in the desired non-zero measured angle between Grand Junction and Atlanta, there are several explanations for the discrepancy between the expected 12 and the estimated 23 degrees of differential phase. First, the employed geometric model assumes certain locations for the phase centers of the antenna onboard GSTAR 3 which were derived from the mechanical specifications for the antennas onboard the GSTAR satellite series. This may not necessarily be the case for the electrical phases. Second, all amplitude dependent effects had yet to be removed from the phase measurement hardware. Third, there may exist unknown mechanical or electronic effects resulting from the accident experienced by GSTAR 3 during its trip to orbit.

Tables 4.1 through 4.4 show a variety of inferred power levels for the different sets of data. Table 4.5 lists various signal CNR maximums and minimums which were recorded during the experiments. There appears to be no correlation between the standard deviations inferred from the measured voltages and the listed CNRs. The reference signal source was Grand Junction for all experiments.

Table 4.5

Maximum and Minimum Measured Carrier-to-Noise Ratios versus "Jammer" Signal Source Location for the Interferometry Experiments

"Jammer" Location	Reference CNR		"Jammer" CNR	
	Maximum	Minimum	Maximum	Minimum
	[dB above the noise floor]			
Grand Junction, CO	14	8	12	3
McLean, VA	13	12	13	2
Grand Junction, CO	24	22	24	22
Atlanta, GA	25	18	13	8

The spectra were offset by 1091 Hz at 9:53 pm EST on the evening of the first experiment and by 1043 Hz at 10:16 pm EST on the evening of the second experiment. These values were acquired by inserting the reference carriers, which had been regenerated by the phase locked loops, into a pair of frequency counters which were phase locked to the same temperature compensated crystal oscillator. The two displayed values were subtracted to produce the frequency differences.

4.5.2 Mapping of Measurement Error

As in the TDOA case, the differential phase measurement is a non-deterministic value with its own set of statistics. This random variable may be mapped from the measurement

domain into the desired geographic contour domain. To do this in a mathematically rigorous form, the functions describing the mapping from the measurement to the geographic domains are required. The relevant equations are discussed for computational map generation purposes in Appendix C. Again, they are non-linear and do not facilitate an easy mapping of the random variable's statistics.

To further complicate a mapping from the measurement domain to the geographical domain, the actual measurements for the interferometric technique are made as a pair of voltages which will each have their own statistics. Although this pair of measurements is reduced to a single differential phase value as was previously discussed, the statistics of the original voltage measurements would now need to be carried through the latter mappings as a 2 dimensional set of probability distribution functions.

For reasons similar to the case of the TDOA measurements, a characterization of the measurement's statistics and mappings between domains is not included in this dissertation. However, the following example is included to illustrate the relationship between measurement statistics and the geographic consequences. After a series of measurements, data reduction, and normalization to the electrical phase reference frame shown in earlier

projections of curves of constant differential phase onto maps, an example differential phase measurement may be considered to be a gaussian random variable with a mean value of 50 electrical degrees with a standard deviation of 10 degrees. Mapping this measured mean and the sum and difference of the standard deviations gives the three geographic contours shown projected onto the map of Figure 4.19. The enclosed area may be considered to be the statistical first sigma region for this particular measurement. Combining this geographic result with that of a TDOA measurement gives a zone of maximum likelihood in which to search for an interfering uplink station.

Because of logistics limitations, an insufficient number of experiments were performed to produce an empirical table of CNR versus geographical error as was done for the TDOA location technique.

4.5.3 Combining TDOA and Interferometric Geographic Results

The simultaneous use of both the TDOA (via GSTAR 1 and GSTAR 2) and Interferometric (via GSTAR 1) methods is illustrated in Figure 1.9. The curves of constant differential delay and phase form intersections which are the three dimensional solutions to the uplink location problem. Although the intersections are not necessarily orthogonal over all of CONUS and their intersections will be

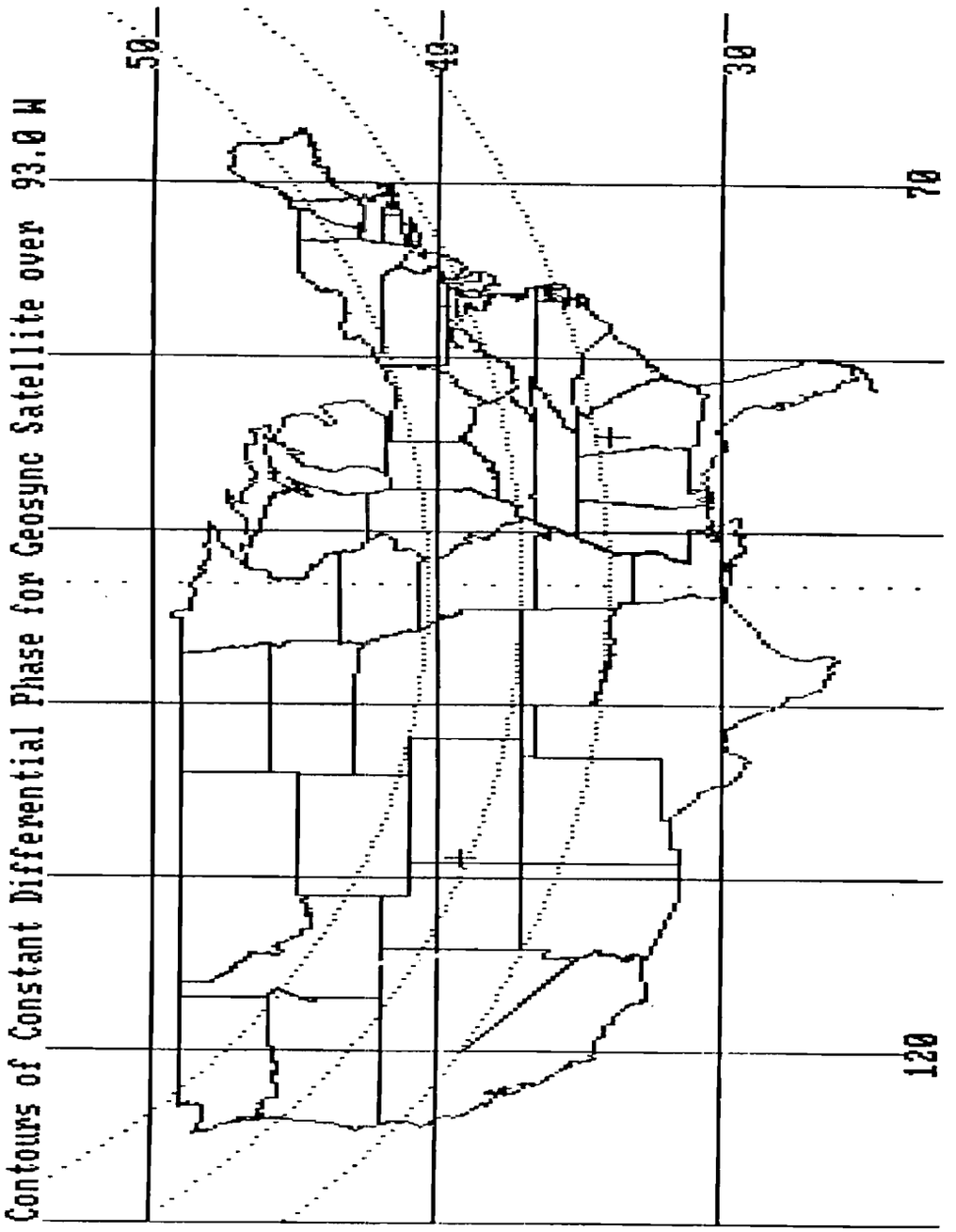

Interferometric Contours of First Sigma Region
Figure 4.19

an area of size determined by carrier-to-noise ratios and geometry determined by the noise statistics, they give much better solutions than an overlap of two sets of differential delay or two sets of differential phase measurement results. To facilitate rapid computer determination of the intersections of the time delay and interferometric curves for an automated scenario, a set of solutions may be generated off-line for rapid recall or an iterative numerical approach may be used.

5. Conclusions

As discussed above, the goal of the presented research was to develop theoretically and to illustrate experimentally the TDOA and interferometric methods for locating a terrestrial satellite uplink station. In each case, the theoretical analysis consisted of understanding the geometry, RF signal power budget, and signal processing issues. Experiments provided measurements of differential delays and phases between actual satellite signals which have been mapped into terrestrial curves corresponding to actual uplink station locations.

The TDOA technique has been successfully performed on numerous occasions both with Georgia Tech and GTE Spacenet facilities to the satisfaction of technically competent observers. All of the experimental observations to date

have been performed with the more difficult "targets-of-opportunity" as contrasted to the provision of a contrived set of signals originating from a previously designated location.

The more complicated interferometric method was successfully tested in two experiments conducted with custom built hardware. The experiments were conducted on 15 February 1990 and 22 February 1990. The results confirm the feasibility of the interferometric system. These tests were observed by Smith and Professors Steffes and Aubrey M. Bush of the Georgia Tech School of Electrical Engineering.

Regardless of the method of parameter measurement, if a stochastic description of the noise characteristics can be acquired, then this can be mapped through the deterministic equations which relate differential delay or phase to terrestrial curves into geographic error probability regions. Thus, for example, the terrestrial intersection of the first sigma region for a typical TDOA measurement with this system and that of a interferometry measurement may be found to occupy an area of 10,000 square miles which contains the potential uplink site. Figure 4.20 geographically illustrates the combination of the earlier TDOA and Interferometric statistical examples.

The originality of this work has been documented in the history (Section 2.0) presented above. The paper by Smith

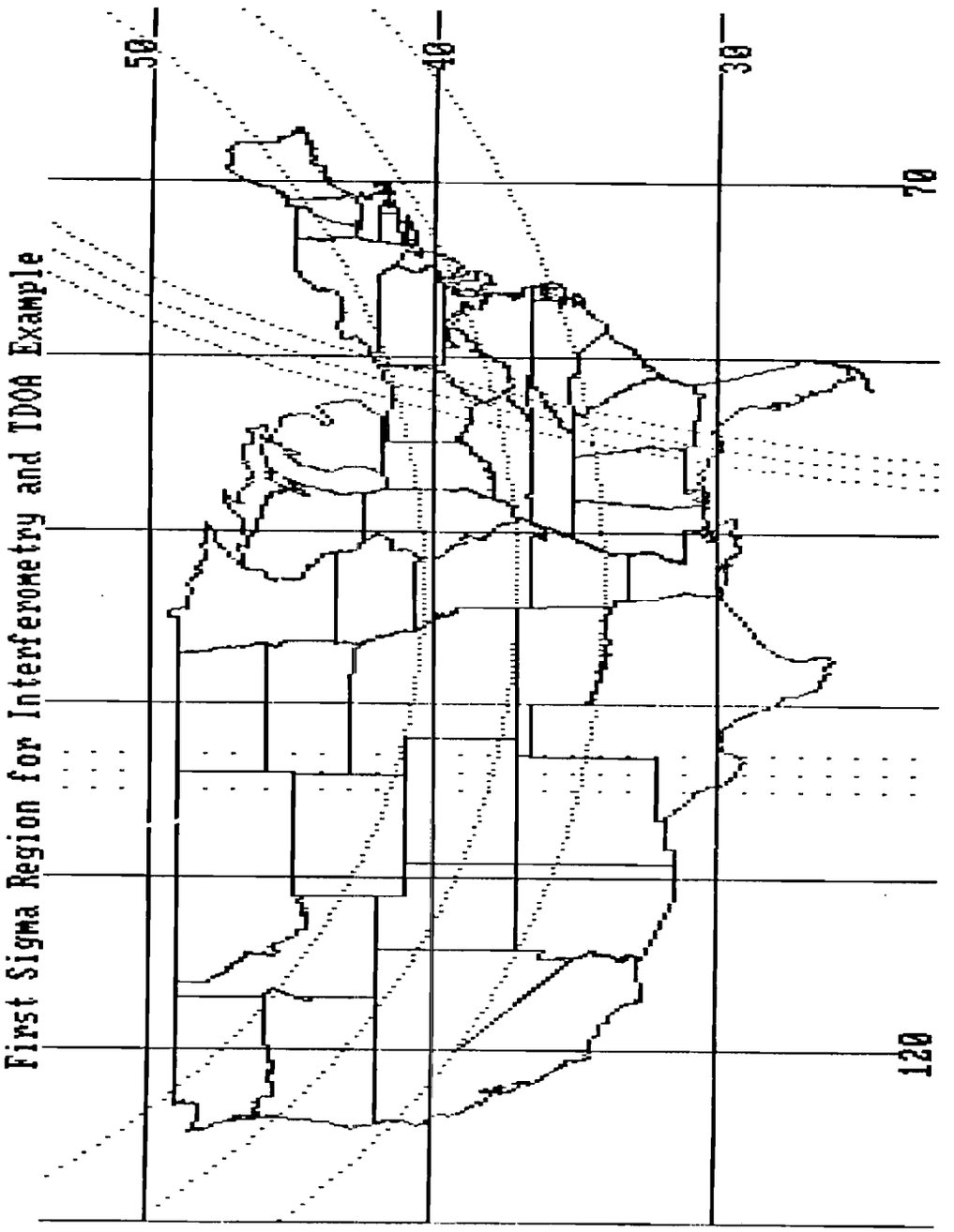

First Sigma Region for Interferometry and TOOA Example
Figure 4.20

and Steffes [8] is the first in the refereed press to describe theoretically and to present experimental results of an operational TDOA system. These efforts provided the first implementation of a Ku-band TDOA system. Although the Hughes documents are not clear on the dates of their C-band TDOA experiments, the Georgia Tech investigators may be the first to implement any sort of a TDOA system. This research is believed to be the first to implement spacecraft-based short baseline interferometry for location of ground stations. The Georgia Tech investigators appear to be the first to demonstrate this type of interferometry.

While the feasibility of the TDOA system has been successfully demonstrated, the Georgia Tech researchers' limited resources did not allow constant maintenance of an operating TDOA system because the hardware was shared with interferometry research and scheduled uplink and downlink sessions. Were the goal to maintain an operational TDOA system, upgrades to the system should include signal processing software, faster analog-to-digital conversion hardware, and various methods of signal correlation that differ from the presented post-demodulation measurement of differential delays employing measurement by operators via an oscilloscope display. Further suggestions are discussed in Section 6.

6. Suggestions for Further Research

This research was the first full attempt at realizing a Satellite Interference Location System. Each aspect of this system could be analyzed to the depth of an individual dissertation. However, the goal of this work was to demonstrate the global system feasibility. This has been done for the TDOA and interferometric techniques.

The following list includes a few areas for further research or modification to the existing system which should further facilitate SILS activities.

6.1 Spacecraft Modification

The Satellite Interference Location System (SILS) development project focused on developing a system which could locate the position of uplink transmitters using existing, on-orbit satellites such as GTE's GSTAR 1 and GSTAR 2. However, as new satellites are designed, it is possible that some relatively simple and low-cost changes in spacecraft antenna design may further facilitate the location of uplink signal sources.

6.1.1 Increasing G/T with Spacecraft Test Transponder

A significant source of difficulty for both the TDOA and interferometric techniques lies with the fact that one of the two signal channels required for each technique

carries an especially low level signal. In the case of the TDOA technique, this occurs because one of the two satellites being used for the time delay measurement is being illuminated only by a low level sidelobe from the uplink transmitter.

A receiving system's "G/T" ratio is a figure-of-merit employed by the microwave community which relates an antenna gain to the system noise temperature. A need for a large antenna gain and low noise temperature imply that a large G/T is desired. This quantity usually is expressed with units of dB/K which is the decibel form of the (linear) antenna gain divided by the system noise temperature in degrees Kelvin. This measure is used to specify receiving Earth stations as well as satellite receivers. For the satellite which may have a beam-forming antenna network to facilitate service to specific geographic areas, the satellite manufacturer will specify the satellite G/T as a function of terrestrial location.

Two approaches to increasing the level of the sidelobe signal received through what previously has been called the "adjacent" satellite can be used. The first is simply to increase the G/T of the ground station which receives the sidelobe signal. While this is an effective solution, the overall CNR of this signal is limited ultimately by the "uplink" CNR, which is related to the spacecraft G/T.

Therefore, any approach for increasing the G/T of the "adjacent" spacecraft would be helpful. It is noteworthy that the antenna systems used with the GSTAR spacecraft actually contain 13 separate beams. In the transmit mode, six of these beams can be used as an "Eastern-US spot beam". The remaining seven can form a "Western-US spot beam". All 13 can be summed to form a continental US (CONUS) beam [18]. However, in receive mode, all 13 beams are presently automatically combined to form a single CONUS beam.

One effective way to increase the G/T of the spacecraft receiver for SILS purposes would be to allow access by a tunable test transponder to any one of the 13 individual receiving beams. Because of the smaller beam size and effective higher gain, the resulting G/T would be significantly higher. A typical scenario would be that an interfering signal appears on GSTAR 2 transponder 6. The adjacent enhanced GSTAR 1 then sets its tunable transponder to channel 6 and scans through each of 13 beams until the best CNR from the sidelobe of the interfering signal is obtained as received by the SILS site. Not only does this facilitate the TDOA/SILS process, but it narrows the possible locations of interfering signal by beam position selection. However, this still requires that transponder 6 on the "adjacent" satellite (GSTAR 1) not be illuminated by an uplink from the same geographic region as the interfering

signal.

6.1.2 Additional Feedhorns for Spacecraft Interferometer

One very cost effective method for improving the ability of a single spacecraft to make interferometric measurements of uplink transmitter location involves placing additional feed horns on the spacecraft. Interferometric measurements of the position of an uplink transmitter are made by using the vertically polarized and horizontally polarized feeds as the two elements of the interferometer. However, because one of the feeds will be orthogonally polarized to the incoming signal, the received signal is extraordinarily weak, making phase comparison by the SILS ground station difficult. If additional co-polarized feeds were available, interferometric measurements can be made with less difficulty. It should be noted that the feed horns used for interferometry need not be nearly as large and complex as the 13 horn arrays used for the regular communications CONUS beams. This is because only the phase of the incoming signal needs to be measured. Any amplitude variations across the beam would have little effect on the resulting interferometric measurement.

Thus, in addition to the 16 feed horns used for each polarization on the current GSTAR spacecraft, an additional horn should be available which capable of providing a very

wide beam (covering CONUS) for each polarization. The two horns (one for each polarization) should be switchable to the inputs of any transponder so as to make improved interferometric measurements possible.

For example, an interfering signal is observed on transponder 5 of an upgraded GSTAR 1. (The signal is vertically polarized and is at a frequency of 14.280 GHz.) Now the "additional" vertically polarized horn can be connected to the input of transponder 13, which normally receives only horizontally polarized signals. Thus, two channels of information are downlinked at 11.980 GHz, one with horizontal polarization (output of transponder 5) and one with vertical polarization (output of transponder 13), and each will carry the interfering signal. However one will carry the interfering signal as received with the normal 13 beam CONUS array, and another with the single horn beam. The difference in the phases of the receiving signals is used to infer uplink station position. If yet an additional horn providing full CONUS coverage could be added for each polarization (a total of 4 horns), then a second baseline would exist, whereby the exact location of the interfering signal could be deduced. It should be noted that the spacing between the additional horns and the main feed arrays are limited by the focal range of the individual reflectors. When using the orthogonally polarized feeds for

the baselines, the spacing between the orthogonally polarized reflectors also contributes to the baselines.

6.1.3 Phase-Locking of the 2300 MHz Spacecraft Local Oscillators

Many of the existing domestic communications satellites employ the polarization re-use technique which is exploited by the interferometric SILS technique. The GSTAR Ku-band series of GTE satellites each have a pair of 2300 MHz oscillators which are the local oscillators for down-conversion from the 14 GHz uplink frequency band to the 12 GHz downlink frequency band. The down-converters of the vertically polarized transponders employ one local oscillator while the down-converters of horizontally polarized transponders employ the other oscillator. The use of these two independent and redundant oscillators facilitates the continued operation of half of the transponders should some portion of one of the down-conversion circuits fail.

The GSTAR spacecraft technical characteristics literature states that the oscillators will experience less than one part per million frequency drift per month [22]. This maximum frequency offset between the oscillators of 2300 Hz does not facilitate simple phase measurement by direct mixing. Therefore, it is suggested that the spacecraft local oscillators be phase locked to a common source.

One method for locking to a common source may be to treat one of the oscillators as a master and drive a second slave oscillator from the master. Should the master fail or drift out of an allowable passband, the second oscillator could continue at its own natural resonant frequency. Thus, the benefits of the redundant second oscillator are retained.

6.2 Computer Controlled TDOA

All of the TDOA measurements were acquired by slope demodulating frequency modulated television signals observed on an adjacent satellite with a manually tunable spectrum analyzer which was also employed to observe the afflicted transponder's output spectrum for the signal of interest. This adjacent baseband signal was compared with that from the primary satellite which was similarly detected or from a satellite television receiver to determine the time difference between signals. This measurement was then mapped into a geographic curve containing the possible uplink locations.

These measurements were performed by having a user manually tune some combination of satellite receivers and spectrum analyzers and then view both baseband signals on a dual trace oscilloscope to generate the differential time measurement. The measured value was then typed into a

computer to be evaluated by a program.

There exist several possibilities to facilitate automating the TDOA measurement process at a SILS site. One route involves buying commercially available test equipment and connecting it via computer interface busses. For example, a pair of Hewlett Packard HP8566B spectrum analyzers which are fully controllable over the IEEE-488 (GPIB or HPIB) digital interface bus may be used as two digitally controllable tuners for producing a pair of baseband outputs. These outputs can be fed to a pair of analog-to-digital converters which are realizable as a multiple trace digital oscilloscope. Such oscilloscopes are available as full test instruments with their own front panel and displays or as outboard data acquisition modules which must be connected to a host computer for user interface. Should two identical spectrum analyzers be used, the locking together of each of their oscillators would be desirable to guarantee that they are observing the same signal.

If the features similar to that found on a pair of $57000 HP8566B spectrum analyzers are not required, a computer controlled downconverter followed by a bank of computer switched filters for slope demodulation similar to that which occurs in the variable bandwidth IF sections of commercially available spectrum analyzers followed by a

video detector can produce the baseband signals. This more custom configuration may more economically suit the application.

6.3 Improved Phase Detectors

Better phase detection hardware is recommended for future interferometric based SILS systems. Some problems with the phase detector which was employed for this system appear to stem from saturation of the amplifiers preceding the mixer that produced the DC voltages that should be related to the desired differential phase. To maintain linear amplifier operation and thus minimum phase distortion over a wide dynamic range, an automatic gain control loop consisting of RF power couplers and electronically variable attenuators is suggested.

The employed phase detector also took pairs of DC measurements between RF paths containing switched lengths of transmission line which purposely introduced an additional fractional wavelength time delay into one of the incoming signal paths. A knowledge of these pairs of voltages, the measurement frequency, and the difference in lengths of transmission line allowed for numerical solution of the differential phase angle independent of the incoming signal amplitude. Because such a scheme is more sensitive to noise induced errors in certain parts of its voltage versus

differential phase characteristic, this method could be optimized to perform in the lower error portions of the mentioned characteristic by introducing a multiplicity of various length computer switched transmission line segments.

6.4 Confirmation for Curves of Constant Differential Phase

Geographic plots of constant differential phase contours were generated in an open loop fashion by assuming the locations of phase centers of the onboard satellite antenna system based on spacecraft mechanical drawings. It is recommended that a survey be taken by having signals transmitted from many different geographic sites. This could be accomplished by having a SNG truck drive north from the southern tip of Texas while stopping occasionally to perform a transmission in conjunction with another facility similar to the GTE TT&C at Grand Junction. A more practical method of performing such a survey would be to accumulate data from "targets-of-opportunity" such as SNG customers over a several week period by having them transmit some signal in conjunction with reference signals from a cooperating SILS reference site as a part of the SNG's uplink initiation procedure.

Appendices

A. TDOA Equation Derivation

This section describes equations which generate a set of terrestrial curves of constant differential delay which may be projected onto a map for use with the TDOA location method. Section 3.1 above outlines a method for generating a series of points whose locus forms one of the desired curves. The relevant known quantities are the longitudes of the two geosynchronous satellites of interest, the radius of the Earth, and the altitude of the geosynchronous satellite.

To generate one curve, a differential time is assumed. Using this differential time, the corresponding differential propagation distance (at the speed of light) is determined. Two new lines, d_{te} and d_{tw}, are generated with lengths differing by this differential distance. Each of these new lines will connect the satellite to the Earth's surface as is illustrated in Figure A.1.

To begin, the shorter of these new lines is set equal to the altitude of one satellite. This shorter line connects one satellite to its subsatellite point. The other line connects the second satellite to the Earth but touches the Earth's surface at some distance from the second subsatellite point. A terrestrial circle is formed around the second subsatellite point with a radius which intersects the second line.

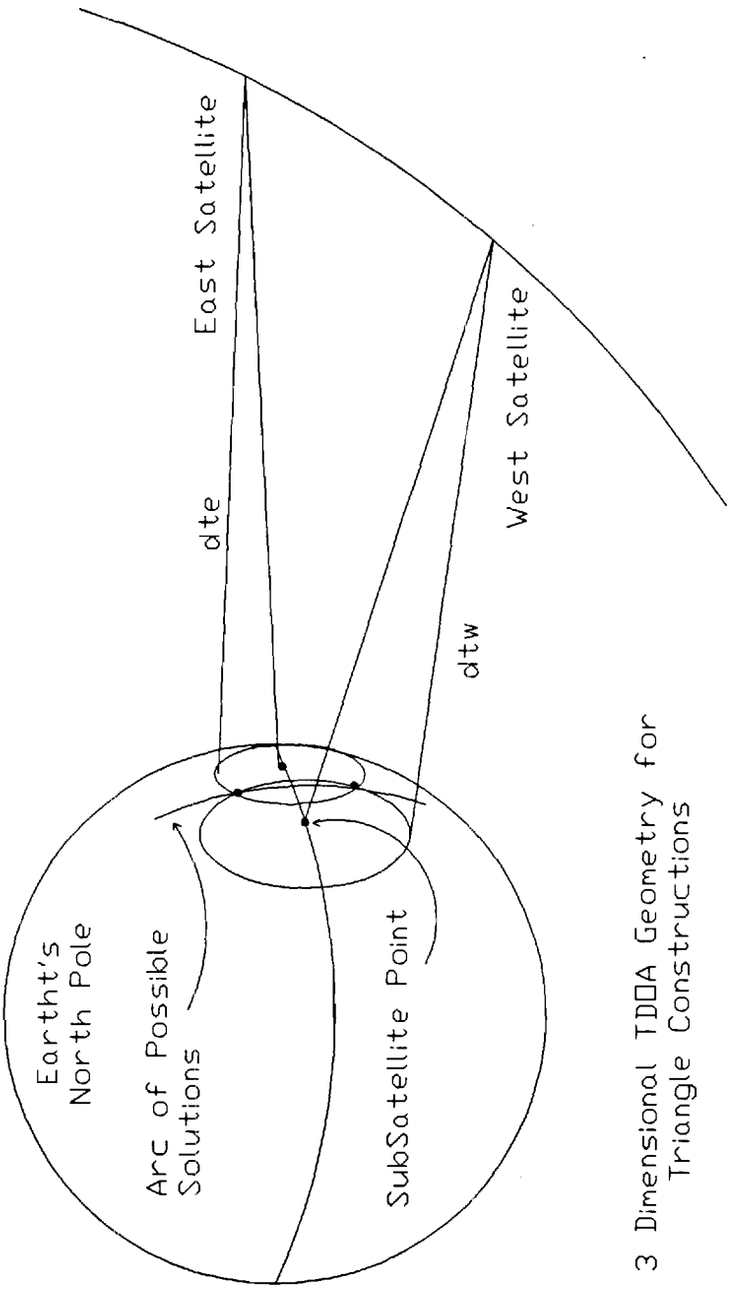

3 Dimensional TDOA Geometry for
Triangle Constructions

Figure A.1

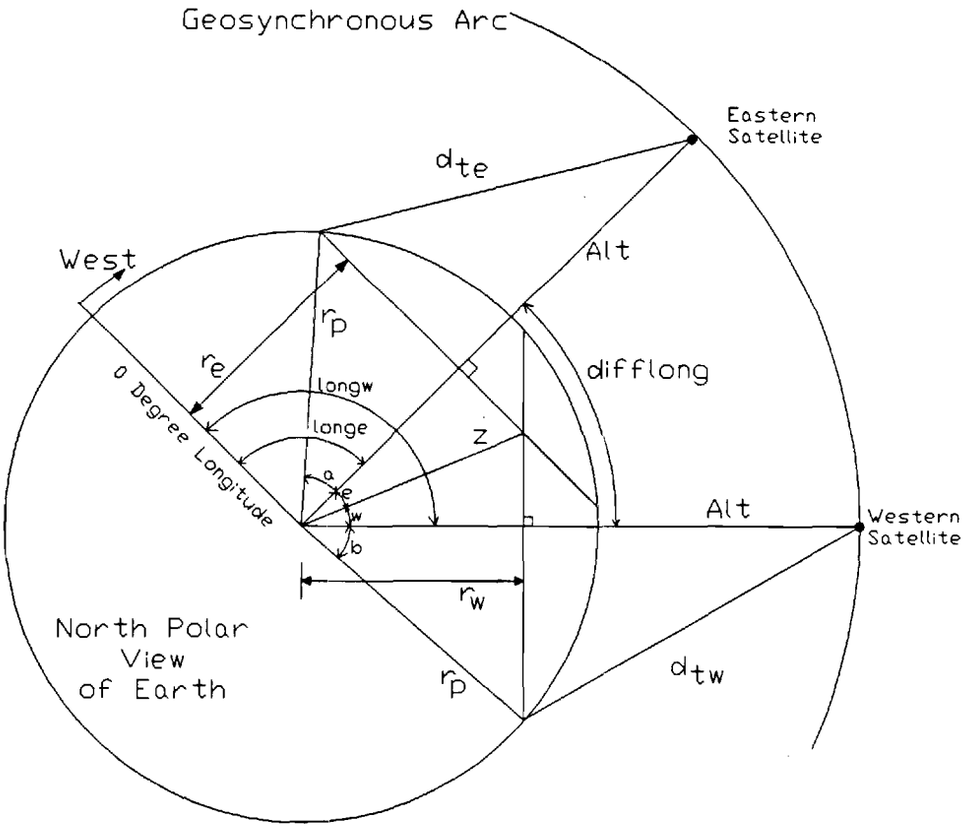

Triangle Construction for Generation of Terrestrial Curves of Constant Differential Delay

Figure A.2

Distances are incrementally added to each new line (d_{te} and d_{tw}) and corresponding subsatellite circles are formed around each subsatellite point. The intersections between these two circles are the points of interest. As the distances are incrementally added to d_{te} and d_{tw}, the locus of the intersections of the two subsatellite circles form the desired terrestrial curves.

Figure A.2 illustrates a two dimensional slice through the Earth's equatorial plane showing the relevant geometry. The known variables are:

alt = [35784 km] altitude to the satellite
r_p = [6378 km] radius of planet Earth
r_{sat} = [42162 km] radius of the satellite's orbit
longe = [degrees east] longitude of the eastern satellite
longw = [degrees west] longitude of the western satellite

$d_{te} = d_{tw}$ + (a fixed differential distance) [km]

The first goal is to solve for angle e in Figure A.2. Adding angle e to longe gives the longitude of the intersection of the subsatellite circles. This is accomplished by application of basic triangle relationships.

From the law of cosines:

Equation A.1:

$$d_{te}^2 = r_p^2 + r_{sat}^2 - 2 * r_p^2 * r_{sat}^2 * \cos(a)$$

Equation A.2:

$$d_{tw}^2 = r_p^2 + r_{sat}^2 - 2 * r_p^2 * r_{sat}^2 * \cos(b)$$

The relationships relating the distances between Earth's center and the planes formed by the eastern and western subsatellite circles and the angles a and b are:

Equation A.3: $r_e = r_p * \cos(a)$

Equation A.4: $r_w = r_p * \cos(b)$

Solving each equation for the common term r_p and combining Equations A.3 and A.4 to remove r_p leaves:

Equation A.5: $$\frac{r_e}{r_w} = \frac{\cos(a)}{\cos(b)}$$

Similarly, angle e and angle w may be related to the cosines of angles a and b by the sharing of side z between two triangles.

Equation A.6: $r_e = z * \cos(e)$

Equation A.7: $r_w = z * \cos(w)$

Thus:

Equation A.8: $$\frac{r_w}{r_e} = \frac{\cos(w)}{\cos(e)}$$

Angles e and w are related by:

Equation A.9: $\text{difflong} = \text{longw} - \text{longe} = e + w$

Therefore, substituting from equation A.9 into Equation A.8 gives:

Equation A.10:

$$\frac{r_w}{r_e} = \frac{\cos(w)}{\cos(e)} = \frac{\cos(\text{difflong} - e)}{\cos(e)}$$

$$= \frac{\cos(\text{difflong})*\cos(e) + \sin(\text{difflong})*\sin(e)}{\cos(e)}$$

$$= \cos(\text{difflong}) + \sin(\text{difflong})*\tan(e)$$

Solving equation A.10 for tan(e) gives:

Equation A.11:

$$\tan(e) = \left[\frac{\dfrac{r_w}{r_e} - \cos(\text{difflong})}{\sin(\text{difflong})} \right]$$

Recalling the relationship from Equation A.5 relating r_w/r_e to cos(a)/cos(b) gives:

Equation A.12:

$$\tan(e) = \left[\frac{\dfrac{\cos(b)}{\cos(a)} - \cos(\text{difflong})}{\sin(\text{difflong})} \right]$$

Again, from the law of cosines:

Equation A.13:

$$\cos(a) = (d_{te}^2 - r_p^2 + r_{sat}^2)/(-2 * r_p^2 * r_{sat}^2)$$

Equation A.14:

$$\cos(b) = (d_{tw}^2 - r_p^2 + r_{sat}^2)/(-2 * r_p^2 * r_{sat}^2)$$

Replacing cos(b)/cos(a) with Equations A.13 and A.14 gives:

Equation A.15:

$$e = \arctan\left[\frac{\frac{(dtw^2 - r_p^2 - r_{sat}^2)}{(dte^2 - r_p^2 - r_{sat}^2)} - \cos(difflong)}{\sin(difflong)} \right]$$

Angle e has been found. Note that angle e is the offset from the eastern satellite longitude. Therefore, the geographic longitude is found by:

Equation A.16:

Longitude = longe + e [degrees]
if T>0 (Uplink west of satellites)

= longe - e [degrees]
if T<0 (Uplink east of satellites)

where: T = [seconds] Differential time of arrival
(Eastern Signal - Western Signal)

The latitude is found by noting that:

Equation A.17: $\cos(a) = \cos(\text{latitude}) * \cos(e)$

Solving for cos(latitude) gives:

Equation A.18: $\cos(\text{latitude}) = \cos(a)/\cos(e)$

Substituting the relationship of Equation A.13 for cos(a) and solving for latitude gives:

Equation A.19

$$\text{Latitude} = +/- \arccos\left[\frac{r_p^2 + r_{sat}^2 - dte^2}{2 * r_p^2 * r_{sat}^2 * \cos(e)} \right]$$

thus providing both the latitude and longitude.

The lines d_{te} and d_{tw} are defined by:

Equation A.20: $T = (dte - dtw)/c$ [seconds]

Again, the variables, their units, and some of their relationships are defined to be:

longe = [degrees] Longitude of eastern satellite
longw = [degrees] Longitude of western satellite
difflong = [km] Absolute value of (longw - longe)
dte = [km] Swept distance from eastern satellite to eastern subsatellite circle
dtw = [km] Swept distance from western satellite to western subsatellite circle
r_{sat} = [42162 km] Radius of Earth geosynchronous orbit
r_p = [6378 km] Radius of Earth
e = [degrees] Intermediate offset longitude between subsatellite circle intersection and satellite longitude
T = [seconds] Differential time of arrival (Eastern Signal - Western Signal)
c = [2.997925×10^8 m/sec] Speed of Light
Latitude = [degrees]
Longitude = [degrees]

One curve of constant differential delay is found by sweeping the shorter line connecting the satellite to Earth's surface from its minimum length (the satellite's altitude) to its maximum length at the limb of the Earth. The intersections of the subsatellite circles formed around the terrestrial intersections these circles and d_{te} and d_{tw} produce the desired curve.

A computer program may plot this curve by stepping d_{te} and d_{tw} over the above mentioned ranges and plotting points at the coordinates defined by the inferred longitude and latitudes. A family of such curves may be generated by assuming a set of delays then repeating the entire procedure to generate one curve for each delay. The computer program

presented in Appendix B does just this and also draws appropriate geographic, political, and cartographic boundaries.

B. TDOA Computer Program to Find Terrestrial Curves of Constant Delay

The following computer program takes as inputs a measured delay, the pair of geosynchronous satellite longitudes, and the SILS site location in latitude and longitude to generate a Mercator projection map of CONUS overlaid with the curve of constant delay appropriate to the given geometry. The additional offset between the satellite of interest and the SILS site is removed to convenience the user. The curve is generated using the equations developed in Appendix A. The program can also continue to generate a family of curves to facilitate an spatially intuitive view of the relationship between measured delays and their geographical mapping.

The program includes an interactive editor to facilitate user friendliness. A 98 kilobyte file (USA.DAT) of points is used to outline the map of the United States of America. This program was written in Borland's Turbo Pascal version 3.01A. The use of a math co-processor is recommended.

```
{WHIT SMITH,  11 December 1988}
{Compute subsatellite delay circle intersections}
{Take a delta-time as an input                4 Feb 1988}
{Variable satellite longitude                 7 Mar 1988}
{Make:  time to sat a variable                9 Dec 1988
          depends on variable SILS site location
        save system defaults in file
        help feature                                      }


PROGRAM main;

{GLOBAL DECLARATIONS}

CONST
REVISION=8;
CR=$0D;             {HEX CARRIAGE RETURN}
ERRMSG=0;           {Error messages on if 1}

 WEST=-130;         {Map extents, degrees of lat and long}
 EAST=-60;
NORTH=55;
SOUTH=22;

Rp=6378.;           {km, Radius of planet - Earth=6378km}
Alt=35784.;         {km, Altitude of satellite = 35784km}
LONGei=103.0;       {Deg, East Satellite Longitude:  GSTAR 1 }
LONGwi=105.0;       {Deg, West Satellite Longitude:  GSTAR 2 }
Tmin=0.1193626;     {Sec, Subsatellite prop delay }
SILSOFFSETi=235;    {uSec, Atlanta diff delay to GSTAR pair}
LONGsilsi=84.40;    {Deg West  - Atlanta}
 LATsilsi=33.78;    {Deg North - Atlanta}



var
rpalt, difsatlong, radsqr: real;   {intermediate variables}
cosdiflong, xmin, ymin, delx, dely: real;
coords: text;
lastx, lasty: real;
longsat1, longsat2, longe, longw, deltat: real;
silsoffset, longsils, latsils: real;


{ ********************************************************
*
*           Trig Pack:   24 April 1987   Rev 2
*
* ********************************************************
```

```
*
*           Tangent
*              input is in radians
*
}
function tan(x: real): real;

var y: real;

BEGIN

y:=cos(x);
if y=0 then
   tan:=9.99999999E30
else
   tan:=sin(x)/y;

END;

{ ********************************************************
*
*           Arccos
*              output is in radians
*
}
function arccos(x: real): real;

BEGIN

if abs(x)>1 then
   if ERRMSG=1 then
      writeln('ERROR: abs(x)>1 in arccos(x)');

if (x=0) then
   arccos:=PI/2
else
   if (x<0) then
      arccos:=PI-arctan( sqrt( abs(1/(x*x)-1) ) )
   else
      arccos:=   arctan( sqrt( abs(1/(x*x)-1) ) );

END;

{ ********************************************************
*
*           Arcsin
*              output is in radians
*
}
function arcsin(x: real): real;
```

```
BEGIN

if abs(x)>1 then
   if ERRMSG=1 then
      writeln('ERROR: abs(x)>1 in arcsin(x)');

if (x=0) then
   arcsin:=0
else if (x=1) then
   arcsin:=PI/2
else if (x=-1)then
   arcsin:=-PI/2
else
   if (x<0) then
      arcsin:=-arctan( sqrt(abs( 1/( 1/(x*x)-1 ) )) )
   else
      arcsin:= arctan( sqrt(abs( 1/( 1/(x*x)-1 ) )) );

END;

{ ********************************************************
*
*        Radians to Degrees
}
function deg(rad: real): real;

BEGIN

deg:=rad*360/2/PI;

END;

{ ********************************************************
*
*        Degrees to Radians
}
function rad(deg: real): real;

BEGIN

rad:=deg*2*PI/360;

END;

{ ******************************************************** }
{ ******************************************************** }
```

```
{-------------------------------------------------------
*
*      Plot Package
*      Maps plot commands into 640 x 200 graphics display
}
procedure plton;

begin

hires;
hirescolor(white);

end;

{--------------
*
}
procedure pltscale(xminarg, yminarg, xmaxarg, ymaxarg: real);

begin

xmin:=xminarg;
ymin:=yminarg;
delx:=xmaxarg-xmin;
dely:=ymaxarg-ymin;

end;

{--------------
*
}
procedure pltxyc(x, y: real; color: integer);

var
u, v: real;

begin

u:=(x-xmin)/delx;
v:=(y-ymin)/dely;

if (0<=u) and (u<1) then
   if (0<=v) and (v<1) then
      plot( round(640*u), 200-round(v*200), color);

end;

{--------------
```

```
*
}
procedure drawxyc(x1, y1, x2, y2: real; color: integer);

var
u1, v1, u2, v2: real;
onscreen: integer;

begin

onscreen:=0;

u1:=(x1-xmin)/delx;
v1:=(y1-ymin)/dely;
u2:=(x2-xmin)/delx;
v2:=(y2-ymin)/dely;

if (-1<=u1) and (u1<2) then
   if (-1<=v1) and (v1<2) then
      onscreen:=1;
if (-1<=u2) and (u2<2) then
   if (-1<=v2) and (v2<2) then
      onscreen:=1;

if onscreen=1 then
      draw( round(640*u1), 200-round(v1*200),
            round(640*u2), 200-round(v2*200), color);

end;


{--------------
*
*    axis:  assume xmin and ymin > 0 for now
*
}
procedure axis(xtic, ytic: real);

var
xleft, xrite, ytop, ybot: real;

begin

xleft:=xtic*(int(xmin/xtic)+1);
xrite:=xleft;
ybot:=ytic*(int(ymin/ytic)+1);
ytop:=ybot;

while (xrite+xtic)<(xmin+delx) do      {tics}
   begin
```

```
    xrite:=xrite+xtic;
    drawxyc(xrite, ybot-0.02*dely, xrite, ytop+0.02*dely,
       white);
    end;
while (ytop+ytic)<(ymin+dely) do
    begin
    ytop:=ytop+ytic;
    drawxyc(xleft-0.02*delx, ytop, xleft+0.02*delx, ytop,
       white);
    end;

drawxyc(xleft, ybot, xrite, ybot, white);    {axis}
drawxyc(xleft, ybot, xleft, ytop, white);

end;

{ ********************************************************
*
*
*
}
procedure initplot;

BEGIN

plton;
pltscale(WEST,SOUTH,EAST,NORTH);
                          {size of frame to contain USA}
lastx:=201; lasty:=201;        {nothing drawn yet}

assign(coords, 'usa.dat');
reset(coords);

difsatlong:=rad(longw-longe);
cosdiflong:=cos(difsatlong);
rpalt:=Rp+Alt;
radsqr:= sqr(Rp)+sqr(rpalt);

END;


{ ********************************************************
*
*
*
}
procedure init;

var i, j: integer;
```

```
BEGIN

clrscr;

          {Initialize lat and long to GSTAR 1 and 2}

silsoffset:=SILSOFFSETi;
longe:=LONGei;
longw:=LONGwi;
longsils:=LONGsilsi;
 latsils:=LATsilsi;

END;


{ ********************************************************
*
*      200, 200 = EOF
*      201, 201 = continous
*      202, 202 = point by point
*
}
procedure drawmap;

var
x, y: real;
i: integer;

BEGIN


while (not eof(coords)) and (lastx<>200) and (lasty<>200) do
   begin
   read(coords, x);
   if (not eof(coords)) then
      read(coords, y);
   x:=-x;   {correct for west longitudes}

   if (lastx=201) or (lasty=201) then
      begin
      lastx:=x;  lasty:=y;
      end;

   if (x<>200) and (y<>200) then
      drawxyc(lastx, lasty, x, y, white);

   lastx:=x;  lasty:=y;
   end;

gotoxy(1,1);
```

```
write('longw = ', longw:6:1, '  longe = ', longe:6:1);

for i:=0 to 80 do          {centerline between sats}
    begin
    y:=i;
    x:=-(longw+longe)/2;
    pltxyc(x, y, white);
    end;

for i:=0 to 80 do          {east and west sats}
    begin
    y:=i;
    x:=-longw;
    pltxyc(x, y, white);
    x:=-longe;
    pltxyc(x, y, white);
    end;

gotoxy(77,4); {Non-scaled, map specific Long/Lat markers}
write('50');
gotoxy(77,12);
write('40');
gotoxy(77,20);
write('30');
gotoxy(69,25);
write('70');
gotoxy(11,25);
write('120');
gotoxy(1,1);


END;

{ ********************************************************
*
*
}
procedure drawlatlong;

var
i: integer;

BEGIN

for i:=-13 to -6 do  {longitudes}
    drawxyc(i*10,0,i*10,60,white);

for i:=0 to 6 do  {longitudes}
    drawxyc(-130,i*10,-60,i*10,white);
```

```
{Insert a cross for SILS site}
drawxyc(-1*longsils-0.5, latsils,
                    -1*longsils+0.5, latsils,     white);
drawxyc(-1*longsils,     latsils-0.5, -1*longsils,
                                      latsils+0.5, white);

END;

{ ********************************************************
*
*    Distance to satellite [km] = f(time [sec])
*
*
}
function distsat(time: real): real;

BEGIN

distsat:=299792.5*time;

END;


{ ********************************************************
*
*   Compute northern INTERSECTION of subsat circles for
*                                                 given dsat
*
*   Input:    dte, dtw:  distance to east/west satellites
*   Output:  lat, long:  northern lat and diff long from
*                          east subsat longitude
*
}
procedure intersect(dte, dtw: real;  var lat, long: real);

var
dterad, dtwrad: real;

BEGIN


{Unique for each itteration}

dterad:= sqr(dte)-radsqr;
dtwrad:= sqr(dtw)-radsqr;

long:=  dtwrad/dterad - cosdiflong;
long:=  arctan( long / sin(difsatlong) );

lat:=   deg(arccos( -dterad/2/Rp/(rpalt)/cos(long) ));
```

```
long:=  deg(long);

{
writeln('dte = ',dte:7:1);
writeln('dtw = ',dtw:7:1);
 }


END;


{ ********************************************************
*
*        Get a differential time value
*
}
procedure editor;

var
i, j, k: integer;
temp, testlonge, testlongw: real;
notyet: boolean;
testchar: char;

BEGIN
         {Get SILS site longitude and latitude}

testchar:='N';
notyet:=TRUE;
while ((testchar='N') or (testchar='n')) do
   begin
   testchar:='Y';
   clrscr;
   writeln('            SILS Site Location Editor');
   gotoxy(1,5);
   writeln('        Latitude = ',  latsils:6:1,
                                   ' [Deg North]');
   writeln('       Longitude = ', longsils:6:1,
                                   ' [Deg West ]');
   gotoxy(1,15);
   writeln('                Satisfied? (Y/N)[Y]');
   writeln;
   write('                        ');
   read(kbd, testchar);
   writeln;
   if ((testchar='N') or (testchar='n')) then
      begin
      writeln('     We'll be sticking to the CONUS region');
      writeln;
      write('     Enter SILS Latitude [Deg North] ');
```

```
                                                readln(testlonge);
        write('     Enter SILS Longitude [Deg West] ');
                                                readln(testlongw);

        testlonge:=abs(testlonge);
        testlongw:=abs(testlongw);


        if (testlonge<80) then          {Good lat/long values?}
           if (testlongw<130) then
              begin
              testchar:='Y';
               latsils:=testlonge;
              longsils:=testlongw;
              end
           else
              begin
              testchar:='N';
              writeln;
      writeln('    -- Bad Latitude or Longitude Value --');
              for i:=1 to 32000 do
                  for j:=1 to 8 do;
              end;
        end;
    end;


          {Get two satellite Longitudes}

testchar:='N';
notyet:=TRUE;
while ((testchar='N') or (testchar='n')) do
   begin
   testchar:='Y';
   clrscr;
   writeln('            Satellite Position Editor');
   gotoxy(1,5);
   writeln('        Eastern Longitude = ', longe:6:1,
                                                ' [deg]');
   writeln('        Western Longitude = ', longw:6:1,
                                                ' [deg]');
   gotoxy(1,15);
   writeln('               Satisfied? (Y/N)[Y]');
   writeln;
   write('                        ');
   read(kbd, testchar);
   writeln;
   if ((testchar='N') or (testchar='n')) then
      begin
 writeln('   We'll be sticking to the Western Hemisphere');
```

```
 writeln;
 write('        Enter 1st Longitude ');  readln(testlonge);
 write('        Enter 2nd Longitude ');  readln(testlongw);

      testlonge:=abs(testlonge);
      testlongw:=abs(testlongw);

      if (testlonge>testlongw) then
         begin                          {Switch east and west}
         temp:=testlonge;
         testlonge:=testlongw;
         testlongw:=temp;
         end;

      if (testlonge<180) then     {Good longitude values?}
         if (testlongw<180) then
            begin
            testchar:='Y';
            longe:=testlonge;
            longw:=testlongw;
            end
         else
            begin
            testchar:='N';
          writeln; writeln('           Bad Longitude Value');
            for i:=1 to 32000 do
                for j:=1 to 8 do;
            end;
      end;
   end;

longsat1:=longe;          {TENATIVE}
longsat2:=longw;


         {Get Measured Differential Time}

deltat:=700;
while( (deltat<-600) or (100<deltat)) do
   begin
   clrscr;
   gotoxy(10,1);
   writeln('Satellite Positions: ', longe:6:1,
                                 'W and ', longw:6:1, 'W');
   writeln;
   write('Enter  differential time observed from');
   write(' SILS Site in microseconds');
   gotoxy(20,5);
   readln(deltat);
```

```
   if ( (deltat<-600) or (100<deltat)) then
      begin
      write('Delta time value of ',deltat:6:1,
                              ' is out of range - try again');
      for j:=1 to 10000 do
          for k:=1 to 30 do;
      end;
   end;


END;


{ ********************************************************
*
*      Display:  Dish angles for Afflicted Satellite
*                                Adjacent  Satellite
*                Offset time to Satellite
}
procedure infopage;

var
costheta1, costheta2, theta1, theta2, dsat1, dsat2: real;
rsat, re: real;
az1, az2, el1, el2: real;


BEGIN


   {Compute Geometry Constants}

rsat := Alt+Rp;
  re := Rp;


{Fixed differential time from satellites to SILS site}

costheta1 := cos( abs( rad( latsils )))
                        * cos( abs( rad( longsat1-longsils)));
    dsat1 := sqrt( rsat*rsat + re*re
                               - 2 * re * rsat * costheta1 );

costheta2 := cos( abs( rad( latsils )))
                        * cos( abs( rad( longsat2-longsils)));
    dsat2 := sqrt( rsat*rsat + re*re
                               - 2 * re * rsat * costheta2 );

silsoffset := (dsat2 - dsat1) * 1000 / 2.997925e8 * 1e6;
                                                      {uSec}
```

```
{Azimuth and Elevation to each satellite}

el1 := arccos( (re*re + dsat1*dsat1
                        - rsat*rsat)/(2 * re * dsat1) );
el1 := deg( el1 ) - 90;

az1 := tan( rad(latsils))/tan(arccos(costheta1));
az1 := deg( arccos(az1) ) + 180;

el2 := arccos( (re*re + dsat2*dsat2
                        - rsat*rsat)/(2 * re * dsat2) );
el2 := deg( el2 ) - 90;

az2 := tan( rad(latsils))/tan(arccos(costheta2));
az2 := deg( arccos(az2) ) + 180;

   {report intermediate variables}

clrscr;
{
writeln('      Intermediate Test Variables'); writeln;

writeln('  latsils = ',  latsils:5:1);
writeln(' longsils = ', longsils:5:1);
writeln(' longsat1 = ', longsat1:5:1);
writeln(' longsat2 = ', longsat2:5:1);
writeln;
writeln('costheta1 = ', costheta1:7:3);
writeln('costheta2 = ', costheta2:7:3);
writeln('    dsat1 = ', dsat1:7:3);
writeln('    dsat2 = ', dsat2:7:3);
writeln;
writeln('       re = ', re:6:1);
writeln('     rsat = ', rsat:7:1);

readln;
}
   {Report AZ/EL information}

clrscr;
writeln('                              Dish Pointing Angles');
writeln('                              --------------------');
writeln;
write('                     Satellite 1');
writeln('            Satellite 2');
writeln;
writeln('  Azimuth [Deg]       ', az1:6:2,
                          '                  ', az2:6:2);
```

```
writeln('Elevation [Deg]       ', el1:6:2,
                              '                  ', el2:6:2);

   {Report Offset Time from SILS Site}

gotoxy(1,10);
write('   ------------------------------------------------------

gotoxy(1,13);
writeln('                              Differential Times');
writeln('                              ------------------');
writeln;

writeln('     SILS Site Observed Delta time = '
                              , deltat:6:1, ' [uSec]');
writeln('             ( + SILS Site offset)    '
                              , silsoffset:6:1);
writeln('                                       --------');

deltat:=deltat+silsoffset;

writeln('     Satellite Observed Delta time = '
                              , deltat:6:1, ' [uSec]');


gotoxy(1,22);
write('   ------------------------------------------------------
writeln;
writeln;
write('          ');
writeln('Hit Carrige Return to generate isochron plot');
readln;

END;

{ ******************************************************
*
*     Scan through one delay
*
*
}
procedure onescan;

var
lat, long: real;
delay, tu1i: integer;
delt, tu1, tu2: real;


BEGIN
```

```
delt:=deltat;          {One scan line for one delta time}
    begin
    delt:=delt*1e-6;
    gotoxy(1,1);
    write('Delta-t = ',delt*1000000.:6:1,'[uSec] ');
    for tu1i:=0 to 110 do
                          {steps of 100uSec over 0 to 11mSec}
        begin
        tu1:=100*tu1i*1e-6;
        tu2:=delt+tu1;
intersect( distsat(tu2+Tmin), distsat(tu1+Tmin), lat, long);
{        if (tu1=0) then
           begin
           gotoxy(1,2);
           write('long(0) = ',long:6:1,'        ');
           end;
 }       long:=long+longe;
        pltxyc(-long, lat, white);
        end;
    end;

write('     (Hit CR to fill out 20 [uSec] plot)');
readln;                {Pause to show only one isochron}
gotoxy(1,1);
write('                                                    ');

for delay:=0 to 12 do  {steps of 20uSec over 0 to 240uSec}
    begin
    delt:=20*delay*1e-6;
    gotoxy(1,1);
    write('Delta-t = ',delt*1000000.:6:1,'[uSec] ');
    for tu1i:=0 to 110 do
                         {steps of 100uSec over 0 to 11mSec}
        begin
        tu1:=100*tu1i*1e-6;
        tu2:=delt+tu1;
intersect( distsat(tu2+Tmin), distsat(tu1+Tmin), lat, long);
{        if (tu1=0) then
           begin
           gotoxy(1,2);
           write('long(0) = ',long:6:1,'        ');
           end;
 }       long:=long+longe;
        pltxyc(-long, lat, white);
        end;
    end;


for delay:=0 to 18 do {steps of 20uSec over 0 to 360uSec}
```

```
    begin
    delt:=20*delay*1e-6;
    gotoxy(1,1);
    write('Delta-t = ',-1*delt*1000000.:6:1,'[uSec] ');
    for tu1i:=0 to 110 do
                        {steps of 100uSec over 0 to 11mSec}
        begin
        tu1:=100*tu1i*1e-6;
        tu2:=delt+tu1;
intersect( distsat(tu2+Tmin), distsat(tu1+Tmin), lat, long);
{        if (tu1=0) then
           begin
           gotoxy(1,2);
           write('long(0) = ',long:6:1,'        ');
           end;
 }       long:=-long+longw;
        pltxyc(-long, lat, white);
        end;
    end;

gotoxy(1,1);
write(' Contours of 20 [uSec]  for Satellite Locations ');
write(longe:6:1, 'W and ', longw:6:1, 'W');

END;

{ ********************************************************
*
*    MAIN LINE PROCEDURE
*
*
}
BEGIN

init;

editor;

infopage;

initplot;
drawlatlong;
drawmap;
onescan;

readln;
textmode;

END.
```

C. Interferometry Equation Derivation

This section describes equations which generate a set of terrestrial curves of constant differential phase which may be projected onto a map for use with the interferometric location method. The relevant known quantities are the longitude of the geosynchronous satellite of interest, Earth's radius, and the altitude of the geosynchronous satellite.

An interferometric baseline connects the satellite to Earth's spin axis as is illustrated in Figure C.1. For the case of the GSTAR satellites, this baseline is believed to be about 55 degrees below the line connecting the satellite to its subsatellite point. The desired terrestrial curves are formed by the intersections of Earth's sphere with a cone formed around the interferometric baseline with its vertex at the satellite.

To generate one curve, a geometric angle, θ_{dp}, which forms the cone around the interferometric baseline is chosen. Angle θ_c is swept from its vertical angle of 0 degrees clockwise to about 20 degrees. The intersection of a line connecting the satellite at point S to Earth's surface at point B is thus swept across Earth's surface forming the desired curve. The challenge lies in locating the longitude and latitude of point B.

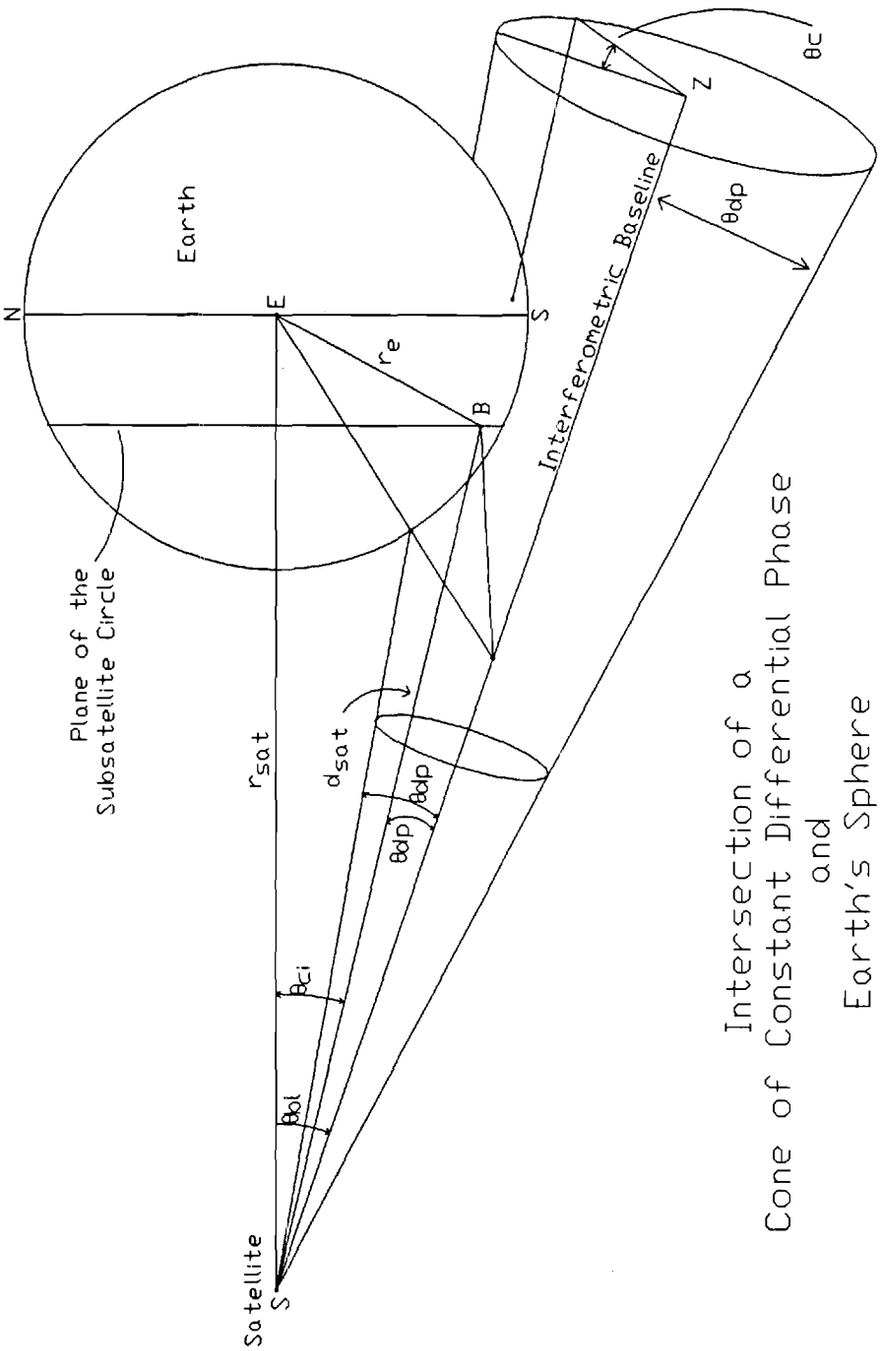

Intersection of a
Cone of Constant Differential Phase and Earth's Sphere

Figure C.1

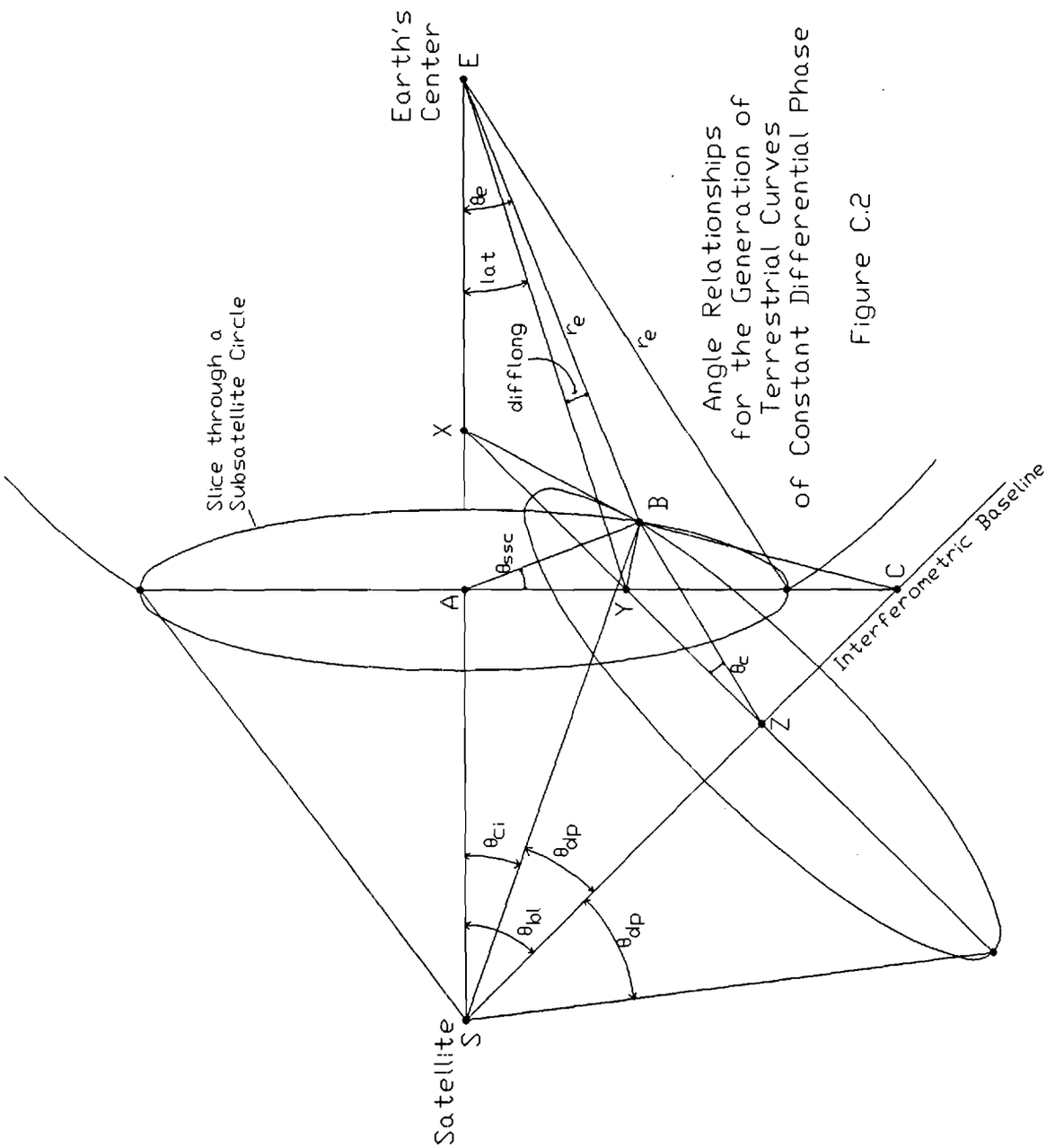

Angle Relationships for the Generation of Terrestrial Curves of Constant Differential Phase

Figure C.2

Note that there is another desired solution at the same latitude and symmetric about the satellite's longitude. This other desired solution is eclipsed by Earth in Figure 6.1. There are also two undesired solutions. These correspond to where line SB emerges on the side of Earth opposite the satellite.

The following construction relates the fixed and chosen variables to the desired latitude and longitude. The construction is broken into parts. Many of the variables are defined geometrically in Figure C.2. The given quantities necessary to determine one pair of longitudes and latitudes are:

Given Quantities

θ_{bl} = Angle ESZ
= Angle from satellite to interferometric baseline

θ_{dp} = Angle BSZ
= Angle of the cone due induced by a phase

θ_c = Angle BZY
= Cone angle swept to generate 1 terrestrial curve

r_e = Radius of Earth
ES = Earth to Satellite distance, orbital radius

The quantities of interest are the angles and not the absolute lengths of the intermediate lines which are defined only to facilitate the geometric construction. Because similar triangles retain their corresponding angles

regardless of scale, some sides of the triangles in the following construction are set equal to unity to facilitate simplicity.

C.3.1 Find θ_{ci}

The first goal is to determine angle θ_{ci} between the line BS connecting the terrestrial point B with the satellite and the line ES connecting the satellite to Earth's center.

Given: θ_{bl}, θ_{dp}, θ_c
Choose: Length of line SZ = 1

Equation C.1: $XZ = SZ * \tan(\theta_{bl}) = \tan(\theta_{bl})$
Equation C.2: $BZ = SZ * \tan(\theta_{dp}) = \tan(\theta_{dp})$

Thus, XZ and BZ are now known in terms of known quantities.

Equation C.3: $XB^2 = BZ^2 + XZ^2 - 2*BZ*XZ*\cos(\theta_c)$

Thus, XB is known in terms of known quantities.

Equation C.4: $SZ = 1 = SX * \cos(\theta_{bl})$
Equation C.5: $SZ = 1 = SB * \cos(\theta_{dp})$

Thus, SX and SB are known.

Equation C.6: $XB^2 = BS^2 + SX^2 - 2*BS*SX*\cos(\theta_{ci})$

Thus, θ_{ci} is known in terms of known quantities.

C.3.2 Find θ_e

The next goal is to find angle θ_e between the line connecting the satellite to Earth's center and the line connecting the terrestrial cone intersection point (Point B) to Earth's center.

Given: θ_{ci}

Equation C.7: $$BE^2 = ES^2 + BS^2 - 2*ES*BS*\cos(\theta_{ci})$$

Thus, Equation C.7 is found to be a quadratic in BS. The desired solution is that with the smaller magnitude. This corresponds to the solution on Earth's surface closest to the satellite. The other solution corresponds to a point on Earth which is not visible to the satellite.

Equation C.8: $$BS^2 = BX^2 + SX^2 - 2*BS*SX*\cos(\theta_e)$$

This gives the desired angle θ_e in terms of known quantities.

C.3.3 Find θ_{ssc}

The next goal is to find angle θ_{ssc} which is the angle in the subsatellite circle plane between the plane containing the satellite's line of longitude and a line connecting the terrestrial intersection point (Point B) and

the line connecting the satellite and Earth's center.

Given: θ_{bl}, θ_{ci}, θ_e
Choose: Length of line AS = 1

Equation C.9: $AS = 1 = BS * \cos(\theta_{ci})$
Equation C.10: $AS = 1 = CS * \cos(\theta_{bl})$

Thus, BS and CS are known.

Equation C.11: $BC^2 = BS^2 + CS^2 - 2*BS*CS*\cos(\theta_{dp})$

Thus, BC is known.

Equation C.12: $AB = AS * \tan(\theta_{ci}) = \tan(\theta_{ci})$
Equation C.13: $AC = AS * \tan(\theta_{bl}) = \tan(\theta_{bl})$

Thus, AB and AC are known.

Equation C.14: $BC^2 = AB^2 + AC^2 - 2*AB*AC*\cos(\theta_{ssc})$

Thus, angle θ_{ssc} is known.

C.3.4 Find the latitude and difflong

Given: θ_e, θ_{ssc}
Choose: Length of line AE = 1

Equation C.15: $AB = AE * \tan(\theta_e) = \tan(\theta_e)$

Thus, AB is known.

Equation C.16: $AY = AB * \cos(\theta_{ssc})$

Thus, AY is known.

Equation C.17: $AY = AE * \tan(lat) = \tan(lat)$

Thus, |lat| = |latitude| is known.

Note that the latitude needs to be specified as being north or south of the equator as follows:

If $|\theta_{ssc}| > 90$ degrees
then the latitude is north of the equator
else the latitude is south of the equator.

Solving for difflong:

Equation C.18: $\cos(\theta_e) = \cos(difflong) * \cos(lat)$

Thus, difflong is known.

C.3.5 Find the longitudes

The longitude offset angle, difflong, now needs to be added to and subtracted from the satellite's longitude to produce the final longitudes of the two terrestrial points.

Given: difflong
longsat = the longitude of the satellite

Equation C.19: western longitude = longsat + difflong
Equation C.20: eastern longitude = longsat - difflong

The final longitude values may need to be adjusted to correct to cartographic convention if the final longitude values cross through the terrestrial 0 or 180 degree longitudes. The latitude is given in Section C.3.4.

The computer program presented in Appendix D sweeps angles θ_{dp} and θ_c to produce the desired terrestrial curves.

D. Interferometry Computer Program to Find Terrestrial Curves of Constant Differential Phase

The following computer program takes as inputs the geosynchronous satellite longitude and the SILS site location in latitude and longitude to generate a Mercator projection map of CONUS overlaid with a family of curves of constant delay appropriate to the given geometry. The curves are generated using the equations developed in Appendix C.

As with the similar TDOA program, this program includes an interactive editor to facilitate user convenience. A 98 kilobyte file (USA.DAT) of points is used to outline the map of the United States of America. This program was written in Borland's Turbo Pascal version 3.01A. The use of a math co-processor is recommended.

```
{WHIT SMITH,  11 May 1988}
{Interferometry:  Plot lines of constant phase over CONUS}

PROGRAM main;

{GLOBAL DECLARATIONS}

CONST
REVISION=2;
CR=$0D;             {HEX CARRIAGE RETURN}
ERRMSG=0;           {Error messages on if 1}

 WEST=-130;         {Map extents, degrees of lat and long}
 EAST=-60;          {-130, -60, 55, 22}
NORTH=55;
SOUTH=22;

Rp=6378.;           {Radius of planet - Earth=6378km}
Re=6378.;           {Radius of planet - Earth=6378km}
Alt=35784.;         {Altitude of satellite = 35784km}
Rsat=42162.;        {Radius of satellite   = 42162km}
Tmin=0.1193626;     {Subsatellite prop delay in seconds }
ANGBASELINE=55.886; {Interferometric baseline}

LONGei=103.0;  {Default East Satellite Longitude:  GSTAR 1 }
LONGwi=105.0;  {Default West Satellite Longitude:  GSTAR 2 }
ATLOFFSET=235;    {Default Atlanta diff delay to GSTAR pair}

var
PI2: real;
angbl, angdp, anggp, angep, angc, angci, ange: real;
angssc, dlat, dlong, longsat, longw, longe, lat: real;

rpalt, difsatlong, radsqr: real;   {intermediate variables}
cosdiflong, xmin, ymin, delx, dely: real;
coords: text;
lastx, lasty: real;
deltat: real;



{ ********************************************************
*
*           Trig Pack:   24 April 1987   Rev 2
*
* ********************************************************
*
*           Tangent
*              input is in radians
```

```
*
}
function tan(x: real): real;

var y: real;

BEGIN

y:=cos(x);
if y=0 then
   tan:=9.99999999E30
else
   tan:=sin(x)/y;

END;

{ ***********************************************************
*
*           Arccos
*              output is in radians
*
}
function arccos(x: real): real;

BEGIN

if abs(x)>1 then
   if ERRMSG=1 then
      writeln('ERROR: abs(x)>1 in arccos(x)');

if (x=0) then
   arccos:=PI/2
else
   if (x<0) then
      arccos:=PI-arctan( sqrt( abs(1/(x*x)-1) ) )
   else
      arccos:=   arctan( sqrt( abs(1/(x*x)-1) ) );

END;

{ ***********************************************************
*
*           Arcsin
*              output is in radians
*
}
function arcsin(x: real): real;

BEGIN
```

```
if abs(x)>1 then
   if ERRMSG=1 then
      writeln('ERROR: abs(x)>1 in arcsin(x)');

if (x=0) then
   arcsin:=0
else if (x=1) then
   arcsin:=PI/2
else if (x=-1)then
   arcsin:=-PI/2
else
   if (x<0) then
      arcsin:=-arctan( sqrt(abs( 1/( 1/(x*x)-1 ) )) )
   else
      arcsin:= arctan( sqrt(abs( 1/( 1/(x*x)-1 ) )) );

END;

{ ************************************************************
*
*        Radians to Degrees
}
function deg(rad: real): real;

BEGIN

deg:=rad*360/2/PI;

END;

{ ************************************************************
*
*        Degrees to Radians
}
function rad(deg: real): real;

BEGIN

rad:=deg*2*PI/360;

END;

{ ************************************************************ }
{ ************************************************************ }

{-------------------------------------------------------------
*
*      Plot Package
*      Maps plot commands into 640 x 200 graphics display
}
```

```
procedure plton;

begin

hires;
hirescolor(white);

end;

{--------------
*
}
procedure pltscale(xminarg, yminarg, xmaxarg, ymaxarg: real);

begin

xmin:=xminarg;
ymin:=yminarg;
delx:=xmaxarg-xmin;
dely:=ymaxarg-ymin;

end;

{--------------
*
}
procedure pltxyc(x, y: real; color: integer);

var
u, v: real;

begin

u:=(x-xmin)/delx;
v:=(y-ymin)/dely;

if (0<=u) and (u<1) then
   if (0<=v) and (v<1) then
      plot( round(640*u), 200-round(v*200), color);

end;

{--------------
*
}
procedure drawxyc(x1, y1, x2, y2: real; color: integer);

var
u1, v1, u2, v2: real;
onscreen: integer;
```

```
begin

onscreen:=0;

u1:=(x1-xmin)/delx;
v1:=(y1-ymin)/dely;
u2:=(x2-xmin)/delx;
v2:=(y2-ymin)/dely;

if (-1<=u1) and (u1<2) then
   if (-1<=v1) and (v1<2) then
      onscreen:=1;
if (-1<=u2) and (u2<2) then
   if (-1<=v2) and (v2<2) then
      onscreen:=1;

if onscreen=1 then
      draw( round(640*u1), 200-round(v1*200),
            round(640*u2), 200-round(v2*200), color);

end;


{ ********************************************************
*
*      200, 200 = EOF
*      201, 201 = continous
*      202, 202 = point by point
*
}
procedure drawmap;

var
x, y: real;
i: integer;

BEGIN


while (not eof(coords)) and (lastx<>200) and (lasty<>200) do
   begin
   read(coords, x);
   if (not eof(coords)) then
      read(coords, y);
   x:=-x;   {correct for west longitudes}

   if (lastx=201) or (lasty=201) then
      begin
      lastx:=x;  lasty:=y;
```

```
      end;

   if (x<>200) and (y<>200) then
      drawxyc(lastx, lasty, x, y, white);

   lastx:=x;  lasty:=y;
   end;

gotoxy(1,1);
write('longsat = ', longsat:6:1);

for i:=0 to 80 do          {east and west sats}
    begin
    y:=i;
    x:=-longsat;
    pltxyc(x, y, white);
    end;

gotoxy(77,4);
write('50');
gotoxy(77,12);
write('40');
gotoxy(77,20);
write('30');
gotoxy(69,25);
write('70');
gotoxy(11,25);
write('120');
gotoxy(1,1);


END;

{ ************************************************************
*
*
}
procedure drawlatlong;

var
i: integer;
longsils, latsils: real;


BEGIN

for i:=-13 to -6 do  {longitudes}
    drawxyc(i*10,0,i*10,60,white);

for i:=0 to 6 do  {longitudes}
```

```
    drawxyc(-130,i*10,-60,i*10,white);

{Insert a cross for SILS site}
longsils:=108.8;   {grand junction}
latsils :=39.1;
drawxyc(-1*longsils-0.5, latsils,     -1*longsils+0.5,
                                      latsils,     white);
drawxyc(-1*longsils,     latsils-0.5, -1*longsils,
                                      latsils+0.5, white);

latsils:=33.8;    {atlanta}
longsils :=84.5;
drawxyc(-1*longsils-0.5, latsils,     -1*longsils+0.5,
                                      latsils,     white);
drawxyc(-1*longsils,     latsils-0.5, -1*longsils,
                                      latsils+0.5, white);

latsils:=39.4;    {woodbine}
longsils :=77.1;
drawxyc(-1*longsils-0.5, latsils,     -1*longsils+0.5,
                                      latsils,     white);
drawxyc(-1*longsils,     latsils-0.5, -1*longsils,
                                      latsils+0.5, white);


END;

{ ********************************************************
*
*    Distance to satellite [km] = f(time [sec])
*
*
}
function distsat(time: real): real;

BEGIN

distsat:=299792.5*time;

END;


{ ********************************************************
*
*   Compute northern INTERSECTION of subsat circles for
*                                              given dsat
*
*   Input:    dte, dtw:  distance to east/west satellites
*   Output:  lat, long:  northern lat and diff long from
*                          east subsat longitude
```

```
*
}
procedure intersect(dte, dtw: real;  var lat, long: real);

var
dterad, dtwrad: real;

BEGIN


{Unique for each itteration}

dterad:= sqr(dte)-radsqr;
dtwrad:= sqr(dtw)-radsqr;

long:=  dtwrad/dterad - cosdiflong;
long:=  arctan( long / sin(difsatlong) );

lat:=   deg(arccos( -dterad/2/Rp/(rpalt)/cos(long) ));
long:=  deg(long);

{
writeln('dte = ',dte:7:1);
writeln('dtw = ',dtw:7:1);
 }


END;


{ ********************************************************
*
*        Get a differential time value
*
}
procedure editor;

var
i, j, k: integer;
temp, testlonge, testlongw, offset: real;
notyet: boolean;
testchar: char;

BEGIN
         {Get two Longitudes}

testchar:='N';
notyet:=TRUE;
while ((testchar='N') or (testchar='n')) do
   begin
```

```
   testchar:='Y';
   clrscr;
   writeln('            Satellite Position Editor');
   gotoxy(1,5);
   writeln('        Satellite Longitude = ', longsat:5:1,
                                                ' [deg]');
   gotoxy(1,15);
   writeln('                Satisfied? (Y/N)[Y]');
   writeln;
   write('                         ');
   read(kbd, testchar);
   writeln;
   if ((testchar='N') or (testchar='n')) then
      begin
writeln('   We'll be sticking to the Western Hemisphere');
writeln;
write('          Enter Longitude ');  readln(testlonge);

      testlonge:=abs(testlonge);

      if (testlonge<180) then   (Good longitude values?)
            longsat:=testlonge
         else
            begin
            testchar:='N';
            writeln;
            writeln('           Bad Longitude Value');
            for i:=1 to 32000 do
                for j:=1 to 8 do;
            end;
      end;
   end;


END;


{ ********************************************************
*
*
*
}
procedure solvelatlong;

var
radical, a, b, c, x, y, z: real;
cosange, cosci, dsatsqr, asqr, bsqr, cosssc, dsat: real;


BEGIN
```

```
{ ------------------------ Satellite Sphere Geometry}

c:= tan( angbl );
a:= tan( angdp );

bsqr:= (a*a + c*c - 2*a*c*cos( angc ) );

z:= 1/cos( angbl );
y:= 1/cos( angdp );

cosci:= (z*z + y*y - bsqr)/(2*y*z);
angci:= arccos( cosci );


if (ERRMSG=1) then begin
writeln('[1]');
writeln('c = ',c:9:3);
writeln('a = ',a:9:3);
writeln('bsqr = ',bsqr:9:3);
writeln('z = ',z:9:3);
writeln('y = ',y:9:3);
writeln('cosci = ',cosci:9:3);
writeln('angci = ',deg(angci):9:3);
end;
{ ------------------------ Cone of Constant Phase Geometry}
{                          Depends on actual distances    }

radical:= Rsat*Rsat*(cosci*cosci - 1) + Re*Re;

cosange:=0;
if (radical>=0) then
   begin
   dsat:= Rsat*cosci - sqrt( radical);

   cosange:= (Rsat*Rsat + Re*Re - dsat*dsat)/(2*Re*Rsat);
   ange:= arccos( cosange );

   if (ERRMSG=1) then
      begin
      writeln('[2]');
      writeln('   dsat = ',dsat:9:3);
      writeln('cosange = ',cosange:9:3);
      writeln('   ange = ',deg(ange):9:3);
      end;

   end;

if (cosange>cos( deg(80) )) then
   begin
```

```
{ ------------------------- Triangle Plane Projection}

   y:=1/cosci;
   x:=1/cos( angbl );

   asqr:= x*x + y*y - 2*x*y*cos( angdp );

   b:= y*sin( angci );
   c:= x*sin( angbl );

   cosssc:= (b*b + c*c - asqr)/(2*b*c);
   angssc:= arccos( cosssc );

if (ERRMSG=1) then begin
writeln('[3]');
writeln('y = ',y:9:3);
writeln('x = ',x:9:3);
writeln('asqr = ',asqr:9:3);
writeln('b = ',b:9:3);
writeln('c = ',c:9:3);
writeln('cosssc = ',cosssc:9:3);
writeln('angssc = ',deg(angssc):9:3);
end;

{ ------------------------- Subsatellite Circle Geometry}

   b:= tan( ange );
   a:= b*cosssc;
   c:= b*sin( angssc );
   dlat:= arctan( a );
   dlong:= arccos( cos( ange )/cos( dlat ) );

if (ERRMSG=1) then begin
writeln('[4]');
writeln('b = ',b:9:3);
writeln('a = ',a:9:3);
writeln('c = ',c:9:3);
writeln('dlat = ',deg(dlat):9:3);
writeln('dlong = ',deg(dlong):9:3);
end;

{ ------------------------- Lat/Long Normalization}

   dlat:=  -deg( dlat  );
   dlong:=  deg( dlong );

   longw:= longsat + dlong;
   longe:= longsat - dlong;
```

```
    if ( abs(angssc)>(PI/2) ) then
                          {Correct for latitude N/S of equator}
       lat:=  dlat
      else
       lat:= -dlat;
    end

        else

    begin
       lat:=0; longe:=0; longw:=0;
    end;

if (ERRMSG=1) then begin
writeln('[5]');
end;


END;


{ ********************************************************
*
*    Assume screen already in plot mode with map in place
*
}
procedure scanphase;

var
i, j: integer;

BEGIN

gotoxy(1,1);
write('Contours of Constant Differential Phase for');
write(' Geosync Satellite over ');
write( longsat:5:1, ' W');

readln;

gotoxy(1,1);
write('                                                ');
write('                                                ');

for i:=0 to 18 do
             {Sweep differential phase over 59 to 63.5 deg}
    begin                              {  in 1/4 degree steps}
    angdp:= rad(59+i/4.0);

    for j:=0 to 128 do
```

```
        begin
        angc:= rad(j/16.0);
                    {Sweep cone angle over 0 to 8 degrees}
                    {  in 1/16 degree steps              }

        solvelatlong;       {Solve for lat and longe/longw}

        angep:= 1630.5*cos(angdp);
                          {Generate electrical phase angle}
        while (angep>360)          {Normalize to [-360,360]}
              angep:=angep-360;
        while (angep<-360)
              angep:=angep+360;

        gotoxy(10,1);
        write('Diff Phase = ', angep:6:2, ' [deg]    ');
        write('Cone Angle = ',  deg(angc):6:2,
                                          ' [deg]    ');

        pltxyc(-longe, lat, white);   {Plot the points}
        pltxyc(-longw, lat, white);

        end;
    end;

gotoxy(1,1);
write('Contours of Constant Differential Phase for');
write(' Geosync Satellite over ');
write( longsat:5:1, ' W');

END;


{ ********************************************************
*
*             Test
*
}
procedure test;

BEGIN

angbl:= rad( 55.9 );
angdp:= rad( 60   );
angc:=  rad(  1   );

solvelatlong;

writeln('    lat = ',lat:9:3);
writeln('  longe = ',longe:9:3);
```

```
writeln('  longw = ',longw:9:3);
writeln('longsat = ',longsat:9:3);
writeln('  angbl = ',deg(angbl):9:3);
writeln('  angdp = ',deg(angdp):9:3);
writeln('   angc = ',deg(angc):9:3);

readln;
END;


{ ************************************************************
*
*
*
}
procedure initplot;

BEGIN

plton;
pltscale(WEST,SOUTH,EAST,NORTH);
                              {size of frame to contain USA}

lastx:=201; lasty:=201;         {nothing drawn yet}

assign(coords, 'usa.dat');
reset(coords);

difsatlong:=rad(longw-longe);    {variable initialization}
cosdiflong:=cos(difsatlong);
rpalt:=Rp+Alt;
radsqr:= sqr(Rp)+sqr(rpalt);

END;


{ ************************************************************
*
*
*
}
procedure init;

var i, j: integer;

BEGIN

PI2:=2*PI;

clrscr;
```

```
longe:=LONGei;     {Initialize lat and long to GSTAR 1 and 2}
longw:=LONGwi;

longsat:=LONGei; {Initialize longitude to eastern satellite}
angbl:=rad( ANGBASELINE );

END;


{ ********************************************************
*
*     MAIN LINE PROCEDURE
*
*
}
BEGIN

init;

{test;}

editor;

initplot;
drawlatlong;
drawmap;

scanphase;

readln;
textmode;

END.
```

E. Interferometry Computer Program to Operate RF Hardware

The following computer program performed real-time operation of the phase detector hardware, controlled the Metrabyte analog-to-digital conversion board, and computed the desired phase angles for the interferometric experiments.

The Metrabyte board had a voltage input which came from the output of the phase detector. A TTL level output from the Metrabyte board switched the phase detector module's additional transmission line length into and out of one of the phase detector's inputs to facilitate the removal of amplitude ambiguities from the final inferred phase.

The program took a pair of voltage measurements and inferred the phase and an input amplitude and thus power into an assumed 50 ohm load. This was displayed to the experimenter. These measured voltages and their times of measurement were also written to a disc file to facilitate later processing. These files were used to generate the mean and standard deviation tables which appear in the interferometry results of section 4.4.2 above.

```
{WHIT SMITH,  3 October 1989 rev 2}
{ Compute magnitude and phase from two DC phase )
{ measurements with }
{ different line lengths switched under computer control }
{ rev 3:  include metrabyte dc offsets }

PROGRAM main;

   {GLOBAL DECLARATIONS}

CONST
REVISION=0;


   {Metrabyte Constants}

{Volts, Input voltage range for Metrabyte board A-D}
VMAX =  2.5;
VMIN = -2.5;

MBBASE=$300;       {MetraByte Base Address (hex)}
WINDOW=2000;       {Running average window size }
DELAY=6400;        {Delay before sampling       }

LONGOFFSET=3.7;    {mV, Offset for long  cal line (4.0)}
SHORTOFFSET=3.7;   {mV, Offset for short cal line (4.5)}

ADLOW=0;           {A to D Inputs}
ADHI=1;
STARTAD=0;

SCANREG=2;         {Scan Registers}

DIGOUT=3;          {Digital Outputs}
DIGIN=4;           {Digital Inputs }

DA0LOW=4;          {D to A Outputs}
DA0HI=5;
DA1LOW=6;
DA1HI=7;

STATUS=8;          {Control}
CONTROL=9;


   {Computational Constants}

VLITE=2.997925e8;
CR=$0D;            {HEX CARRIAGE RETURN}
```

```
ESC=27;             {escape key}
ERRMSG=0;           {Error messages on if 1}

TYPE
REGISTER = RECORD
           AX, BX, CX, DX, BP, SI, DI, DS, ES, FLAGS:
           INTEGER;
           END;


var
dispmin, dispsec: real;
datafile:  text;
samples: real;
lastdiffang: real;

{*********************************************************
*
*
*  RETURN THE TOD CLOCK'S SECONDS COUNT
*     IN HUNDREDS OF SECONDS
*
}
FUNCTION SECONDS: INTEGER;

VAR
REGS: REGISTER;

BEGIN

REGS.AX:=$2C00;    {GET TOD FROM DOS FUNCTION 2C}
MSDOS(REGS);
SECONDS:=100*(REGS.DX DIV 256) + (REGS.DX MOD 256)

END;


{*********************************************************
*
*
*
}
FUNCTION minutes: INTEGER;

VAR
REGS: REGISTER;

BEGIN

REGS.AX:=$2C00;    {GET TOD FROM DOS FUNCTION 2C}
```

```
MSDOS(REGS);
minutes:=100*(REGS.CX DIV 256) + (REGS.CX MOD 256)

END;

{ ********************************************************
*
*           Trig Pack:   24 April 1987   Rev 2
*
* ********************************************************
*
*           Tangent
*              input is in radians
*
}
function tan(x: real): real;

var y: real;

BEGIN

y:=cos(x);
if y=0 then
   tan:=9.99999999E30
else
   tan:=sin(x)/y;

END;

{ ********************************************************
*
*           Arccos
*              output is in radians
*
}
function arccos(x: real): real;

BEGIN

if abs(x)>1 then
   if ERRMSG=1 then
      writeln('ERROR: abs(x)>1 in arccos(x)');

if (x=0) then
   arccos:=PI/2
else
   if (x<0) then
      arccos:=PI-arctan( sqrt( abs(1/(x*x)-1) ) )
   else
      arccos:=   arctan( sqrt( abs(1/(x*x)-1) ) );
```

```
END;

{ ********************************************************
*
*           Arcsin
*              output is in radians
*
}
function arcsin(x: real): real;

BEGIN

if abs(x)>1 then
   if ERRMSG=1 then
      writeln('ERROR: abs(x)>1 in arcsin(x)');

if (x=0) then
   arcsin:=0
else if (x=1) then
   arcsin:=PI/2
else if (x=-1)then
   arcsin:=-PI/2
else
   if (x<0) then
      arcsin:=-arctan( sqrt(abs( 1/( 1/(x*x)-1 ) )) )
   else
      arcsin:= arctan( sqrt(abs( 1/( 1/(x*x)-1 ) )) );

END;

{ ********************************************************
*
*        Radians to Degrees
}
function deg(rad: real): real;

BEGIN

deg:=rad*180/PI;

END;

{ ********************************************************
*
*        Degrees to Radians
}
function rad(deg: real): real;

BEGIN
```

```
rad:=deg*PI/180;

END;

{ ************************************************************
*
*         Common Logs
}
function log(x: real): real;

BEGIN

if x<=0 then
   log := -300
else
   log:=ln(x)/ln(10);

END;

{ ************************************************************ }
{ ************************************************************ }



{ ************************************************************
*
*   Analog Inputs
*
*     Input:  channel numbers 0-15
*     Output: 0-((2^12)-1 = 4095)
*
* Errors: Returns -1 if channel number not in range [0,15]
*         Returns -2 if hardward acknowledgement timeout
*
}
function getanalog(channel: integer): integer;

var
timer: integer;

BEGIN

if (channel>15) then getanalog:=-1 else
  if (channel<0) then getanalog:=-1 else
    begin
    port[MBBASE+SCANREG]:=channel + $100*channel;
                                    {point to analog channel}
    port[MBBASE+STARTAD]:=channel;
```

```
                                                    {start conversion}
    timer:=10;                                     {check for timeout}
    while (port[MBBASE+STATUS]>127) and (timer>0) do
          timer:=timer-1;                {should take < 12 uSec}
    if timer=0 then
       begin
       getanalog:=-2;
       writeln('getanalog:  timeout on A/D completion');
       end
    else
       getanalog := (port[MBBASE+ADLOW] div 16)
                                    + (port[MBBASE+ADHI] * 16);
    end;


samples:=samples+1;

END;

{ ********************************************************
*
*                     Digital Outputs
*
*     Output:
*
*          15 >= (one nybble to OP3-OP0)  >= 0
*
*
}
procedure putdigital(data: integer);

BEGIN

data := abs(data) mod 16;
                {Guarentee that output nybble is in range}

port[MBBASE+DIGOUT]:=data;  {Output the data}

END;


{ ********************************************************
*
*           Screen Output Metrabyte status register
*
}
procedure showstatus;

var
i, j: integer;
```

```
BEGIN

i:=port[MBBASE+STATUS];
write(' status = ', i:5);
write(  '     status upper nybble = ',
                                ((i div 16)        ):2 );
writeln('     status lower nybble = ',
                                ( i - (i div 16)*16):2 );
END;

{ ******************************************************
*
*          Repeat voltage samples from A/D converter
*
* Average WINDOW samples from the requested channel mod 16
*
* Return the averaged voltage
*
}
function getamp(channel: integer): real;

var
i, analog: integer;
tempk, tempc, tempf, volts: real;


BEGIN

if samples>9999 then samples:=0;

channel := channel mod 16;
volts:=0;               { Low pass filter by averaging   }
                        { over a window of length WINDOW }
for i:=1 to WINDOW do
    volts := volts + getanalog(channel);

getamp := volts*(VMAX-VMIN)/4096/WINDOW + VMIN;

{writeln('from getamp - volts = ', volts:5:3, ' [volts]');}

samples := samples + WINDOW;

end;

{ ******************************************************
*
*    Itteratively solve for amplitude and phase
*
```

```
}
procedure phase;

var
manual:  boolean;
i, j: integer;

freq,       {Hz, frequency of measurement}
length,     {meters, length of diff phase transmission line}
vf,    {fraction of c, velocity factor of transmission line}
anglen,     {angle induced by transmission line length}

bracket,    {intermediate itterative limits}

vshort,     {short line measured DC voltage}
vlong,      {long  line measured DC voltage}

amp,        {resulting amplitude           }
diffang,    {resulting angle = f(amp)      }
diffang0    {storage for first diffang     }
:real;

testchar: char;

   {nonlinear function to evaluate}

function itterate(diffang: real): real;
  begin
  itterate := vshort*cos( diffang + anglen )
                                      - vlong*cos( diffang );
  end;


BEGIN

              {editor}

{defaults}
freq:=135;           {frequency in MHz}
length:=0.263;
     {specific to differential phase module number 2 about }
  { 45 deg at 70 MHz, physical length of cal line in meters}
vf:=66;              {cal line velocity factor in percent}
vshort:=300.0;       {initialize in mV}
vlong:=-519.6 ;

testchar:='a';       {anything other than ESC}

manual:=FALSE;     {Manual versus automatic acquisition mode}
```

```
while 1>0 begin  {loop forever}

if manual then
 begin          {get from keyboard, ask only once}
 clrscr;
 gotoxy(1, 10);
 write('short length voltage                V(short) ['
                                  , vshort:6:1, ' mV] = ');
 readln(vshort);
 write(' long length voltage                 V(long) ['
                                  ,  vlong:6:1, ' mV] = ');
 readln(vlong);
 writeln;
 writeln('              ----------------------------');
 writeln;
 write(' measurement frequecy                      freq ['
                                  ,  freq:5:2, ' MHz] = ');
 readln(freq);
 write(' differential cable length         length ['
                            ,  length:5:3, ' meters] = ');
 readln(length);
 write(' cable velocity factor                        vf ['
                                   ,  vf:4:1, ' %] = ');
 readln(vf);
 end;

if vshort>=9999 then
   manual:=FALSE;

if not manual then
   begin                {get from Metrabyte board}

   putdigital(0);              {Turn off calibrate relay}
   write('  turn off relay  ');
   for i:= -DELAY to DELAY do
       for j:=1 to 5 do;
   vshort:= getamp(9)*1000;       {convert to millivolts}
   vshort:= vshort + SHORTOFFSET;
              {correction for metrabyte hardware offset}

   putdigital(15);             {Turn on  calibrate relay}
   write(' turn on relay ');
   for i:= -DELAY to DELAY do
       for j:=1 to 5 do;
   vlong := getamp(9)*1000;       {convert to millivolts}
   vlong := vlong + LONGOFFSET;
              {correction for metrabyte hardware offset}

   putdigital(0);              {Turn off calibrate relay}
```

```
   write('  turn off relay  ');
   {readln;}
   end;


freq:=freq*1e6;          {convert MHz to Hz}
vshort:=vshort/1000;     {convert mV to V}
vlong:=vlong/1000;       {convert mV to V}
vf:=vf/100;              {convert percent to unitless}

   {deduce cal cable angle from cable length, freq, and vf}
anglen:=((freq/VLITE/vf)*length*360);

clrscr;

writeln('                    MEASURED VOLTAGES'); writeln;
writeln(' short length voltage          V(short) = '
                                , vshort*1000:6:1, ' mV');
writeln('  long length voltage           V(long) = '
                                , vlong*1000:6:1,  ' mV');

dispsec:=seconds/100;
dispmin:=minutes/100;
WRITE(datafile, dispmin:2:2, ' ',dispsec:2:2 );  {SAVE DATA}
writeln(datafile, vshort, ' ', vlong);

writeln; writeln;
writeln('             HARDWARE DEPENDENT PARAMETERS');
writeln;
writeln(' measurement frequecy                freq = '
                              , freq/1e6:5:2, ' MHz');
writeln(' switched cable length             length = '
                                , length:5:3, ' meters');
writeln(' switched cable angle           cable angle = '
                                , anglen:4:1, ' deg');
writeln(' cable velocity factor                vf = '
                                , (vf*100):4:1, ' %');

anglen:=rad(anglen);
            {convert cable length to radians from degrees}


{ ********************************************************
*
*    Itterate
*
*
}
              {initial conditions}
```

```
diffang:=-PI;

              {itterative solution 1}

bracket:=1;
while ( (diffang<PI) and (bracket>0.00001) )
   begin
   bracket:=bracket/10;
{  writeln('bracket = ', bracket:8:6);
}
   while
     ( (diffang<PI) and
       ( itterate(diffang)*itterate(diffang+bracket) > 0 )
     )
       begin
       diffang:=diffang+bracket;
       end;
   end;

if diffang>PI then
   begin
   writeln('CRASH1:  diffang = ', deg(diffang):6:2);
   end;


diffang0:=diffang+bracket;
amp:=vshort/cos(diffang);

writeln; writeln;
writeln('                          RESULTS'); writeln;


if amp<0 then
begin

{---------------}

diffang:=diffang0;

              {itterative solution 2}

bracket:=1;
while ( (diffang<PI) and (bracket>0.00001) )
   begin
   bracket:=bracket/10;
{  writeln('bracket = ', bracket:8:6);
}
   while
     ( (diffang<PI) and
```

```
        ( itterate(diffang)*itterate(diffang+bracket) > 0 )
      )
        begin
        diffang:=diffang+bracket;
        end;
   end;
write('2nd Solution:    ');
end    {end of amp<0}
else
write('1st Solution:    ');

if diffang>PI then
   begin
   writeln('CRASH:  diffang = ', deg(diffang):6:2);
   end;

amp:=vshort/cos(diffang);

if amp<0 then
   begin
   writeln('CRASH:  0>amp = ', amp:6:3);
   end;

  write('   Power = ', (1000*amp*amp/50):6:3, ' mW = ');
writeln( (10*log(amp*amp/50)+30):5:1, ' dBm');
writeln('                 Amplitude = ', amp:6:3, ' volts');
writeln('                       ang = '
                              , deg(diffang):5:1, ' degrees');
writeln;
  write('                   diffang = '
                           , deg(abs(diffang-lastdiffang)):5:1 );
writeln(' degrees');


{---------------}
{readln;  ***}
if manual then
   read(kbd, testchar)
else
   writeln;

{writeln('char = ', ord(testchar) );
readln;}

if ord(testchar)=ESC then  {terminal condition}
   begin
   clrscr;
   halt;
   end;
```

```
freq:=freq/1e6;
vf:=vf*100;
vshort:=vshort*1000;
vlong:=vlong*1000;
lastdiffang:=diffang;
end;
END;


{ ************************************************************
*
*
*
}
procedure init;

var i, j: integer;

BEGIN

clrscr;
port[MBBASE+CONTROL]:=0;    {Initialize Metrabyte board}
putdigital(0);              {Turn off calibrate relay  }
lastdiffang:=0;

ASSIGN(datafile,'pdoa.dat');  {OPEN THE TOTE STACKER
                                    STATE FILE}

       {TEST FOR THE EXISTENCE OF FILE}
{$I-}
RESET(datafile);
{$I+}


IF (IORESULT<>0) THEN
   BEGIN   {FILE IS EMPTY}
   CLOSE(datafile);
   ASSIGN(datafile,'pdoa.dat');  {OPEN FILE}
   REWRITE(datafile);   {CLEAR FILE TO WRITE NEW STATE}
   WRITE(datafile, dispmin:2:2, dispsec:2:2 );  {SAVE DATA}
   CLOSE(datafile);
   WRITE('PDOA data file was empty or nonexistant')
   END
ELSE
   BEGIN   {ELSE READ IN AND INITIALIZE THE LOCAL VARIABLES}
   WRITE('PDOA file exists');
   RESET(datafile);
   CLOSE(datafile)
   END;
```

```
ASSIGN(datafile,'pdoa.dat');  {OPEN FILE}
REWRITE(datafile);   {CLEAR FILE TO WRITE NEW STATE}

END;


{ ************************************************************
*
*    MAIN LINE PROCEDURE
*
*
}
BEGIN

init;

{header;}

phase;

END.
```

F. Interferometric Hardware and Schematics

Figures 4.13 and 4.15 include in block diagram form the RF signal processing hardware which was assembled to perform the interferometric measurements at the SILS site. All custom electronics were designed to operate from a 12 VDC supply with the exception of the operational amplifier circuit in the PLLs which use +/- 12 VDC. The following text describes the schematics found in the associated Figures.

Phase Locked Loops. The phase locked loops were built to facilitate a 60 to 80 MHz tuning and lock range with appropriate output power to facilitate the RF power levels required in other portions of the circuit. Their loop filters employ the "perfect integrator" operational amplifier circuit to guarantee that the output phase equals that of the input signal. This should be compared to other filter topologies which do not guarantee phase equality between input and output signals during a locked condition. The extra pole at the complex Laplacian origin provided by this integrator facilitates this requirement.

The design methods presented in Manassewitsch [20] and Gardner [21] were used to choose the components with a narrow loop bandwidth being a design goal to facilitate the exclusion of received noise. The originally computed

component values did not produce satisfactory operation of the loops. Lock was easily broken upon the hardware experiencing mechanical or electrical transients. However, after "tweaking" the component values to widen the loop bandwidth and overcoming a few faulty components and pieces of laboratory equipment, satisfactory PLL operation was attained.

The phase locked loop electrical schematic of Figure F.1 shows manually adjustable offsets to compensate for current offsets into the operational amplifier inputs and DC offsets from the phase detector output. After incorporation of the "bleeder" resistor across the integration capacitor, neither of these compensation circuits should be necessary. However, the variable offset were left in place. The integrator does just that with whatever small input offset occurs until the operational amplifier hits its supply rails without the "bleeder" resistors.

It was discovered that the "perfect integrator" operational amplifier circuit employed in the PLLs works best when it's output is less than a few millivolts. Operation was poor when the integrator had been allowed to ramp up to the almost 5 volts required to tune the VCOs to the desired 70 MHz range. The final circuit provided tuning by the summing of a manually controlled DC voltage with the integrator's output. The PLLs were tested for phase lock by

locking each loop to a low phase noise CW source then mixing the PLL output with a copy of the CW input and detecting a DC output. This DC voltage varied appropriately with a phase change induced by varying the cable lengths to the phase detector.

Phase Detector. As is discussed in the earlier text, the phase detector is realized as an enhanced mixer with pre-amplification and a switchable length of transmission line to facilitate the removal of amplitude ambiguities. The DC output is low pass filtered with a RC network. Were a high impedance voltage sensor not used then a voltage follower circuit would be required to facilitate a low impedance output and buffering. Schematics for the phase detector module are shown in Figure F.2.

Amplifiers. The gain blocks are purchased Mini-Circuits ZHL-1A amplifiers [19] and modules constructed from various Mini-Circuits MMIC amplifiers.

Filters. Because CW or 100 kHz wide signals were used as the interfering signal during live satellite tests, 250 kHz wide SAW bandpass filters centered at 70 MHz were used following helical resonator filters to limit the extraneous channel noise power into the phase comparator. Figure F.3 shows the schematics incorporating these purchased SAW filters surrounded by the required impedance transformation networks and MMIC amplifiers needed to recover the insertion

loss of the filters. The helical resonators were 6 MHz wide bandpass filters designed to isolate one television signal at a 70 MHz IF. Without the 6 MHz filters, the pre-amplifiers preceding the SAW filters were overwhelmed by the satellite channel noise power.

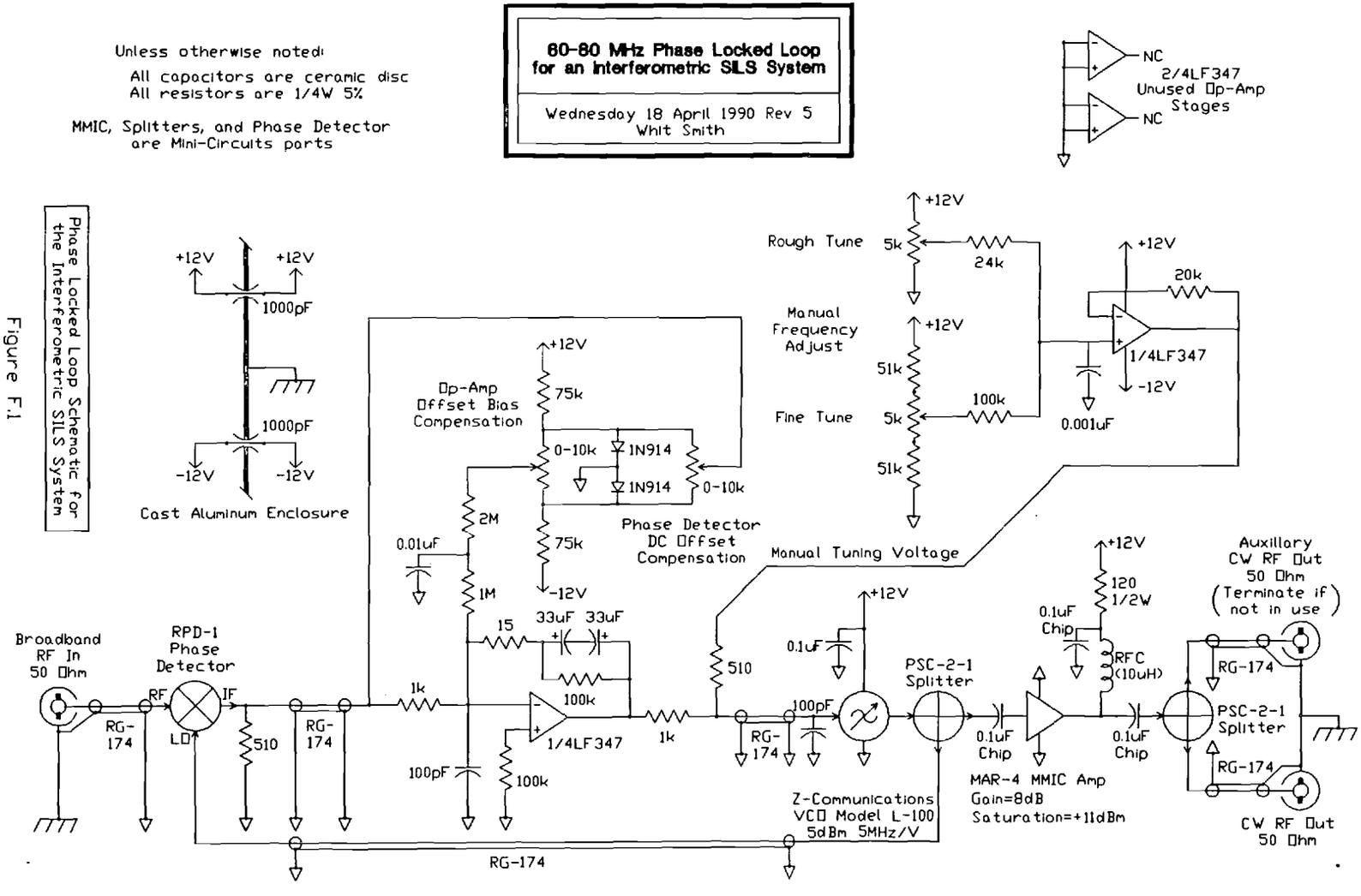
60-80 MHz Phase Locked Loop
for an Interferometric SILS System
Wednesday 18 April 1990 Rev 5
Whit Smith
Unless otherwise noted:
All capacitors are ceramic disc
All resistors are 1/4W 5%
MMIC, Splitters, and Phase Detector
are Mini-Circuits parts
NC
2/4LF347
Unused Op-Amp
Stages
NC
Phase Locked Loop Schematic for the Interferometric SILS System
+12V
+12V
1000pF
1000pF
-12V
-12V
Cast Aluminum Enclosure
Rough Tune
5k
24k
+12V
20k
Manual
Frequency
Adjust
+12V
51k
1/4LF347
-12V
100k
Fine Tune
5k
0.001uF
51k
Op-Amp
Offset Bias
Compensation
+12V
75k
0-10k
1N914
1N914
0-10k
2M
0.01uF
75k
Phase Detector
DC Offset
Compensation
Manual Tuning Voltage
1M
-12V
15
33uF 33uF
Broadband
RF In
50 Ohm
RPD-1
Phase
Detector
RF
IF
LO
RG-
174
510
RG-
174
1k
100k
100pF
100k
1/4LF347
1k
510
RG-
174
0.1uF
+12V
100pF
PSC-2-1
Splitter
0.1uF
Chip
MAR-4 MMIC Amp
Gain=8dB
Saturation=+11dBm
0.1uF
Chip
+12V
120
1/2W
RFC
(10uH)
Auxillary
CW RF Out
50 Ohm
(Terminate if
not in use)
RG-174
PSC-2-1
Splitter
RG-174
CW RF Out
50 Ohm
Z-Communications
VCO Model L-100
5dBm 5MHz/V
RG-174

Figure F.1

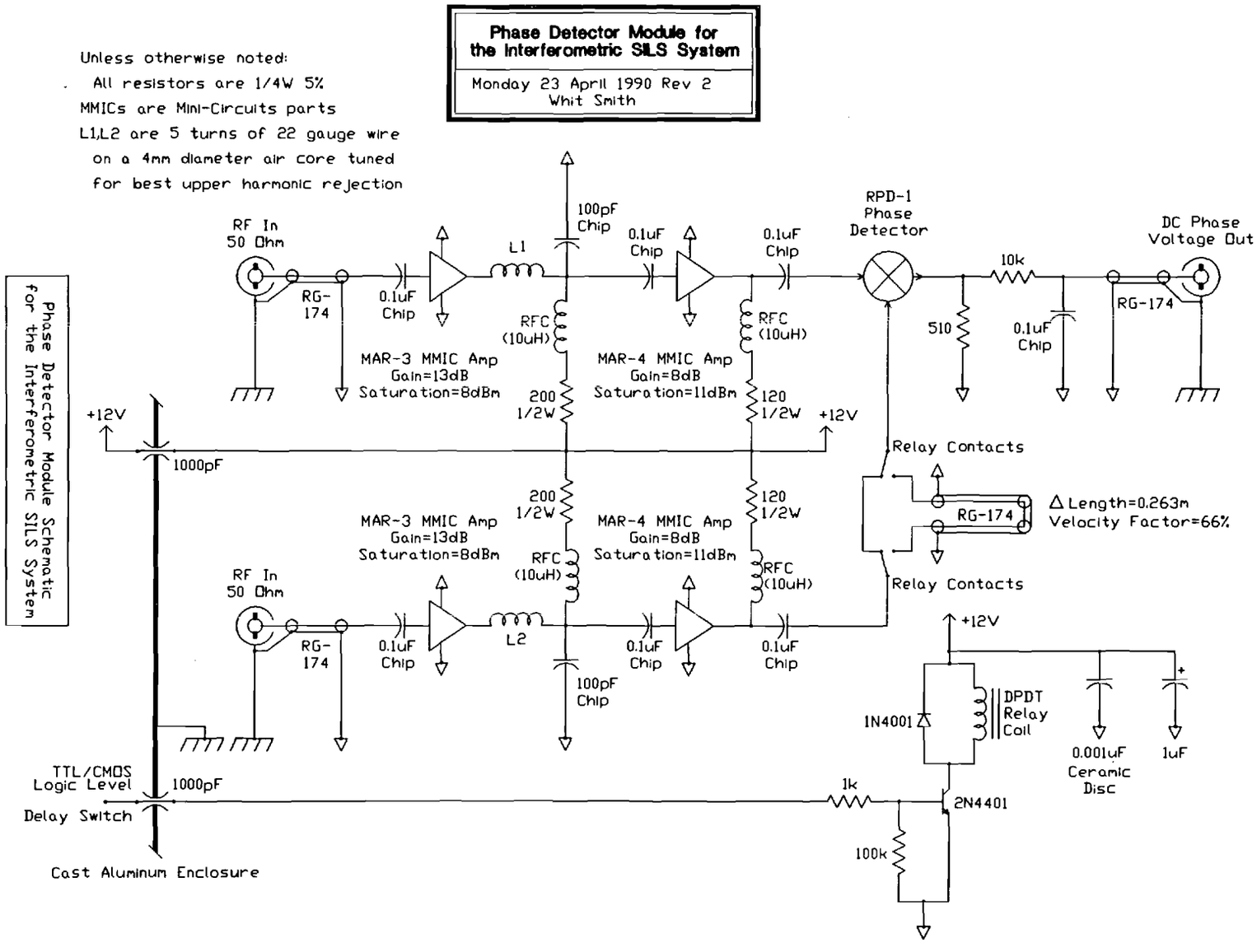
Phase Detector Module for the Interferometric SILS System
Monday 23 April 1990 Rev 2
Whit Smith
Unless otherwise noted:
All resistors are 1/4W 5%
MMICs are Mini-Circuits parts
L1,L2 are 5 turns of 22 gauge wire on a 4mm diameter air core tuned for best upper harmonic rejection
Phase Detector Module Schematic for the Interferometric SILS System
RF In 50 Ohm
RG-174
0.1uF Chip
L1
100pF Chip
0.1uF Chip
0.1uF Chip
RFC (10uH)
MAR-3 MMIC Amp Gain=13dB Saturation=8dBm
200 1/2W
MAR-4 MMIC Amp Gain=8dB Saturation=11dBm
120 1/2W
RPD-1 Phase Detector
DC Phase Voltage Out
10k
510
0.1uF Chip
RG-174
+12V
1000pF
Relay Contacts
RG-174
Δ Length=0.263m
Velocity Factor=66%
L2
100pF Chip
1N4001
DPDT Relay Coil
0.001uF Ceramic Disc
1uF
TTL/CMOS Logic Level
Delay Switch
1k
2N4401
100k
Cast Aluminum Enclosure

Figure F.2

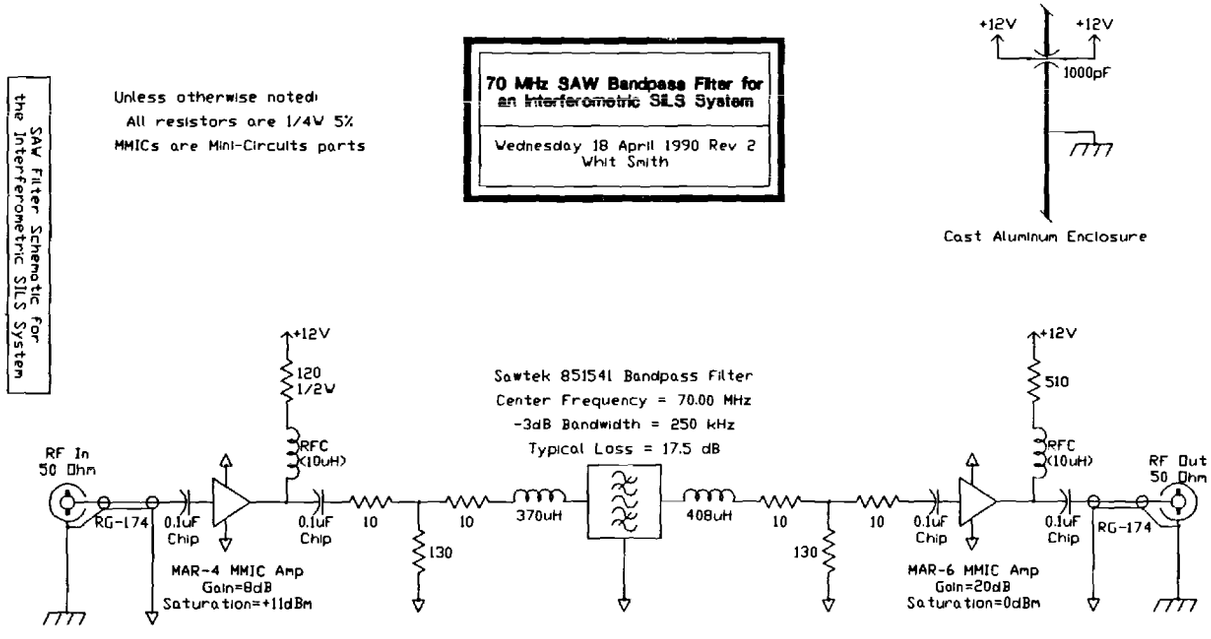
SAW Filter Schematic for the Interferometric SILS System
Unless otherwise noted:
All resistors are 1/4W 5%
MMICs are Mini-Circuits parts
70 MHz SAW Bandpass Filter for an Interferometric SILS System
Wednesday 18 April 1990 Rev 2
Whit Smith
+12V
+12V
1000pF
Cast Aluminum Enclosure
+12V
120
1/2W
RFC
(10uH)
RF In
50 Ohm
RG-174
0.1uF
Chip
MAR-4 MMIC Amp
Gain=8dB
Saturation=+11dBm
0.1uF
Chip
10
10
130
Sawtek 85154I Bandpass Filter
Center Frequency = 70.00 MHz
-3dB Bandwidth = 250 kHz
Typical Loss = 17.5 dB
370uH
408uH
10
10
130
+12V
510
RFC
(10uH)
0.1uF
Chip
MAR-6 MMIC Amp
Gain=20dB
Saturation=0dBm
0.1uF
Chip
RG-174
RF Out
50 Ohm

Figure F.3

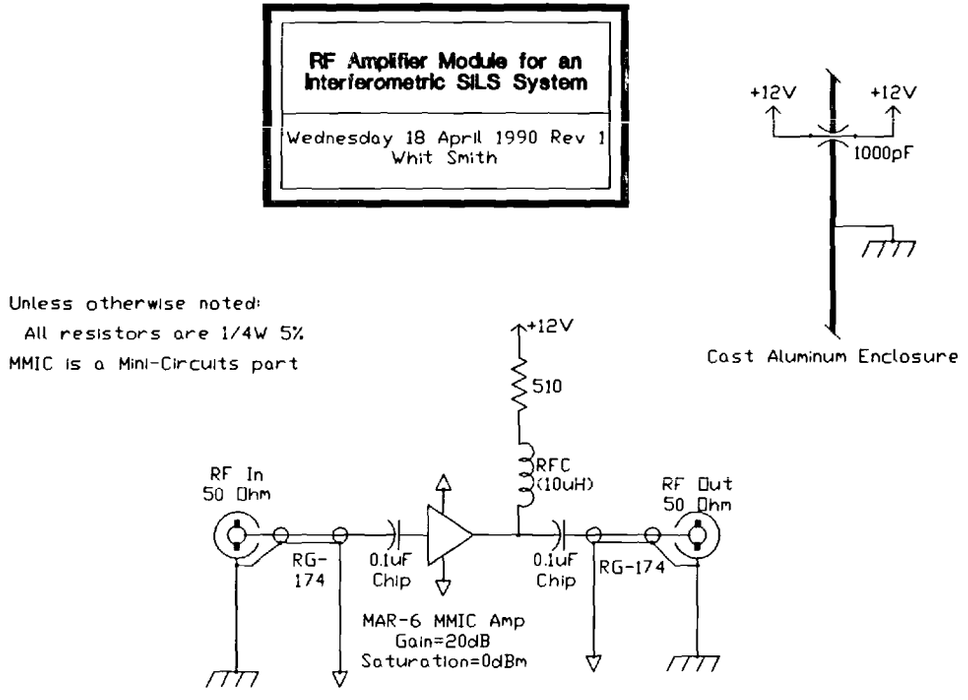

Figure F.4

Intermediate RF Amplifier Schematic for the Interferometric SILS System

Bibliography

[1] Aviation Week and Space Technology, 5 May 1986, "Tapes Studied for Clues in HBO Interference," p28.

[2] Newsweek, 12 May 1986, "A Thing That Went Bump in the Night," p75.

[3] Time, 12 May 1986, "Captain Midnight's Sneak Attack," p101.

[4] Marcus, Michael J. (1987) Satellite Security: Legacy of "Captain Midnight," Telecommunications, Vol. 21, June 1987, 61-62.

[5] Johnson, Gordon (1987) Contel Corporation, Atlanta, Georgia, personal communication.

[6] Chestnut, Paul C., (1982) Emitter Location Accuracy Using TDOA and Differential Doppler, IEEE Transactions on Aerospace and Electronic Systems, Vol. AES-18, No. 2, March 1982, 214-218.

[7] Harris, Richard and Reed Burkhart, "Location of Terrestrial Based Satellite Interference," IEEE 1987 Aerospace Applications Conference, Vail, Colorado, 9 February 1987.

[8] Smith, William W. and Paul G. Steffes, (1989) "Time Delay Techniques for a Satellite Interference Location System," IEEE Transactions on Aerospace and Electronic Systems, AES-25, 2 (March 1989), 224-231.

[9] Operation and Maintenance Manual for Harris 6.1 Meter Delta Gain Ku-Band Satellite Earth Station Model 5346 (1985), Harris Corporation, Kilgore, Texas, p2-2.

[10] Weiss, Anthony J., (1987) "Bounds on time-Delay Estimation for Monochromatic Signals," IEEE Transactions on Aerospace and Electronic Systems, Vol. AES-23, No. 6, November 1987, 798-808.

[11] Weiss, Anthony J. and Zvi Stein, "Optimal Below Threshold Delay Estimation for Radio Signals," IEEE Transactions on Aerospace and Electronic Systems, Vol. AES-23, No. 6, November 1987, 726-730.

[12] Friis, H. T., Proceedings of the IRE 34, 254 (1946).

[13] Scientific-Atlanta 1990 Network Systems Group Product Catalog (1990), Series 8060 6-Meter Earth Station Antenna insert, Scientific-Atlanta, Incorporated, Norcross, Georgia.

[14] Operation and Maintenance Manual for Harris 6.1 Meter Delta Gain Ku-Band Satellite Earth Station Model 5346 (1985), Harris Corporation, Kilgore, Texas, 2-2.

[15] Operation and Maintenance Manual for Harris 6.1 Meter Delta Gain Ku Band Satellite Earth Station model 5346, Harris, 1985, p2-2.

[16] Jurgens, Richard D., EE 8901 Report: Ground Station Integration and Performance Characterization, Summer 1987.

[17] Cook, Jim, Scientific Atlanta Staff Scientist, Personal Communications, 9 October 1987.

[18] Antenna Design Proposal for GSTAR from RCA Government Systems Division/Astro-Electronics.

[19] Mini-Circuits RF/IF Signal Processing Handbook, (1987-1988) Volume 2, Mini-Circuits Incorporated, Brooklyn, NY.

[20] Manassewitsch, Vadim, Frequency Synthesizers: Theory and Design, (1980), 2nd Edition, John Wiley and Sons, New York, p263-8. (PLL Design).

[21] Gardner, Floyd M., Phaselock Techniques, (1979), 2nd Edition, John Wiley and Sons, New York, p9-14. (PLL Design).

[22] Technical Characteristics of GSTAR Satellites, (December 1985), GTE Spacenet Corporation, McLean, Virginia.

[23] Belden Electric Wire and Cable Catalog Number 885, (1987) Belden Corporation, Electronic Division, Richmond, Indiana.

[24] Federal Communications Commission Rules and Regulations, (November 1987), Volume 5, Part 25.209, p178-9.

[25] Gagliardi, Robert M., Satellite Communications, (1984), Van Nostrand Reinhold Company, Incorporated, New York. (RF Link and CNR Equations).

Vita

William Whitfield Smith, Jr. (Whit) was born in Goldsboro, North Carolina, on August 17th, 1959. He received the B.E.E and M.S.E.E. degrees in 1982 and 1986 from the Georgia Institute of Technology, Atlanta, from which he plans to graduate with his Ph.D. in Electrical Engineering in June 1990.

During his undergraduate career, he designed, built, and installed industrial computer controls for a variety of firms. From 1982 until 1984, he was employed by the Broadcast Products Division of the Harris Corporation where he designed and developed high power commercial broadcast transmitters and their control equipment. He has also pursued various Graduate Research Assistantships and consulting activities during his graduate student career which have resulted in at least one patent.